8-2012

EFFECTS OF THE ACTA2 R258C MUTATION ON VASCULAR SMOOTH MUSCLE CELL PHENOTYPE AND PROPERTIES

Katerina L. Byanova

EFFECTS OF THE *ACTA2* R258C MUTATION ON VASCULAR SMOOTH MUSCLE CELL PHENOTYPE AND PROPERTIES

by

Katerina Lyubomirova Byanova, B.A.

APPROVED:

_____
Dianna M. Milewicz, M.D., Ph.D., Advisor

_____
Fernando Cabral, Ph.D.

_____
Guangwei Du, Ph.D.

_____
Jeffrey Frost, Ph.D.

_____
Ali J. Marian, M.D.

APPROVED:

_____
Dean, The University of Texas
Graduate School of Biomedical Sciences at Houston

EFFECTS OF THE *ACTA2* R258C MUTATION ON VASCULAR SMOOTH MUSCLE CELL PHENOTYPE AND PROPERTIES

A

THESIS

Presented to the Faculty of

The University of Texas

Health Science Center at Houston

And

The University of Texas

M. D. Anderson Cancer Center

Graduate School of Biomedical Sciences

in Partial Fulfillment

of the Requirements

for the Degree of

MASTER OF SCIENCE

by

Katerina L. Byanova, B.A.

Houston, Texas

August 2012

Dedication

This work is dedicated to all patients and families suffering from or at risk of developing TAAD, who donated time and samples for our studies. Our work would be impossible without you.

Acknowledgements

First and foremost, I would like to thank Dr. Dianna Milewicz for giving me the opportunity to stay on and pursue a master's degree in her lab and work on this project. It has been two memorable years, for which I am truly grateful.

Next, I would like to thank my committee – Dr. Cabral, Dr. Du, Dr. Frost and Dr. Marian - for helping me out along the way, for pushing me to deepen my understanding and develop critical thinking skills, and for giving me informal feedback, access to resources and encouragement in the past two years.

I would not have accomplished nearly as much as without the help of Callie Kwartler, who not only introduced me to the lab, but also offered friendship, a helping hand and great advice along the way. Dr. Limin Gong's technical and moral support has also been indispensable from the moment I joined the lab. A big thank you goes to all my labmates and to Dr. R. Jay Johnson for sharing the past few years and for remaining patient with me even on bad days.

The faculty and students in the Cell & Regulatory Biology Program offered a lot of valuable feedback and encouragement throughout, for which I am thankful. Dr. Richard Clark's mentorship and his contagious passion for science were an excellent morale boost and a source of inspiration from early on.

Finally, I would not be where I am today if not for my wonderful family and fiancé. Albeit from far away, my mother and grandmother have been my pillars and sources of inspiration, strength and determination. Having my fiancé, Dr. Antoine Vernon, by my side, has made the hard times more bearable and the good times even better. Antoine, I cannot imagine getting this far without your love, support and delicious dinners. Thank you.

EFFECTS OF THE *ACTA2* R258C MUTATION ON VASCULAR SMOOTH MUSCLE CELL PHENOTYPE AND PROPERTIES

Publication No._____

Katerina Lyubomirova Byanova, B.A.

Advisor: Dianna M. Milewicz, M.D., Ph.D.

Thoracic Aortic Aneurysms and Dissections (TAAD) are the fifteenth leading cause of death in the United States. About 15% of TAAD patients have family history of the disease. The most commonly mutated gene in these families is *ACTA2*, encoding smooth muscle-specific α-actin. *ACTA2* missense mutations predispose individuals both to TAAD and to vascular occlusive disease of small, muscular arteries.

Mice carrying an *Acta2* R258C mutant transgene with a wildtype *Acta2* promoter were generated and bred with $Acta2^{-/-}$ mice to decrease the wildtype: mutant *Acta2* ratio. $Acta2^{+/+\ R258C\ TG}$ mice have decreased aortic contractility without aortic disease. $Acta2^{+/-\ R258C\ TG}$ mice, however, have significant aortic dilatations by 12 weeks of age and a hyperproliferative response to injury. We characterized smooth muscle cells (SMCs) from both mouse models under the hypothesis that mutant α-actin has a dominant negative effect, leading to impaired contractile filament formation/stability, improper focal adhesion maturation and increased proliferation.

Explanted aortic SMCs from $Acta2^{+/+\ R258C\ TG}$ mice are differentiated - they form intact filaments, express higher levels of contractile markers compared to wildtype SMCs

and have predominantly nuclear Myocardin-Related Transcription Factor A (MRTF-A) localization. However, ultracentrifugation assays showed large unpolymerized actin fractions, suggesting that the filaments are brittle. In contrast, *Acta2*$^{+/- R258C TG}$ SMCs are less well-differentiated, with pools of unpolymerized actin, more cytoplasmic MRTF-A and decreased contractile protein expression compared to wildtype cells. Ultracentrifugation assays after treating *Acta2*$^{+/- R258C TG}$ SMCs with phalloidin showed actin filament fractions, indicating that mutant α-actin can polymerize into filaments.

Both *Acta2*$^{+/+ R258C TG}$ and *Acta2*$^{+/- R258C TG}$ SMCs have larger and more peripheral focal adhesions compared to wildtype SMCs. Rac1 was more activated in *Acta2*$^{+/+ R258C TG}$ SMCs; both Rac1 and RhoA were less activated in *Acta2*$^{+/- R258C TG}$ SMCs, and FAK was more activated in both transgenic SMC lines compared to wildtype. Proliferation in both cell lines was significantly increased compared to wildtype cells and could be partially attenuated by inhibition of FAK or PDGFRβ. These data support a dominant negative effect of the *Acta2* R258C mutation on the SMC phenotype, with increasing phenotypic severity when wildtype: mutant α-actin levels are decreased.

Table of Contents

List of Illustrations

List of Tables

List of Abbreviations

Acta2/ACTA2	Smooth-muscle specific alpha-actin (mouse/human)
Akt/PKB	Protein Kinase B
BAV	Bicuspid aortic valve
Cnn1	Calponin 1
DMEM	Dulbecco's modified eagle medium
Elk1	E twenty-six (ETS)-like transcription factor 1
ERK1/2	Extracellular signal-regulated kinases 1/2
EtOH	Ethanol
F actin	Filamentous actin
FA	Focal adhesion
FAK	Focal adhesion kinase
FITC	Fluorescein isothiocyanate
FTAAD	Familial thoracic aortic aneurysm an/or aortic dissection
G actin	Globular (monomeric) actin
IB	Immunoblot
IEF	Isoelectric focusing (2D) gel
IF	Immunofluorescence
LDS	Loeys-Dietz syndrome
MMP	Matrix metalloproteinase
MRTF-A	Myocardin-related transcription factor A
MRTF-B	Myocardin-related transcription factor B

MS	Marfan syndrome
Myh11	Myosin heavy chain
PBS	Phosphate buffered saline
Pi	Inorganic phosphate
PI3K	Phosphoinositide-3 kinase
PMSF	Phenylmethanesulfonylfluoride
PDGFRβ/*Pdgfrb*	Platelet-derived growth factor receptor beta
PVDF	Polyvinylidene fluoride
Sm22α	Transgelin
SmBM	Smooth muscle basal medium
SMC	Smooth muscle cell
SM-MHC	Smooth muscle- myosin heavy chain
SRF	Serum response factor
STAAD	Sporadic thoracic aortic aneurysms and/or aortic dissections
TAAD	Thoracic aortic aneurysms and/or aortic dissections
TBS-T	Tris-buffered saline with Tween-20
TCF	Ternary complex factor
TGF-β1	Transforming growth factor beta 1
TIRF Microscopy	Total internal reflection fluorescent microscopy
vEDS	vascular (type IV) Ehlers-Danlos Syndrome
VSMC	Vascular smooth muscle cell
WT	Wildtype

CHAPTER ONE: Introduction

Thoracic Aortic Aneurysms and Aortic Dissections (TAAD)

Epidemiology

Thoracic aortic aneurysms and dissections (TAAD) are the eighteenth leading cause of death in the United States (thirteenth leading cause in people over 65 years of age), and they account for approximately 15,000 deaths every year (1). Aortic dissections are medical emergencies – if left untreated, they cause death in about ⅓ of all patients within 24 hours of the onset and 75% of patients within two weeks (2), with a death rate of approximately 1% per hour from the onset of the dissection (3; 4).

An aortic aneurysm is an enlargement of the vessel wall, which can progress to a dissection – a tear in the wall that creates a false lumen and diverts the blood flow away from the main channel (2-3; 5-6). Aortic aneurysms are classified based on the region of the aorta where they form - the aortic root, ascending aorta, aortic arch, descending aorta, or abdominal aorta (1; 3; 5-6). Ascending, descending and aortic arch aneurysms are also commonly referred to as thoracic aortic aneurysms. Aortic dissections, on the other hand, have two separate classification systems that are commonly used – the Stanford system and the DeBakey system. A Stanford type A dissection is one of the ascending aorta, the aortic arch or the descending aorta, which originates in the ascending aorta or aortic arch. Stanford type B dissections originate in the descending aorta (1-4). A DeBakey class I dissection is an expansive dissection that originates in the ascending aorta; class II, on the other hand, is a more localized dissection of the ascending aorta. Class III is dissection of the descending aorta, which also tends to lead to extensive tearing along the aortic wall (**Fig. 1.1)** (1-3).

A

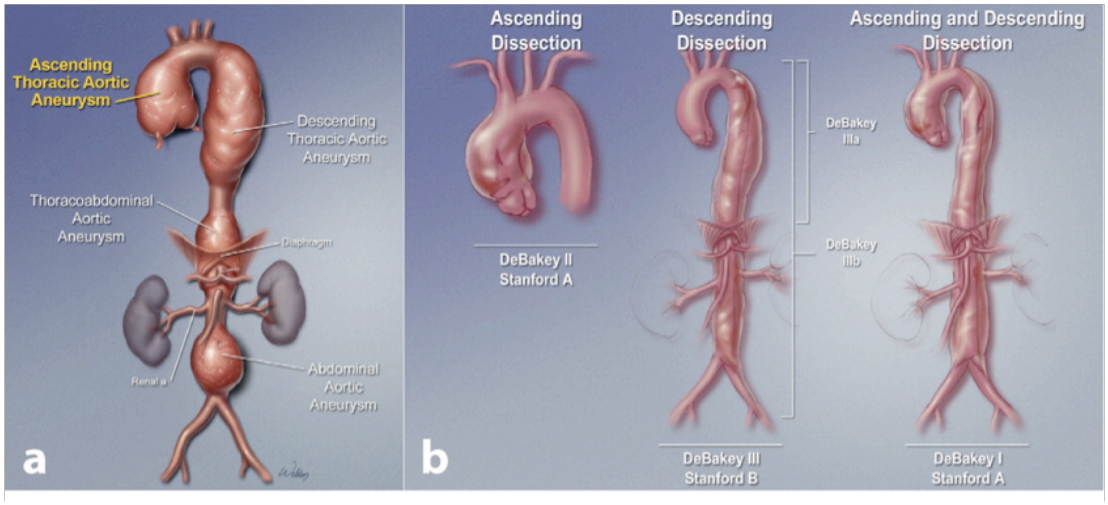

Figure 1.1: Thoracic Aortic Aneurysms and Dissections. **A.** a**.** Illustration of the locations along the aorta where aneurysms commonly occur and b. the Stanford and DeBakey aortic dissection classification systems. Republished with permission of Annual Reviews, from [Genetic basis of thoracic aortic aneurysms and dissections: Focus on smooth muscle cell contractile dysfunction. Milewicz, D. M., Guo, D. C., Tran-Fadulu, V., Lafont, A. L., Papke, C. L., Inamoto, S., Kwartler, C.S. & Pannu, H. 9, 2008]; permission conveyed through Copyright Clearance Center, Inc.

Symptoms of aortic dissection include, but are not limited to, sharp chest pain, which may radiate as the dissection spreads, sudden drop or, conversely, increase in blood pressure (distal dissections would cause an increase in blood pressure, while proximal dissections could lead to either an increase or a decrease), sweating, difficulty breathing, numbness of limbs, fainting and loss of consciousness (2; 5). Aortic dissections are often misdiagnosed as heart attacks because of the similarities in the clinical presentation (2; 5). Because dissections can severely compromise the aortic function and progress to complete rupture and death, they are treated as medical emergencies, requiring timely surgical intervention and repair.

The current standard of care for patients with TAAD is a repair surgery (2). The aorta can be surgically repaired either at the aneurysm stage or after a dissection is found (2;

5-6). If the aneurysm is discovered early, patients can undergo preventive surgery. However, as the disease progresses to dissection, the surgery becomes emergent, and survival rates decrease. Only about 50% of patients with acute dissections make it to the emergency room, and even fewer are diagnosed in time because of the overlap of the symptoms with other, more frequent conditions, such as myocardial infarction, heartburn, pulmonary embolism or pericarditis (2). A simple X-ray cannot rule out the possibility of a dissection; the most accurate tests for diagnosing an aortic dissection are computer tomography and transesophageal echocardiograms (2; 4). Even after a dissection is diagnosed and surgery is recommended, the survival rate remains low because a large proportion of patients who undergo the repair surgery do not survive the procedure (3). Therefore, it is imperative to identify patients at risk for a dissection before the onset of the acute event so that they can be monitored and treated in a timely manner.

Major risk factors for TAAD include hypertension, bodybuilding, and smoking/drug use (1-3; 5-7). Therefore, lifestyle adjustments and anti-hypertensive drugs such as the beta-blocker metoprolol are commonly prescribed to patients at risk of aneurysm development (1-2; 5). If patients cannot tolerate beta-blockers, they are often administered calcium channel blockers, which also help reduce blood pressure in these patients (1-2). Additional risk factor is male gender (1-5). There are genetic risk factors as well, such as syndromic mutations as in Marfan, Loeys-Dietz and vascular Ehlers-Danlos syndromes, and also congenital abnormalities such as bicuspid aortic valve (BAV). Finally, an aortic dissection can be a complication as a result of vasculitis, coronary artery bypass graft or cardiac catheterization (2-3).

Much work has been done by our lab and others to improve awareness of this condition and help identify populations, families and individuals who may be at risk of aortic aneurysms and dissections. The ultimate goal is to be able to diagnose a patient early and monitor and manage their aneurysm progression so that it cannot proceed to dissection.

Arterial Structure

The walls of all arteries are made up of three layers – the intima, media and adventitia (2; 5-6; 8). The intima is an endothelial cell monolayer that makes up the innermost portion of the aortic wall and lines the lumen of the vessel. The media is the middle layer, and it is made up of elastic fibers and smooth muscle cells arranged in concentric circles around the lumen (6; 8-9). Between the intima and the media lies an elastin layer termed "internal elastic lamina," and between the media and adventitia lies the "external elastic lamina" (8-9). The adventitia is made up of large amounts of extracellular matrix components, fibroblast cells and nerve endings (**Fig. 1.2A, top)**. The arterial wall is further held together by a network of collagens, which provides rigidity to the vessel (8).

There are two kinds of arteries found in the body – small muscular arteries and large elastic arteries. The carotid arteries are one example of muscular arteries. In these vessels, the medial layer between the internal and external elastic laminas is entirely composed of smooth muscle cells without any additional elastin (9). The aorta, on the other hand, is an example of an elastic artery. It is the largest vessel in the human body, and it carries blood directly out of the left ventricle of the heart. The aorta's media is composed of multiple single-cell-thick layers of smooth muscle cells, lying between layers of elastin fiber. Each

unit composed of a layer of SMCs between two elastin fibers is called a "lamellar unit" (**Fig. 1.2B**) (8; 10). The smooth muscle cells (SMCs) are attached to the lamellae via fibrillin 1-rich microfibrils and other extracellular matrix proteins such as fibronectin or vitronectin (6; 8). The points of contact of the microfibrils with the SMC plasma membrane are called dense plaques (or focal adhesions when the cells are grown in culture). Finally, due to its large size the aorta uniquely has its own network of vessels bringing nutrients to the adventitial fibroblasts, called the *vasa vasorum* (8).

Unlike in muscular arteries, the additional elastin in large vessel walls allows these vessels to resist pulsatile blood flow by providing elastic recoil and by aiding tensile force generation across the wall. Elastic lamellae are laid during development and remain unchanged during adulthood regardless of the accumulation of insults to the vessel wall. The number of elastic lamellae varies depending on the specific region of the vessel – for example, there are fewer lamellar units in the abdominal aorta compared to the ascending aorta (8).

Pathological examinations of dissected patient aortas consistently show three "hallmark" features of the diseased aorta: medial degeneration, loss of elastic fibers and accumulation of proteoglycans in the medial space (**Fig. 1.2A, bottom**). Medial degeneration refers to the disarray of smooth muscle cells in the medial wall. There may be regions of focal loss of SMCs present in the vessel as well, but it has not been ascertained yet whether there is a loss of smooth muscle cells with aortic disease progression or, to the contrary, a gain (5-6; 8). In patients with aortic dissections, the elastic lamellae appear fragmented, distended or may be missing. Proteoglycans, which are heavily glycosylated proteins secreted by nearby cells, accumulate in diseased aortas because they serve to fill

spaces left as a result of the matrix fragmentation and cellular disorganization (5-6; 8). Proteoglycans usually appear at the very early stages of aneurysm formation, and can serve as an early marker for disease (11).

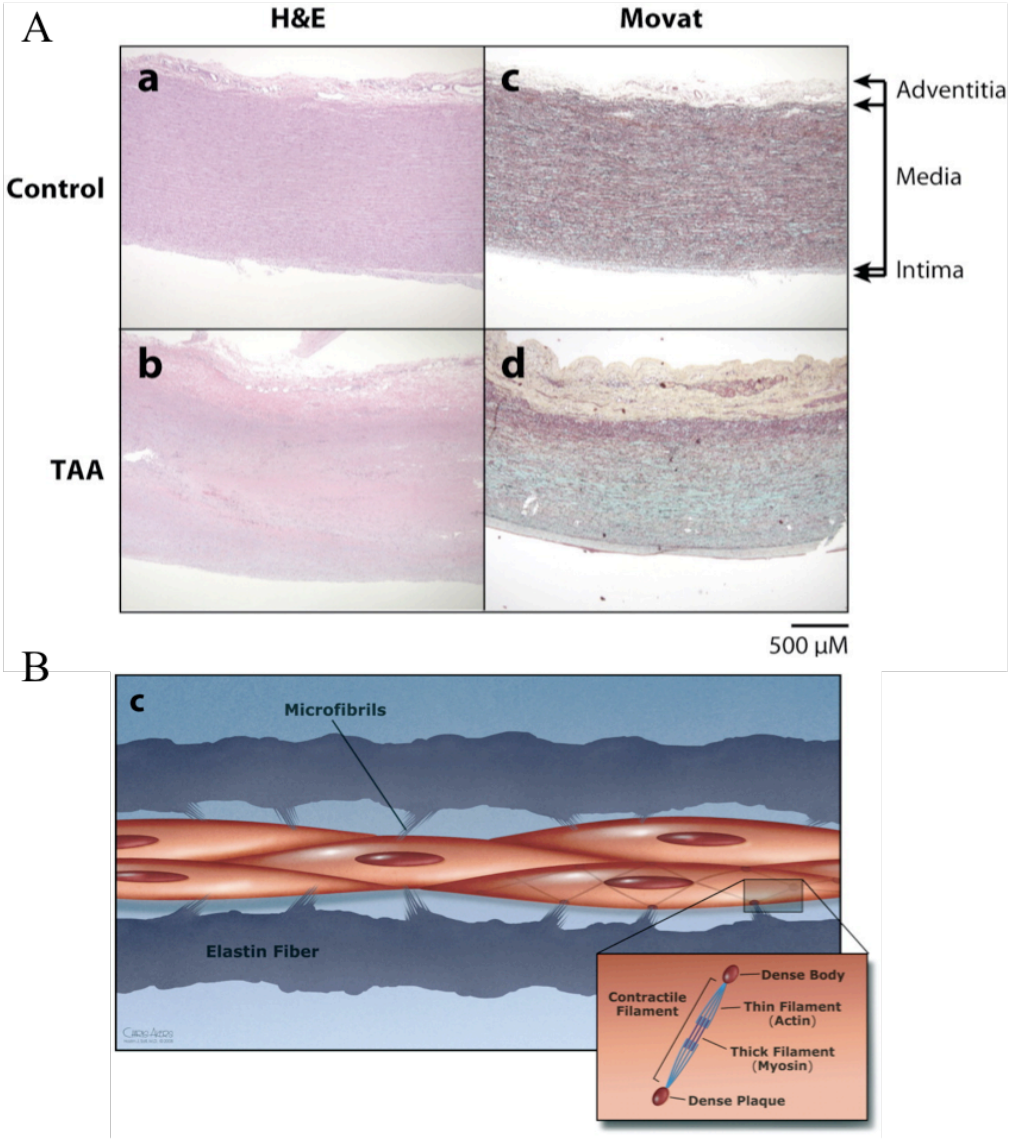

Figure 1.2: Structure and Organization of the Aorta A. Hematoxylin and Eosin staining and Movat staining of aortic tissue from control (a,c) and TAA patients (b,d) shows the three-layer organization of the aortic wall. In control patients, cells are neatly arranged in layers (a) in-between elastic fibers (c, elastin shown in black). In TAA patients, cells are disorganized (b), and there is a loss of elastin fibers and accumulation of proteoglycans (c, proteoglycans appear blue). Republished with permission of Annual Reviews, from [Genetic basis of thoracic aortic aneurysms and dissections: Focus on smooth muscle cell contractile dysfunction. Milewicz, D. M., Guo, D. C., Tran-Fadulu,

V., Lafont, A. L., Papke, C. L., Inamoto, S., Kwartler, C.S. & Pannu, H. 9, 2008]; permission conveyed through Copyright Clearance Center, Inc. **B.** Illustration of a lamellar unit, composed of elastin fibers, single layer of smooth muscle cells and microfibrils linking the cells to the fibers. Inset illustrates the smooth muscle contractile unit. Adapted with permission of Annual Reviews, from [Genetic basis of thoracic aortic aneurysms and dissections: Focus on smooth muscle cell contractile dysfunction. Milewicz, D. M., Guo, D. C., Tran-Fadulu, V., Lafont, A. L., Papke, C. L., Inamoto, S., Kwartler, C.S. & Pannu, H. 9, 2008]; permission conveyed through Copyright Clearance Center, Inc.

Finally, studies of TAAD consistently point towards an increase in matrix metalloproteinases (MMPs), which are Zn ion-dependent enzymes that cleave extracellular matrix proteins, contributing to the end-stage pathology. Recent work suggests that MMPs play a key role in the pathogenesis of TAAD, and that treatment of aortas with the non-specific MMP inhibitor doxycycline can reverse the aneurysm phenotype in rodent models of disease (7-8; 12).

Taken together, the current understanding of aneurysm pathogenesis is that accumulation of risk factors, a genetic predisposition, or both, can send stimuli to the SMCs, causing them to secrete more extracellular matrix proteins, as well as MMPs. This early change leads to a dysregulation of the extracellular matrix, cleaving of the elastic fibers and disarray of the SMCs as a result of compromised lamellar units. In the later stages there is also accumulation of macrophages in the adventitia and potentially, an increase in oxidative stress, which may cause SMC apoptosis and further increases in MMP activity. Once the aortic wall integrity is compromised and the elasticity is lost, aneurysms progress even more rapidly and ultimately proceed to dissection (6; 8).

Vascular Smooth Muscle Cells (VSMCs)

Research on TAAD has highlighted the importance of the medial layer of the aorta in disease onset and progression, with a special focus on vascular smooth muscle cells (VSMCs) because of their contractile and secretory properties, which contribute to the TAAD pathology (6).

Quiescent smooth muscle cells are spindle-shaped, and they express high levels of contractile genes and proteins. Unlike skeletal myocytes and cardiomyocytes, smooth muscle cells do not contain sarcomeres, but instead they have crisscrossing actomyosin units, each of which is structured similarly to that in other muscle, with two myosin molecules sliding along actin filaments with the aid of ATP (13). Each contractile unit is connected to the others via dense bodies within the cells or via dense plaques at the plasma membrane. Quiescent smooth muscle cells make up the medial layer of the aorta. They are able to contract in unison, together with the elastic lamellae, in response to blood flow. While the elastic lamellae are key to withstanding high stress and strain on the aorta, the smooth muscle cells are master organizers and serve to guide the contractile response and force generation in the vessel wall (6; 8; 14).

Smooth muscle cells are unique among muscle cells in that, upon stimulation from mechanical forces or a range of cytokines, they are able to switch from their quiescent phenotype to a less contractile but more migratory, secretory and proliferative phenotype (**Fig. 1.3**) (14). When smooth muscle cells receive a signal to become dedifferentiated, they undergo a switch that leads to low contractile gene and protein expression but an increase in proliferation, migration and the synthesis of collagens and other extracellular matrix

proteins. This transition is extremely important in response to vascular injury, for example, because it allows smooth muscle cells to migrate into the damage site, proliferate to produce more cells and also secrete the necessary factors and extracellular matrix proteins to help rebuild the injured area of the vessel (14-16). Dysregulation of the smooth muscle phenotypic switch contributes to a range or pathologies, such as post-angioplasty restenosis and atherosclerosis (8). In fact, work in our lab suggests that increased smooth muscle cell proliferation as a result of genetic mutations in a range of genes contributes to diverse occlusive vascular diseases, such as ischemic stroke, Moyamoya disease or fibrotic early-onset carotid artery disease (9; 17). Together, these observations have been termed "hyperplastic vasculomyopathy" (9).

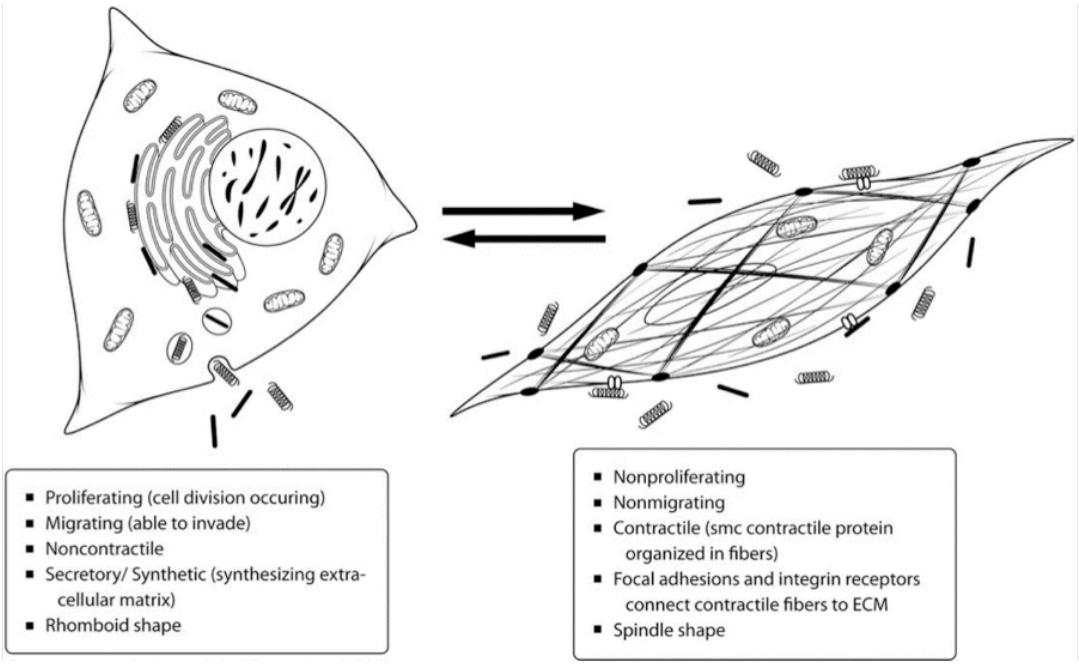

Figure 1.3: Smooth Muscle Cell Phenotypic Plasticity. Reprinted by permission from Macmillan Publishers Ltd: Genetics in Medicine, (9), copyright (2010).

SMC phenotype switching

The current paradigm in smooth muscle cell biology is that the SMC phenotype is controlled by one major signaling axis, the Serum Response Factor (SRF): Myocardin-Related Transcription Factor (MRTF) axis, which integrates mechanical and cytokine cues and directs the transcriptional changes that induce the subsequent phenotypic switch (14; 18-19). SRF is a highly promiscuous and ubiquitously expressed transcription factor, which binds one or more CArG box elements in the promoter region to activate transcription of over 200 genes (14; 19-20). SRF interacts with a range of transcriptional cofactors to confer specificity. One such family of transcription factors that is specific to cardiomyocytes and smooth muscle cells is the family of myocardin-related transcription factors (MRTFs), which includes myocardin, MRTF-A (also known as MKL1, which stands for acute megakaryoblastic leukemia factor 1/ MAL1), and MRTF-B (MKL2) (21). These three co-factors have overlapping but also distinct sets of target genes. Knockout mouse models of each of the three members of the MRTF family have been generated to help identify the differences between the three co-factors. *Myocd*$^{-/-}$ mice exhibit embryonic lethality at day 10.5, due to defects in heart development compounded by additional profound loss of SMCs in the vasculature (22). *MRTF-B*$^{-/-}$mice also die prenatally due to a defect in pharyngeal arch development; they additionally show a defect in SMC differentiation in the ascending aorta, specifically in cells of neural crest origin (19; 23-24). *MRTF-A*$^{-/-}$ mice, on the other hand, are viable but the mothers cannot nurse their young (19; 24-25).

Two of the three members of the MRTF family, MRTF-A and MRTF-B, have been found to be able to translocate from the cytoplasm to the nucleus (19; 26). In fact, this 'shuttling' of MRTF plays a key role in the regulation of contractile gene expression.

Monomeric (G) actin can bind to MRTFs in the cytoplasm, sequestering it outside of the nucleus. When MRTF is out of the nucleus, SRF is free to bind other co-factors such as ternary complex factor (TCF) or Elk-1 (19; 21; 27), and drive the expression of growth-related genes. In order for differentiation to be induced, actin polymerization triggered by the small G-protein RhoA is required; this triggers the translocation of MRTFs to the nucleus (19; 21; 26; 28-29). Once in the nucleus, MRTFs bind SRF and promote the expression of contractile and cytoskeletal markers, causing a positive feedback loop to reinforce the differentiation signal. Importantly, while myocardin also binds SRF and drives contractile gene expression, it is constitutively nuclear (26; 30) and does not respond to Rho-activated actin polymerization (30), but is regulated by the ubiquitin proteasome system (31).

Regulation of actin polymerization

There are six types of actin in the human body, and four of those are found in smooth muscle cells, which together make up approximately 40% of total smooth muscle protein: smooth-muscle specific α-actin, cytoskeletal β-actin, and both smooth-muscle specific and non-muscle γ-actin, all of which share over 95% homology (32). Smooth muscle-specific α-actin the most abundant of all forms – approximately two thirds of all actin in SMCs is α-actin, compared to β-actin (21%) and γ-actin (12%), and it localizes with myosin in the smooth muscle contractile units (32, 33). Cytoskeletal filaments, on the other hand, are predominantly composed of γ-actin, and β-actin is most frequently cortically localized (32).

Actin polymerization plays a key role in mounting the SMC response to tension, and it involves both cytoskeletal changes and contractile filament formation (32; 34). According

to the classical understanding, actin polymerization is initiated when actin monomers bind ATP, which activates them and promotes the formation of oligomers first and then a cluster of actin molecules, or a nucleus. This nucleus of polymerization recruits more ATP-bound actin and elongation occurs. As actin is stabilized in the filament, ATP hydrolysis occurs and actin remains ADP-bound (35). A filament usually remains stable with the aid of capping and stabilizing proteins like calponin, or tropomyosin, and it is considered that the ADP-bound, older actin filaments are less stable than the younger, ATP-bound filaments (36-37). Interestingly, Kueh and colleagues (2008) suggest that that the ADP-bound form is in fact more stable because it allows for a canonical helix to form. The mature filament, however, is targeted much more frequently by cofilin, the binding of which reintroduces disorder in the helix and causes an increase in the filament shrinking rates (36).

A major regulator of actin filament formation and contractility in vascular SMCs is the small G-protein RhoA (29; 34; 38-40). Activation of RhoA can be driven by upstream signaling cues, for example by activated focal adhesion kinase (FAK) (39), angiotensin II type 1 receptor (41), or activated integrin-linked kinase (ILK) (29), which in turn are promoted by mechanical stress (29) or individual extracellular matrix components (40). RhoA regulates polymerization via induction of mDia, and p160ROCK, a Rho kinase, which activates LIM kinase (LIMK) and, in turn, cofilin, leading to actin reorganization. Further, Rho kinase inhibits the myosin light-chain phosphatase, allowing for myosin light chain phosphorylation to persist and thus increasing contractile filament crosslinking in the SMCs (29; 39). Thus, RhoA controls actin reorganization, contractility, and contractile gene expression via the SRF: MRTF axis, making it a key regulator of the SMC phenotype (19; 28).

While RhoA is important for regulating actin reorganization in differentiated vascular SMCs, other small G-proteins can also regulate actin polymerization in migratory cells, for example, where turnover of actin filaments and cytoskeletal rearrangements are rapid and transient. Such regulatory G-proteins include Rac1 and Cdc42, which, together with RhoA, are localized in the focal adhesions and activated in response to the changing composition of these adhesions (39).

Focal adhesions

Focal adhesions are the points of contact between the plasma membrane and the extracellular matrix. Clustered around integrin receptor heterodimers, focal adhesions are multi-protein complexes, which are important for both signal- and mechano-transduction in SMCs. Focal adhesions act as "sensors" for mechanical stretch, and they trigger the activation of signaling cascades involved in proliferation, migration, survival, and cytoskeletal remodeling (39; 42). Focal adhesions are not static; instead they can "mature" in response to cues from actin polymerization and myosin force generation (43-44). During focal adhesion maturation, the adhesions not only become larger and more complex, but they also change in composition (44-45). For example, Kuo *et al* (2011) showed that treating fibroblast cells with blebbistatin, which inhibited myosin motor function, caused adhesions to appear smaller (less mature) and enriched in Rac1 activators, unlike untreated cells, which had mature focal adhesions, differentially enriched in RhoA activators. Enrichment with Rac1 activators promotes proliferative signaling and prevents further focal adhesion maturation; enrichment in RhoA activators in more mature adhesions, on the other hand, promotes further actin polymerization, cytoskeletal remodeling and further focal adhesion

maturation (38; 46-47). We were able to replicate the findings by Kuo and colleagues (2011) in SMCs with a myosin mutant, which caused a decrease in myosin function: compared to wildtype SMCs, the SMCs with impaired myosin function had increased Rac1 activation, decreased RhoA activation, smaller focal adhesions and a dedifferentiated phenotype; the differentiated phenotype was restored by activating RhoA in these cells (48). Thus, focal adhesions play a key role in regulating the SMC phenotype and response to the environment by mediating interactions with the extracellular matrix and responding to actin polymerization and signaling cues within the cells.

Embryonic origins of VSMCs

Because smooth muscle cells are widely distributed in a number of organs and organ systems, they also have diverse embryonic origins. Even different segments of the aorta are populated by SMCs of distinct embryonic origins (49). For example, the aortic root is made up of secondary heart field-derived SMCs, the ascending aorta, aortic arch and the base of the left and right carotid arteries, right subclavian artery and the innominate artery are made up of neural crest cell-derived SMCs, while the descending aorta contains SMCs originating from somite cells, and the abdominal aorta is made up of mesodermally-derived cells (49). Studies of the SMC properties in the different regions of the aorta suggest that there is a differential response to common cues, such as TGF-β1: a study by Gadson *et al* (1997), for example, established that although both neural crest-derived and mesoderm-derived SMCs required TGF-β1 for contraction in a collagen gel contraction study, the response was much greater in mesoderm-derived SMCs. Furthermore, when administered at the same concentrations, TGF-β1 was able to induce proliferation in neural crest-derived SMCs but

caused growth arrest in mesoderm-derived SMCs (49; 51). Further, studies involving the translocation and grafting of different cell types in other portions of the aorta suggest that the basis of SMC phenotype and behavior depends on embryonic origin and not on environmental factors. Taken together, these findings add another layer of complexity when studying SMC function and dysregulation in disease and set a requirement for cell-lineage specific studies.

Genetic Basis of TAAD

TAAD is a clinical feature of several syndromes (Marfan syndrome, Loeys-Dietz syndrome, vascular Ehlers-Danlos syndrome); it can also be inherited in the absence of syndromic features (termed familial TAAD, or FTAAD), or can occur sporadically (termed STAAD). Syndromic cases account for 5% of all aortic dissections; familial cases are approximately 15%, and the rest are sporadic (3; 5-8; 52).

Syndromic presentation

TAAD is a common and fatal outcome for patients with Marfan syndrome (MS), Ehlers-Danlos type IV (vascular EDS, or vEDS), and Loeys-Dietz syndrome (LDS). Additional syndromes that may lead to TAAD include filamin A deficiencies, arterial toruosity syndrome (caused by mutations in the glucose transporter *GLUT10*), and bicuspid aortic valve (BAV) syndrome (3; 5; 8). Specific findings related to several of these syndromes in relation to TAAD are presented below.

Marfan syndrome is a common connective tissue disorder, which affects approximately one in 5000 newborns in the United States (53-54). Patients with Marfan syndrome present with a range of skeletal features (great height, extremely long limbs, *pectus excavatum* - sunken chest, cleft palate), as well as pulmonary, ocular and cardiovascular symptoms (53-54). Upon examination, the aortas of patients with Marfan syndrome reveal a loss of SMCs, loss of elastin, and an increase in MMPs. The causal gene defect was identified in patients with Marfan syndrome in 1991– a dominant negative mutation in *FBN1*, which codes for the extracellular matrix protein fibrillin (5-6; 8). Fibrillin is the main constituent of microfibrils, which connect the layers of elastin to the smooth muscle cell layers in the media. Fibrillin mutations lead to a defect in transforming growth factor beta (TGF-β1) signaling: TGF-β1 is normally sequestered by fibrillin in the extracellular matrix in an inactive form (6; 54). Fibrillin mutations prevent the sequestration of TGF-β1 and thus lead to enhanced TGF-β1 signaling, which affects multiple pathways in smooth muscle cells and adventitial fibroblasts. It has been proposed that dysregulated TGF-β1 signaling drives aortic aneurysm formation in MS patients (8; 55). A National Institutes of Health clinical trial is currently underway for patients with Marfan syndrome after promising results were obtained from mouse models of the disease, which showed a dramatic reversal of aneurysms when treated with losartan, an angiotensin II receptor blocker (54). While the benefits of the losartan treatment have been established in mice carrying a mutation in *Fbn1*, the exact mechanism by which an angiotensin receptor II blocker mediates TGF-β1 blockade is not yet clear (55). More recently, another FDA-approved drug, pravastatin, was also shown to reverse Marfan aneurysms to a similar extent as losartan, albeit without preserving the aortic architecture as well as losartan (56).

Loeys-Dietz syndrome is caused by mutations in the *TGFBR1/2* genes, and affects approximately 500 people worldwide, with the number increasing as knowledge about this condition, first identified in 2005, is spreading (57-58). Common features in patients with the disease include wide-set eyes, translucent and thin skin, bifid uvula, cleft palate, as well as early-onset aortic disease (1; 3; 8; 57; 59). Interestingly, patients with Loeys-Dietz syndrome, display very similar clinical features to patients with Marfan syndrome, as well as dysregulated TGF-β1 signaling in spite of the fact that the identified mutations have a predicted loss of TGF-β1 receptor function (6; 8). Experiments using losartan and pravastatin are currently underway to evaluate their potential benefit for LDS patients in addition to Marfan syndrome patients.

Finally, vascular Ehlers-Danlos syndrome (vEDS) is caused by a mutation in procollagen 3, encoded by the gene *COL3A1*, and it affects as many as 1 in 5000 people (1; 6). Patients with vEDS have thin, translucent skin and impaired wound healing, joint hypermobility and distinctive facial features, including large protruding eyes, small chin, thin lips and nose. These patients frequently present with spontaneous aortic dissections or organ rupture without prior history of aneurysms (3; 6; 8). It has been suggested that the dissections occur at focal points as a result of accumulation of environmental insults to the same site, such as hypertension or physical injury (8). In 2010, Ong *et al* reported a clinical trial conducted in France and Belgium using the β2-adrenergic receptor blocker and β1 activator celiprolol for the treatment of patients with vEDS. Use of celiprolol led to a threefold decrease in the frequency of deadly events in patients with vEDS (60).

Sporadic TAAD

A patient with sporadic TAAD is one who presents with an aortic aneurysm or dissection without prior family history and who does not carry any of the Mendelian mutations associated with syndromic or familial TAAD. Sporadic TAAD is by far the most common form of TAAD among patients. These patients are usually older, and it is believed that a combination of genetic and environmental factors, and the accumulation of insults to the aorta with time, might jointly contribute to disease. The most common environmental risk factor is hypertension, followed by smoking and obesity (6). STAAD patients are at a great risk because currently there are no proven strategies for recognizing who in the general population might carry a predisposition for developing an aortic dissection.

Our lab and others have been working to identify the genetic risk factors associated with sporadic TAAD, focusing on rare variants that are found in patient cohorts but not in controls. Rare variants are genetic events, which are not as frequent in the general population as single nucleotide polymorphisms (SNPs), but are more prevalent than Mendelian mutations. Rare variants do not necessarily segregate with disease in families, and could be found at lower frequencies among healthy individuals too; thus, rare variants might contribute to the development and predisposition to TAAD, but they are unlikely to cause disease without any additional risk factors (48; 61- 62).

So far we have identified two kinds or rare variants - copy number variations (CNVs) and missense alterations. While a number of CNVs were identified in patients with sporadic disease, they all disrupted very few and specific pathways, most frequently genes related to contraction and focal adhesions (61). One such example is a copy number variation in a region on chromosome 16p13.1, which was present in approximately 1% of

patients in the STAAD cohorts studied, but only in 0.09% of control cohorts. Interestingly, this duplication was also present in some patients with family history of the disease, though it did not segregate with disease in these families. The 16p13.1 region comprises a number of genes, but the most likely candidate for increasing the risk of dissection in sporadic TAAD patients is the variation in *MYH11*, the gene that codes for smooth-muscle myosin heavy chain, an essential component of the acto-myosin contractile apparatus in vascular smooth muscle cells (62). The pathways, which could cause smooth muscle cell dysfunction and thus greater risk for an aortic aneurysm and dissection as a result of the increased *MYH11* copy number, are currently being elucidated.

A second rare variant that we chose to characterize is a missense R247C alteration, also in *MYH11*. This alteration was enriched in TAAD cohorts, as well as cohorts of patients with occlusive vascular disease, and it was predicted that it leads to a 10-12 fold increase in the risk for a dissection in these individuals. Interestingly, a paralogous mutation in cardiac myosin, *MYH7,* R249Q, has already been characterized in cases of hypertrophic cardiomyopathy, supporting the hypothesis that the *MYH11* R247C alteration could contribute to TAAD. Indeed, a double knock-in mouse model of the R247C alteration showed decreased aortic contractility *ex vivo* and decreased ATPase activity *in vitro,* but it did not develop aortic disease. $Myh11^{R247C/R247C}$ mice also exhibited a pathologic highly proliferative response to carotid artery injury by carotid artery ligation. Further, explanted primary aortic smooth muscle cells from these mice were dedifferentiated and significantly more proliferative. These SMCs also had smaller focal adhesions and increased expression of focal adhesion kinase (FAK) and Rac1, but decreased RhoA activation. Treating the cells with the bacterial endotoxin CN03 caused RhoA to become constitutively activated, which

was able to rescue the de-differentiated phenotype of the smooth muscle cells. Therefore, although the *Myh11* R247C missense mutation did not confer an aortic disease phenotype, it appeared to increase the risk of an aortic event by affecting the smooth muscle cell phenotype and aortic contractility and the risk of an occlusive vascular event by leading to increased proliferation in response to injury *in vivo* (48).

Finally, LeMaire and colleagues (2011a) conducted a genome-wide association study of patients with STAAD, looking at common genetic variants, which may increase the risk for aortic disease, and found such (SNPs) on chromosome 15q21.1, a region that encompasses *FBN1*, the gene coding for fibrillin 1, and causes Marfan Syndrome. This finding draws yet another link between the different presentations of TAAD and suggests that lessons from the study of syndromic patients may be applicable to TAAD patients at large, and that extracellular matrix defects and smooth muscle contractile defects likely share similar downstream effects, resulting from the dysregulation of the smooth muscle cell phenotype.

Familial TAAD

About 15% of patients with aortic aneurysms and dissections have first-degree relatives with the condition. These patients have single gene mutations, which are dominant negative and have variable expression and decreased penetrance (3; 5- 6; 8; 52). Our lab and others have identified a number of genes that cause familial TAAD, which broadly segregate in two categories – TGF-β1-signaling pathway genes and contractile genes.

Role of impaired TGF-β1 signaling in FTAAD

Transforming growth factor beta is a potent and versatile cytokine, which has a role in development and regulates a number of different cell types in adult tissues. TGF-β1 signals through its receptors, TGFBR-1 and -2, via two pathways. The canonical TGF-β1 pathway causes the activation of regulatory Smads (Smad2 and Smad3), which dimerize and associate with Smad4 in order to translocate into the nucleus where they drive the expression of a number of genes. Non-canonical TGF-β1 signaling is independent of Smad activation, and it results in the activation of a number of different mitogen-activated protein kinases (MAPKs). In total, TGF-β1 drives a range of cellular processes, which in smooth muscle range from differentiation to proliferation, migration and survival. TGF-β1 is an autocrine and paracrine signal, and it is found in an inactive form in complex with Latency Associated Peptide (LAP) and Latent TGF-β1-Binding Protein (LTBP), which together form a Large Latent Complex (LLC) and associate with microfibrils in the extracellular matrix (8).

So far, we have identified three genes which are altered in our families and belong to the TGF-β1 pathway: *TGFBR1, TGFBR2,* and *SMAD3*. *TGFBR1/2* mutations account for approximately 1-2% of the families with inherited TAAD; these mutations lead to Loeys-Dietz syndrome in some patients, but they do not lead to syndromic presentation in the studied families (5; 64). These mutations cause early-onset aortic disease, medial disarray, loss of elastin fibers in the aortic wall and dedifferentiation of SMCs. Interestingly, these SMCs are also less proliferative than wildtype SMCs. While canonical signaling was not significantly altered, non-canonical signaling through p38 MAPK and Akt was decreased, but the exact mechanism has not been determined (64).

Mutations in *SMAD3* are responsible for about 2% of all cases of FTAAD (5; 65). Interestingly, in addition to aortic disease, some of the TAAD families carrying alterations in this gene have also had history of aneurysms in other vessels. Even though the changes occurring in the vascular SMCs of patients with *SMAD3* mutations have not yet been characterized, aortic tissue from these patients indicates an increase in *SMAD3* staining, as well as in phosphorylated *SMAD2*. These observations were not consistent with data from *Smad3*$^{-/-}$ fibroblasts, which point towards a dedifferentiated phenotype, with cells expressing low levels of downstream canonical TGF-β1 targets, such as connective tissue growth factor (CTGF) and collagens (65). While the reason for the discrepancy has not been clarified yet, it highlights the level of complexity that is added when interactions with other cell types and the extracellular matrix are taken into consideration.

Role of contractile gene mutations in FTAAD

So far mutations in three contractile genes have been identified in families with FTAAD - *MLCK*, *MYH11* and *ACTA2*, which together account for approximately 13% of all cases of FTAAD.

MLCK (also known as *MYLK*) is the gene for myosin light-chain kinase, a serine/threonine kinase, which is responsible for the phosphorylation of myosin regulatory light chain at Ser19 and the activation of the smooth muscle-specific, as well as nonmuscle, myosin motors for acto-myosin contraction. Two mutations have been identified in families with TAAD, indicating that *MLCK* mutations are responsible for approximately 1% of FTAAD cases. Interestingly, patients with mutations in *MLCK* develop acute aortic dissections without developing aortic aneurysms first (66).

Mutations in *MYH11* are responsible for approximately 1-2% of FTAAD and are consistently identified in conjunction with patent ductus arteriosus (PDA) (67-69). These mutations cause medial degeneration, SMC disarray as well as focal SMC hyperplasia, loss of elastic fibers, accumulation of proteoglycans (67-69). Interestingly, Pannu *et al* (2007) also reported an increased vascularization in the aortic wall, with the vasa vasorum penetrating as far as the medial layer, as well as occlusions of the vasa vasorum itself, which stained positively for SM alpha-actin, indicating that the occluding cells were smooth muscle-like. Finally, in addition to predisposing to TAAD, *MYH11* mutations were found to segregate with occlusive vascular disease in the families reported by Pannu *et al* (2007), indicating a contribution to occlusive pathology in addition to aneurysm formation.

The most commonly mutated gene in families with TAAD is *ACTA2,* which codes for smooth muscle-specific α-actin (70). It is altered in approximately 10% of all families with history of TAAD. Many mutations have been identified in α-actin to date, which are all predicted to have a dominant negative effect (17; 69-76). Recently, a *de novo* and extremely severe *ACTA2 R179H/L* mutation was identified, which predisposes to multi-system SMC dysfunction (72).

Similar to *MYH11* mutations*, ACTA2* mutations also lead to focal hyperplasia and smooth muscle cells disarray in the aortic wall, coupled with loss of elastin fibers, proteoglycan accumulation and occlusion of the vasa vasorum by smooth-muscle α-actin-positive cells (**Fig.1.4A**) (70). Importantly, *ACTA2* mutations in FTAAD families also segregate with a range of occlusive vascular diseases such as livedo reticularis (vascular rash resulting from occlusions in dermal capillaries), iris flocculi (pigmentation tumors of the iris), Moyamoya disease (MMD; early-onset cerebrovascular disease, which leads to vessel

occlusion, compensatory but insufficient microvascularization at the site of occlusion and stroke), early-onset stroke and early-onset fibrotic coronary artery disease (CAD; **Fig. 1.4B**) (17; 70). Detailed analysis of family history also reveals that different mutations in *ACTA2* predispose to different but distinct sets of occlusive diseases. For example, patients with R149C mutations more frequently develop early-onset CAD, unlike patients with R258H/C mutations, who show a higher frequency of early-onset stroke (17). Therefore, despite shared aortic pathology, specific mutations can also lead to unique but equally devastating additional pathologies.

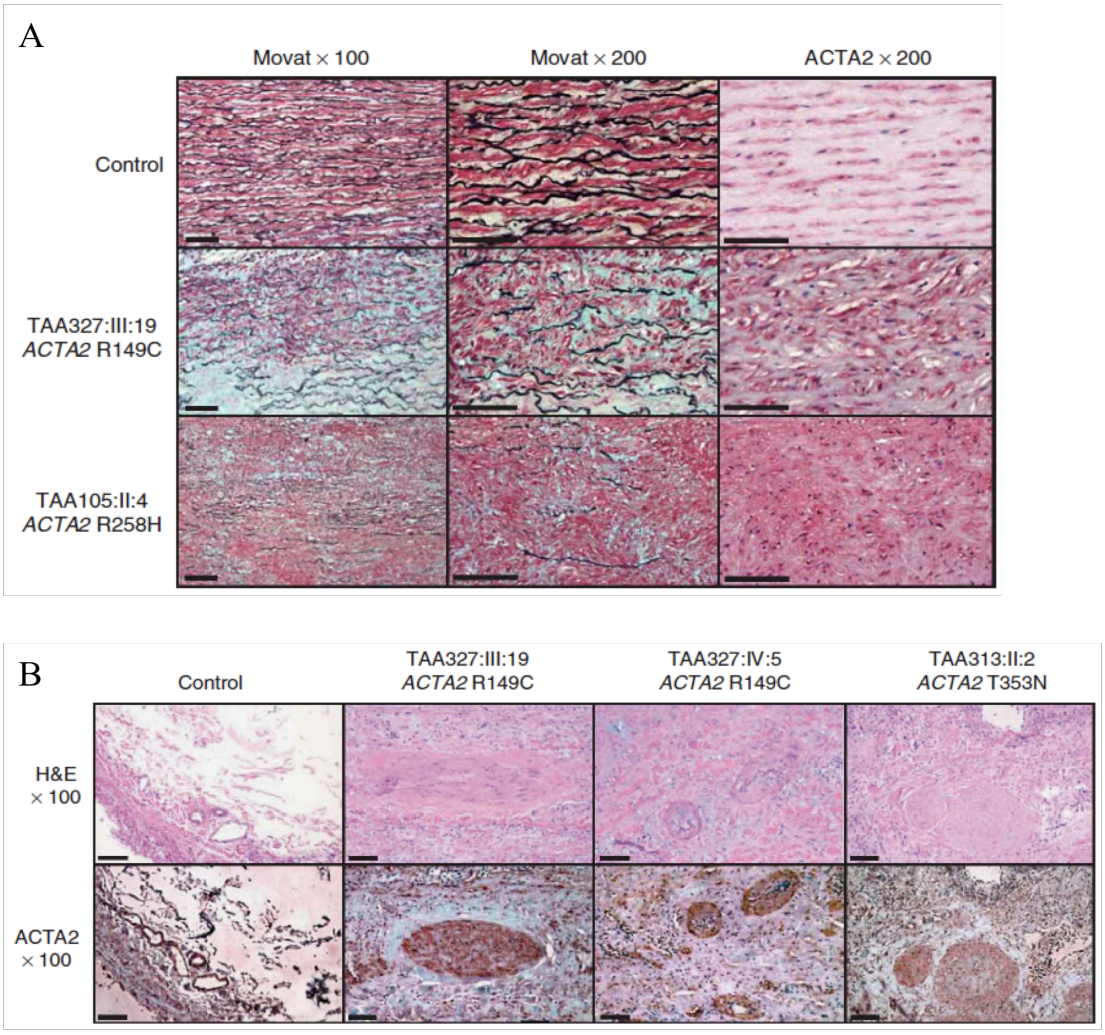

Figure 1.4: Mutations in *ACTA2* Lead to TAAD and Vascular Occlusive Diseases. A. Aortic pathology in patients with two different *ACTA2* mutations. Both show proteoglycan

accumulation (in blue), loss of elastin fibers, SMC disarray. **B**. The *vasa vasorum* of patients with *ACTA2* mutations is completely occluded (top panel) with cells that stain positive for α-actin (bottom panel), indicating these cells are smooth muscle-like. Reprinted by permission from Macmillan Publishers Ltd: Nature Genetics, (70), copyright (2007).

While the reasons for the different occlusive pathologies associated with each *ACTA2* mutation have not been determined, the cause most likely relates back to the three-dimensional α-actin structure and the specific conformational and functional defect that each mutation confers. Actin monomers consist of four subdomains, each of which plays a specific role in ATP binding, protein-protein interactions and filament formation (17; 70). Work on cardiac actin (*ACTC1*), mutations in which predispose to familial hypertrophic and dilated cardiomyopathies, indicates that mutations in subdomains 1 and 4 affect the ability of cardiac actin to interact with other proteins, while mutations in subdomain 3 affect actin filament formation (77). In smooth muscle-specific α-actin, mutations that confer a greater risk for developing premature CAD, such as R149C and R118Q, are all found in the hydrophobic cleft of the actin molecule (17; 70). The *ACTA2* R258C/H mutation, on the other hand, is found in subdomain 4 of α-actin, which plays a role in the opening and closing of the ATP binding pocket (17; 70). It has not yet been properly studied how each mutation alters the ability of smooth muscle actin to bind other molecules, such as calponin, cofilin, gelsolin or profilin, which regulate actin filament polymerization, severing or stability. Recent work by Bergeron *et al* (2011) was the first to identify specific changes resulting from different *ACTA2* mutations found in TAAD patients by studying two neighboring mutations using a *S. cerevisiae* expression system. The authors compared the N115T and R116Q mutations found in patients with TAAD, and found striking differences in nucleotide exchange rates and in sensitivity to severing proteins like cofilin, where the N115 mutation

was hyposensitive, and the R116Q mutant was hypersensitive (78). These are only two examples in a large field that is yet to be explored in more detail.

Role of *ACTA2* in TAAD Pathogenesis

Since *ACTA2* was identified as a common cause of familial TAAD, work in our lab has focused on determining the mechanisms of disease pathogenesis in patients with *ACTA2* mutations using primary aortic smooth muscle cells and dermal fibroblasts from patients, as well as mouse models.

Staining for α-actin in smooth muscle cells explanted from the aortas of patients with *ACTA2* mutations confirm a dominant negative effect of the *ACTA2* mutations on contractile filament formation. In fact, polymerization of α-actin into actin filaments is disrupted to a different extent in all mutations (**Fig. 1.5A)**. Alpha-actin polymerization was similarly disrupted in explanted patient dermal fibroblasts, which were treated for 72 hours with TGF-β1 to induce transformation into myofibroblasts and, consequently, contractile protein expression. Further, both SMCs and fibroblasts were shown to proliferate significantly more than cells obtained from age-, race- and gender-matched normal controls (**Fig. 1.5B**) (70). These observations are in agreement with the vascular pathology observed by immunohistochemistry (**Fig. 1.4**) (17; 70). Together, these findings led to the hypothesis that the effects of *ACTA2* mutations are twofold. First of all, mutations in *ACTA2* lead to decreased contractility in the aorta by disrupting the SMC contractile apparatus and, hence, mechanotransduction across the medial layer (6). In addition, *ACTA2* mutations cause a

hyperplastic compensatory response in smaller arteries, where SMCs are solely responsible for maintaining the contractility of the vessel, leading to vascular occlusive disease (9).

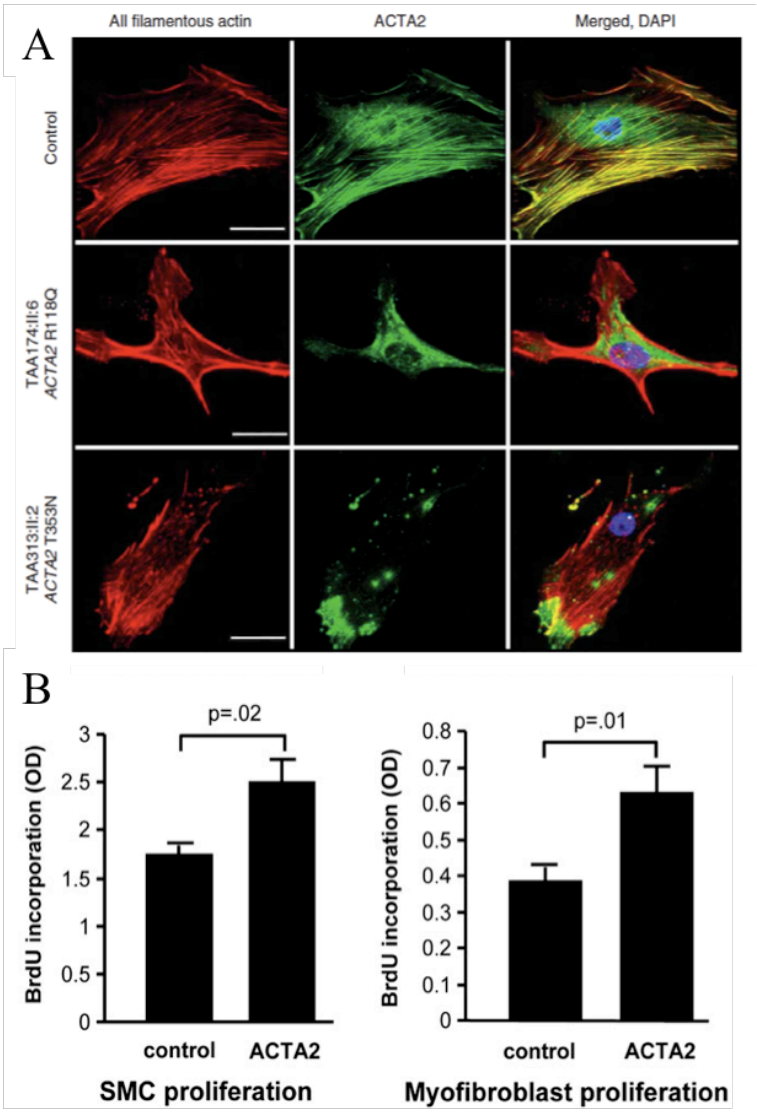

Figure 1.5: **Pathology of Cells from Patients with *ACTA2* Mutations. A.** SMCs from patients with *ACTA2* mutations have disrupted α-actin filament formation. Adapted by permission from Macmillan Publishers Ltd: Nature Genetics, (70), copyright (2007) **B.** Explanted SMCs and dermal fibroblasts from patients with *ACTA2* mutations proliferate more than control cells in culture. Reprinted from The American Journal of Human Genetics, 84, Dong-Chuan Guo, Christina L. Papke, Van Tran-Fadulu, Ellen S. Regalado, Nili Avidan, Ralph Jay Johnson, Dong H. Kim, Hariyadarshi Pannu, Marcia C. Willing, Elizabeth Sparks, Reed E. Pyeritz, Michael N. Singh, Ronald L. Dalman, James C. Grotta, Ali J. Marian, Eric A. Boerwinkle, Lorraine Q. Frazier, Scott A. LeMaire, Joseph S. Coselli, Anthony L. Estrera, Hazim J. Safi, Sudha Veeraraghavan, Donna M. Muzny, David A. Wheeler, James T. Willerson, Robert K. Yu, Sanjay S. Shete, Steven E. Scherer,

C.S. Raman, L. Maximilian Buja, and Dianna M. Milewicz, Mutations in Smooth Muscle Alpha-Actin (*ACTA2*) Cause Coronary Artery Disease, Stroke, and Moyamoya Disease, Along with Thoracic Aortic Disease, 617-627, Copyright (2009), with permission from The American Society of Human Genetics.

Characterization of the *ACTA2* R258C Mutation Using a Transgenic Mouse Model

Because only limited patient smooth muscle cells samples are available, and because dermal fibroblasts present a limited alternative system, we proceeded to study the disease phenotype caused by individual mutations by using a transgenic mouse model carrying mutations in *Acta2*.

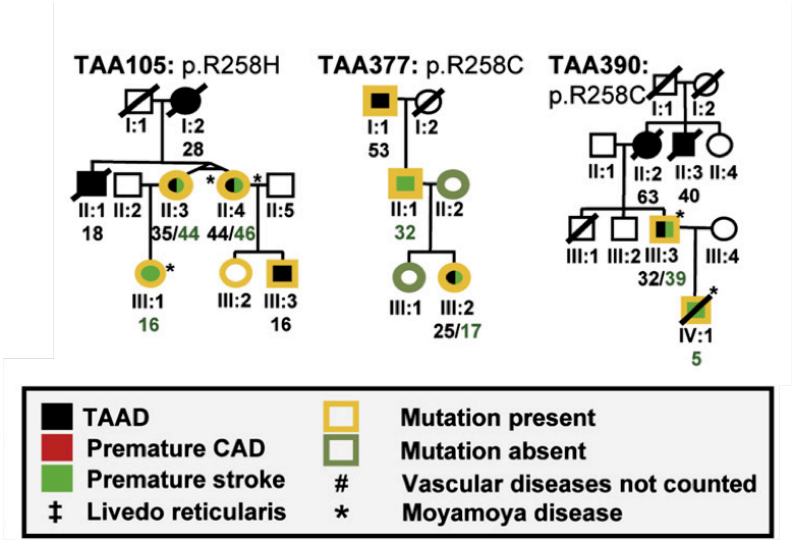

Figure 1.6: ***ACTA2* R258C Segregates with TAAD and Premature Stroke in Three Families.** Reprinted from The American Journal of Human Genetics, 84, Dong-Chuan Guo, Christina L. Papke, Van Tran-Fadulu, Ellen S. Regalado, Nili Avidan, Ralph Jay Johnson, Dong H. Kim, Hariyadarshi Pannu, Marcia C. Willing, Elizabeth Sparks, Reed E. Pyeritz, Michael N. Singh, Ronald L. Dalman, James C. Grotta, Ali J. Marian, Eric A. Boerwinkle, Lorraine Q. Frazier, Scott A. LeMaire, Joseph S. Coselli, Anthony L. Estrera, Hazim J. Safi, Sudha Veeraraghavan, Donna M. Muzny, David A. Wheeler, James T. Willerson, Robert K. Yu, Sanjay S. Shete, Steven E. Scherer, C.S. Raman, L. Maximilian Buja, and Dianna M. Milewicz, Mutations in Smooth Muscle Alpha-Actin (*ACTA2*) Cause Coronary Artery Disease, Stroke, and Moyamoya Disease, Along with Thoracic Aortic Disease, 617-627, Copyright (2009), with permission from The American Society of Human Genetics.

We chose to characterize the R258C/H mutation first. This mutation was first identified in three families, in which over 70% of the mutation carriers developed aortic disease and approximately 50% had history of early-onset ischemic strokes (starting as early as 5 years of age; **Fig. 1.6**) (17). A cDNA construct was generated using the *Acta2* gene with the R258C mutation in exon 7 and a wildtype smooth muscle *ACTA2* promoter up to intron 1, attached to the remaining construct at an AatII site. A HindIII site at the 3' UTR region containing a neomycin resistant gene was also included (**Fig. 1.7A**) (79). Using the smooth muscle α-actin-specific promoter allowed for the transgene to be expressed together with wildtype actin exclusively in cells that express this actin isoform. In addition, a second, independent transgenic line was generated to verify that the observed phenotype was not due to a disruption at the site of transgene insertion but by the transgene itself (**Appendix 1 & 2**). Further, mutant α-actin expression was confirmed by quantitative real-time PCR and by isoelectric focusing (IEF) blot using aortic tissue protein (**Fig. 1.7B**), which was able to resolve the mutant from wildtype protein.

Next, the mice carrying the transgene on a wildtype background were bred with $Acta2^{-/-}$ mice so that in two generations, three different genotypes were obtained: $Acta2^{+/+\ R258C\ TG}$, $Acta2^{+/-\ R258C\ TG}$ and $Acta2^{-/-\ R258C\ TG}$ (**Fig. 1.7C**) (81). Aortic tissue protein was then isolated from the $Acta2^{-/-\ R258C\ TG}$ mice and immunoblotted for SM α-actin in order to show that the mutant protein is expressed (**Fig. 1.7D**). Thus, three different mouse models were developed with a transgene under a wildtype promoter so that mutant actin expression is tissue-specific and occurring simultaneously with the wildtype expression, and the mutant protein expression was confirmed by qPCR, immunoblot, and IEF blot.

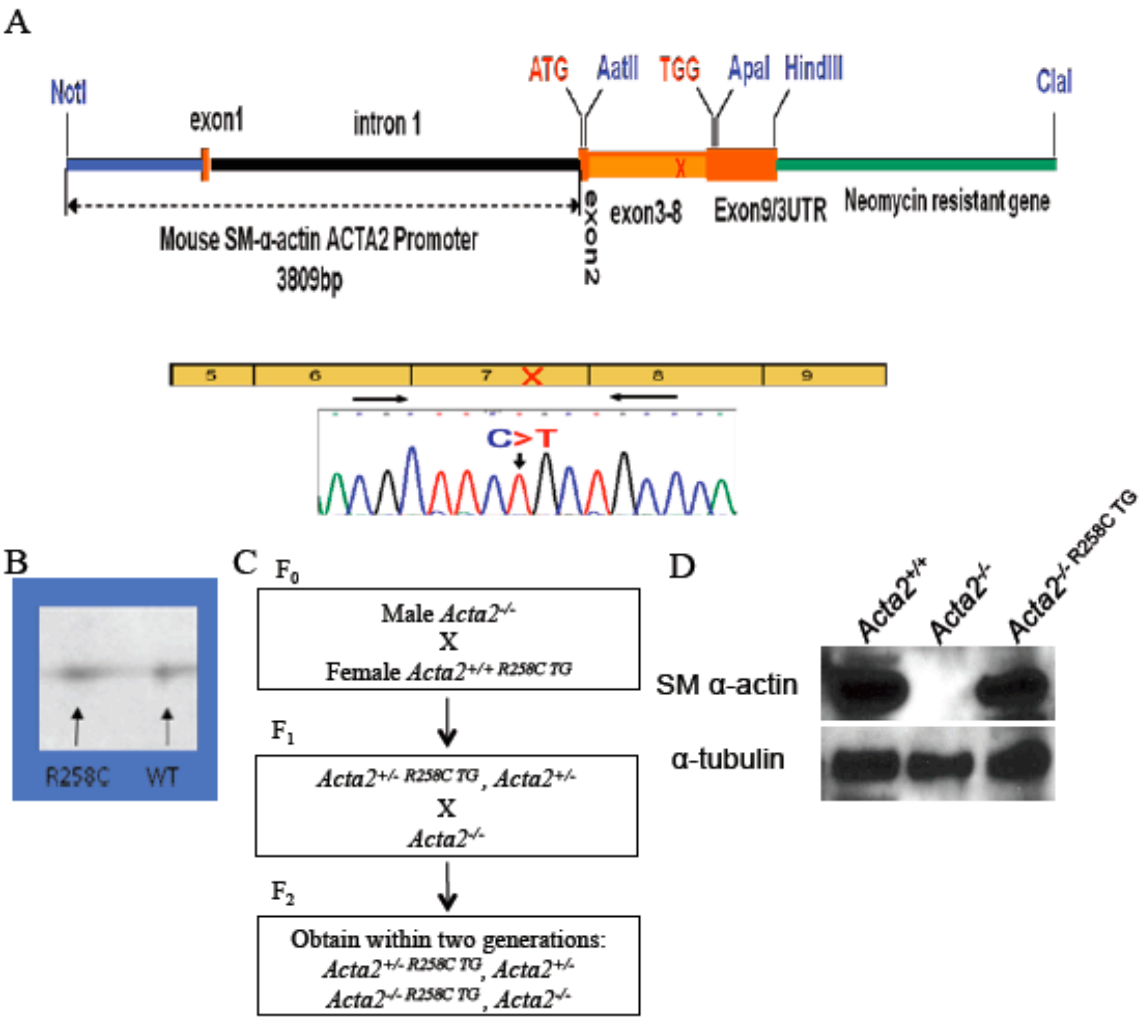

Figure 1.7: Generation of the *Acta2* $^{R258C\ TG}$ mice. A. Construct design for mutant transgene, containing a wildtype α-actin promoter up to intron 1. From J. Cao, MD, PhD (79), with permission **B.** IEF blot confirming mutant α-actin expression in the aorta. From A. Chang, PhD (80), with permission **C.** Breeding scheme for generating *Acta2*$^{+/-\ R258C\ TG}$ and *Acta2*$^{+/-}$ mice. From C. Villamizar (81), with permission. **D.** Immunoblot showing α-actin expression in aortic tissue from *Acta2*$^{-/-\ R258C\ TG}$ mice.

We proceeded to characterize the *Acta2*$^{+/+\ R258C\ TG}$ and the *Acta2*$^{+/-\ R258C\ TG}$ mice. We predicted that, like in TAAD patients, the *R258C* mutation will have a dominant negative effect and that this disruptive effect will have similar, if less severe, physiological manifestations in the mice as in the patients, including aneurysm formation and occlusive

disease phenotype. Further, we hypothesized that decreasing the number of wildtype alleles in our transgenic mouse models would exacerbate the phenotype.

Characterization of the *Acta2*$^{+/+\ R258C\ TG}$ and the *Acta2*$^{+/-\ R258C\ TG}$ mice has indicated that both mice develop aortic enlargements as early as 12 weeks of age, but the difference from the normal controls was significant only for the *Acta2*$^{+/-\ R258C\ TG}$ aortas (**Fig. 1.8C**) (81). The number of elastic lamellae laid at development was also significantly larger in these mice compared to the other genotypes. Interestingly, both *Acta2*$^{+/+\ R258C\ TG}$ and the *Acta2*$^{+/-\ R258C\ TG}$ mice have significantly increased cell density, which, decreases by 24 weeks of age but remains significantly greater than wildtype medial cell density (**Fig. 1.8A,B**) (81). Importantly, aortic contractility in the *Acta2*$^{+/+\ R258C\ TG}$ SMCs was significantly lower in the thoracic and ascending aortas compared to the wildtype controls (**Fig. 1.8D**) (82). This finding provides evidence towards a dominant negative effect of the mutation on the whole aorta structure and function.

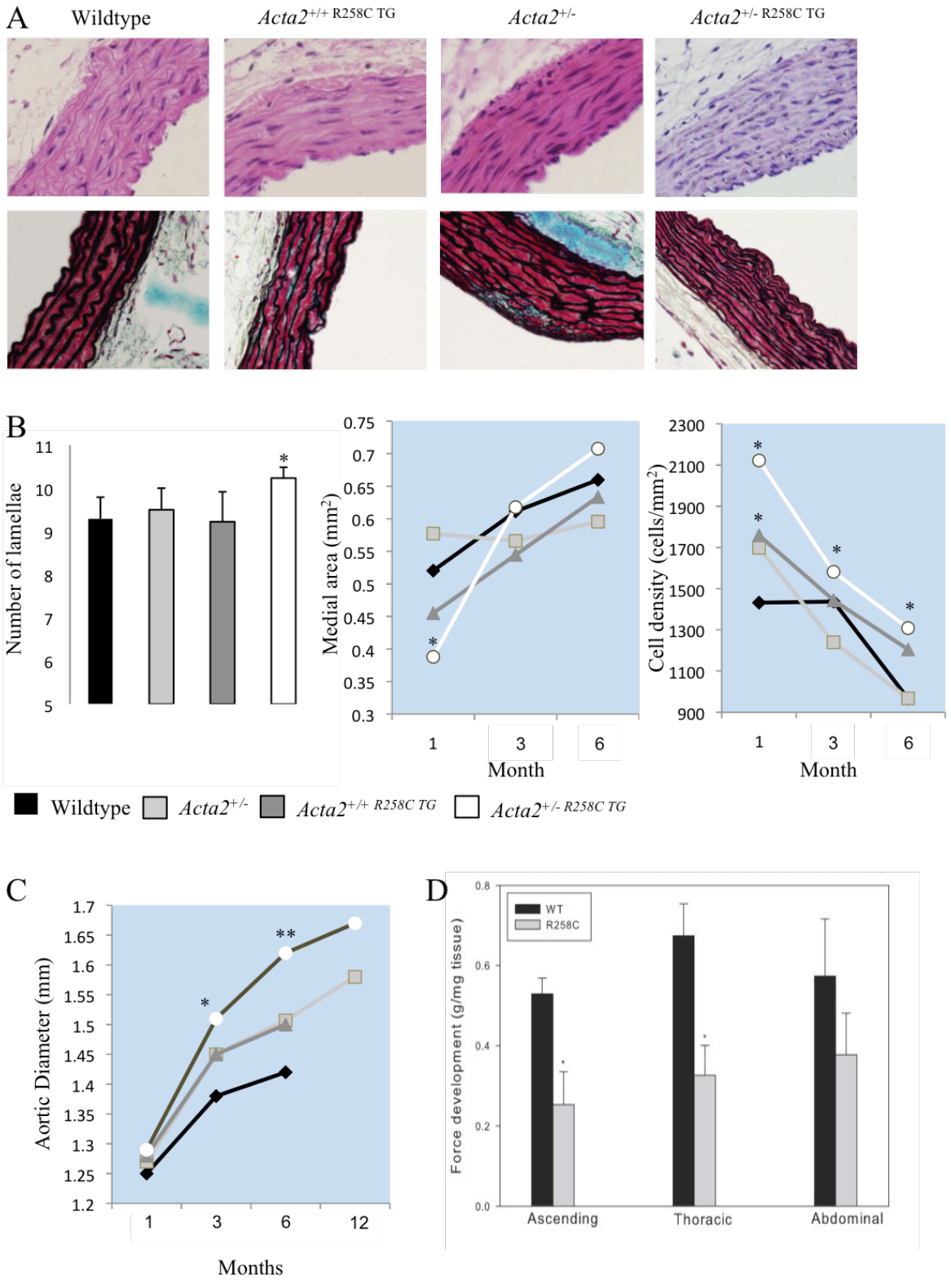

Figure 1.8. Aortic Pathology of the *Acta2*$^{+/+\ R258C\ TG}$ and *Acta2*$^{+/-\ R258C\ TG}$ Mice. A. H&E and Movat staining of aortas from wildtype, *Acta2*$^{+/+\ R258C\ TG}$, *Acta2*$^{+/-}$ and *Acta2*$^{+/-\ R258C\ TG}$

mice at 12 weeks. From C. Villamizar (81), with permission. **B.** Quantification of number of lamellae at 4 weeks, medial area and cell density from staining over 6 months. From C. Villamizar (81), with permission **C**. Aortic diameter determined by echocardiography up to 1 year of age. From C. Villamizar (81), with permission. **D.** Aortic contractility is significantly decreased in the ascending and thoracic aorta of *Acta2*$^{+/+\ R258C\ TG}$ mice. From J. Huang, PhD (82), with permission. *p<0.05, **p<0.01.

In order to assess whether the *Acta2*$^{+/+\ R258C\ TG}$ and the *Acta2*$^{+/-\ R258C\ TG}$ mice exhibited a pathologic proliferative response *in vivo*, we used a carotid artery ligation model, first described by Kumar & Lindner (1997). Briefly, the left carotid artery of mice is ligated completely proximal to the bifurcation, causing extensive aortic remodeling and neointima formation, which occludes up to 80% of the lumen in normal mice (83). Importantly, the cells that make up the neointima are smooth muscle cells that migrate from the media into the lumen and proliferate extensively. Thus, the carotid artery ligation model assesses the vascular response to injury in mice. Aortic remodeling and neointima formation are characterized and quantified when mice are sacrificed for histology 21 days later, with the right carotid artery serving as control. When we performed carotid artery ligations and quantified the neointima development 21 days post-injury, we found that the *Acta2*$^{+/-\ R258C\ TG}$ mice had significantly more neotintima formation compared to wildtype, as estimated by the area of the intima, of the media and the ratio of the media to the neointima. The *Acta2*$^{+/+\ R258C\ TG}$ mice did not have a significant pathologic response to injury (**Fig. 1.9A,B**) (81). Yet, it was in the *Acta2*$^{+/+\ R258C\ TG}$ mice that we recorded two cases of spontaneous stroke. Unfortunately, we were unable to preserve the tissue and perform a necropsy to identify the exact location of the occlusion.

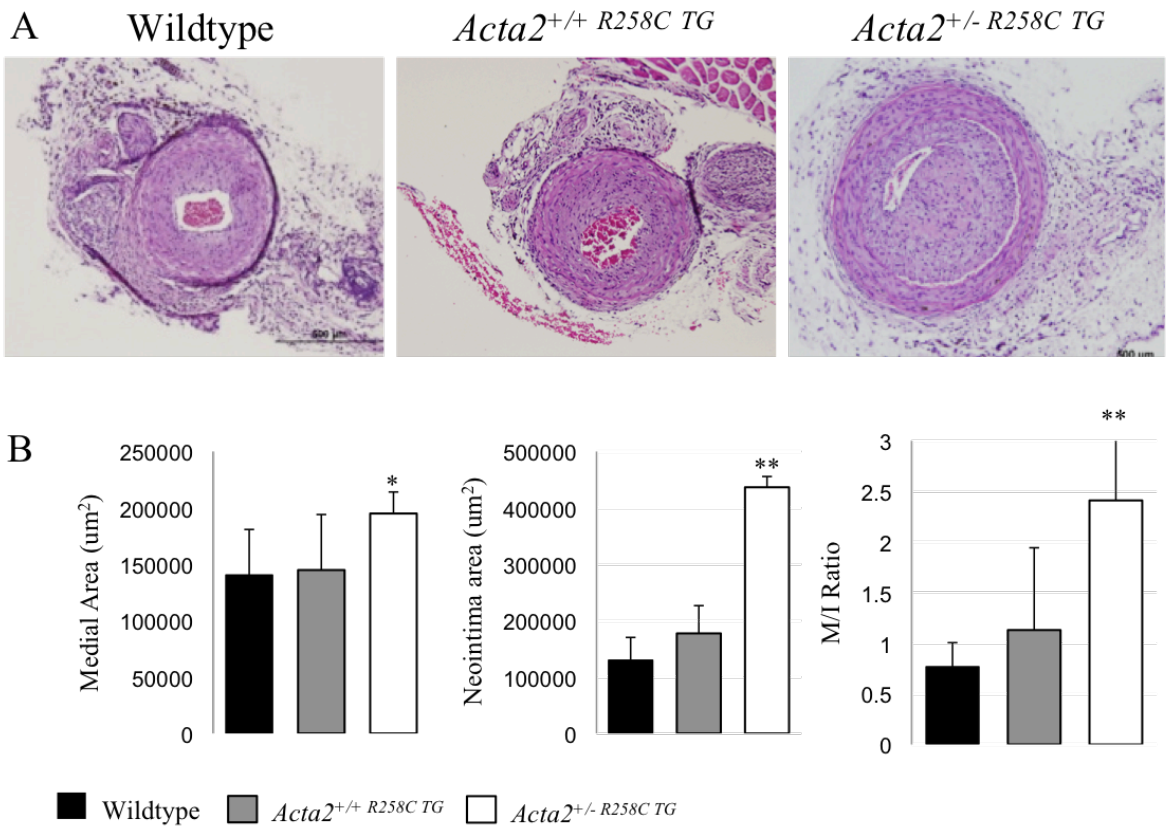

Figure 1.9: Neointima Formation Following Carotid Artery Ligation in *Acta2*$^{+/+\ R258C\ TG}$ and *Acta2*$^{+/-\ R258C\ TG}$ Mice. **A.** Carotid artery ligation lead to severe occlusions in the *Acta2*$^{+/+\ R258C\ TG}$ and *Acta2*$^{+/-\ R258C\ TG}$ mice. **B.** Medial area, neointima area and the ratio of the media to neointima are significantly increased in *Acta2*$^{+/-\ R258C\ TG}$ mice, but not in the *Acta2*$^{+/+\ R258C\ TG}$ mice. **p<0.01. From C. Villamizar (81), with permission.

To summarize, while the *Acta2*$^{+/+\ R258C\ TG}$ mice have a slight aortic dilatation, they do not develop aneurysms, nor do they show a significant hyperproliferative response as a result of vascular injury. However, they have decreased aortic contractility, increased cell density by 8 weeks and a rare occurrence of strokes. The *Acta2*$^{+/-\ R258C\ TG}$ mice do not have a recorded case of stroke so far, but they show robust aortic dilatation starting at 12 weeks of age, significantly greater number of elastic lamellae, significantly increased cell density and a significant, pathologic increase in neotintima formation after injury. This data confirms a dominant negative effect of the mutation, highlights similarities in the pathological

hallmarks in the mouse models and the human patients, as well as between the *Acta2*$^{+/+\ R258C\ TG}$ and *Acta2*$^{-/-}$ mice, and robust evidence for the increased severity of the phenotype with the loss of one wildtype *Acta2* allele.

The *in vivo* phenotype of mice with the R258C mutation posed the question whether these findings could be translated to the aortic SMCs, too. That lead us to hypothesize that introducing a mutation in α-actin will lead to (1) impaired filament formation, (2) altered focal adhesion maturation and (3) increased proliferation. Further, we predicted that the decrease in relative wildtype to mutant α-actin content would exacerbate the disease phenotype of the aortic SMCs of these mice as well.

CHAPTER TWO: Materials and Methods

Aortic SMC Isolation

Aortas were isolated from 5- to 8-week old wildtype, *Acta2*$^{+/+\ R258C\ TG}$, *Acta2*$^{+/-\ R258C\ TG}$ and *Acta2*$^{+/-}$ mice. Three explants were obtained from the *Acta2*$^{+/+R258C\ TG}$ mice, four explants from the wildtype mice, one from *Acta2*$^{+/-}$ and one from *Acta2*$^{+/-\ R258C\ TG}$; each explant was made up of 3-5 mouse ascending or descending aortas. Whole aortas were obtained under sterile conditions and transferred into biopsy media (Waymouth's basal medium, Gibco Life Technologies, Grand Island, NY) and either immediately processed or stored at 4°C. The ascending aorta was separated from the descending aorta at the start of the left subclavian artery; the two were then processed and grown separately. The adventitia was gently shaved off and the aortas were washed consecutively in 70% EtOH, sterile PBS (Gibco Life Technologies, Grand Island, NY) and aortic biopsy medium (Waymouth's basal medium). The tissue was cut into small pieces (≤0.5-1 mm diameter) and incubated for 14-18 hours at 37°C in 5 ml aortic biopsy medium with 0.5 mg collagenase type I, 0.095 mg of elastase type I and 0.125 mg of soybean trypsin inhibitor. The digestion was stopped at the end of the incubation with 2.5 ml of sterile, filtered fetal bovine serum (FBS; Atlanta Biologicals, Lawrenceville, GA) and 2.5 ml of complete SMC medium. The cells and tissues were then spun down, resuspended in complete SMC medium and left in 25 cm^2 flasks in an incubator set at 37°C and 5% CO_2.

Experiments were conducted only on cultured SMCs from the ascending aorta. Wildtype and *Acta2*$^{+/-}$ cells were used as controls. All cells were no higher than passage 5. All genotypes were passage-matched for each experiment, and each experiment was conducted between two and six times. Cells for all experiments were plated on collagen IV-

coated flasks, plates and dishes. Briefly, collagen IV (Sigma-Aldrich, St. Louis, MO) was resuspended in 0.25% sterile glacial acetic acid and left at 4°C for several hours before use. The collagen IV stock solution was then resuspended in a 1:19 ratio in sterile PBS. Dishes were coated and then left to incubate for at least 45 min before cell plating. Extra collagen IV was removed from dishes before seeding.

SMC Culture and Storage

Smooth muscle cells were grown in $25cm^2$ and $75cm^2$ cell culture flasks in incubators set at 37°C, 5% CO_2. Cells were grown in complete smooth muscle medium, which was made up of Smooth muscle Basal Medium (SmBM, Lonza, Walkersville, MD) supplemented with 20% fetal bovine serum (FBS; Atlanta Biologicals, Lawrenceville, GA), 2% HEPES (1M), 1% 100x Antibiotic-Antimycotic, 1% 200mM L-glutamine, 1% 100mM MEM sodium pyruvate (Gibco Life Technologies, Grand Island, NY), as well as growth factor aliquots: human Fibroblastic Growth Factor (hFGF-B, 1ml), insulin (0.5 ml) and human Epidermal Growth Factor (hEGF; 0.5 ml; Lonza SmGM-2 SingleQuots, Walkersville, MD). All components were first filtered through a 0.45 μm sterile filter before being added to the SmBM. Cells were detached from flasks using 0.25% trypsin (Gibco Life Technologies, Grand Island, NY) and passed when they reached 80-90% confluency.

Cells were stored in 1 ml aliquots of SMC freeze media (for 50 ml: 40 ml complete SMC media, 5 ml filtered FBS, 5 ml DMSO (Sigma-Aldrich, St. Louis, MO)) at first in -80°C freezers and then permanently in liquid nitrogen tanks.

RNA Isolation and Quantitative Real-time PCR

SMCs were seeded on collagen IV-coated dishes and left overnight to attach. They were subsequently incubated in 1% serum media (serum-starving media: 1% FBS, 2% HEPES (1M), 1% 100x Antibiotic-Antimycotic, 1% 100x L-glutamine, 1% 100x sodium pyruvate in SmBM) for 24 hours. The media was then aspirated, and cells were washed once in PBS, which was completely removed afterwards. Dishes were either placed on ice for immediate use or stored at -80°C.

For RNA isolation, 1 ml of Trizol (Invitrogen, Carlsbad, CA) was added to each dish, which was then left on ice for at least 5 min. Cells were detached with a cell lifter and moved to a centrifuge tube. Two hundred microliters of MB grade chloroform (Fisher Scientific, Pittsburgh, PA) were added to each tube. Tubes were then shaken vigorously for 15 sec and left to incubate at room temperature for 5 min. The samples were then spun down at 4°C for 20 minutes at 1,200 x *g*.

After the cells were centrifuged, the transparent top layer was transferred to a new centrifuge tube and 750 µL of 100% isopropanol (Fisher Scientific, Pittsburgh, PA) was added to each tube. Tubes were inverted 20 times and then left either overnight at -20°C or for 5 minutes at room temperature. Samples were then spun down at 4°C for 30 minutes at 16,100 x *g*. Once the spin was completed, the liquid was discarded and 750µL of 75% ethanol (EtOH, Fisher Scientific, Pittsburgh, PA) was added to each tube. The pellet at the bottom was resuspended by tapping the tube with finger several times, and spun down again at 4°C and 16,100 x *g* for 20 min. The EtOH was removed completely and the pellets were air-dried on ice for 20 min before resuspending in 50 µL of RNase-free water and

quantifying the RNA concentration at OD 260 nm using a NanoDrop (Thermo Scientific, Wilmington, DE).

The isolated RNA was then used for cDNA synthesis using High Capacity cDNA Archive Kit (Life Technologies, Carlsbad, CA) according to the manufacturer's protocol. Briefly, 5µL RNA, 5µL 10x RT buffer, 10x random primers, 2.5 µL dNTPs and 2 µL of Multiscribe RT (50U/µL), together with 30.5 µL RNase-free water were mixed and placed in a thermal cycler for 10 min at 25°C followed by 2 hrs at 37°C. We used Applied Biosystems' TaqMan probes and followed the manufacturer's protocol when we performed quantitative real-time PCR of mRNA expression using an Applied Biosystems Prism 7900 HT Sequence Detection System (Applied Biosystems, Foster City, CA). All samples were run in triplicate and standardized to *Gapdh*.

Protein Isolation

Cells were grown in 35-mm collagen IV-coated dishes at density of 75,000 cells/dish. After seeding, cells were allowed to attach overnight in complete smooth muscle medium. They were subsequently serum-starved in 1% serum medium for 24 hours, washed once in PBS and snap frozen in liquid nitrogen for the preservation of phosphorylated proteins. Dishes were then stored at -80°C until use. Protein was isolated from cells using RIPA buffer (50 mM Tris-HCl pH 7.4, 150 mM NaCl, 1% NP-40, 0.25% sodium deoxycholate, 1 mM EDTA) with 10µL/ml phosphatase inhibitor cocktails 2 and 3 (Sigma-Aldrich, St. Louis, MO), and 30µL/ml protease inhibitor cocktail (P8340; Sigma-Aldrich, St. Louis, MO). Between 50 and 100 µL of the solution were added to each dish, depending on

the dish size. Cells were scraped using cell lifters and the solution was transferred to a centrifuge tube. Samples were shaken on an orbital shaker at 4°C for 30 min and then spun down at 16,100 x *g* at 4°C for 30 minutes. Supernatant was then transferred to a clean tube and quantified using a standard Bradford assay, measuring absorption at 650 nm. Samples were stored at -20°C until further use.

Western Blot

Five to ten micrograms of protein sample was loaded onto pre-cast Tris-HCL SDS-PAGE gels (BioRad, Hercules, CA), separated by SDS PAGE, and transferred to polyvinylidene difluoride membranes (Millipore, Bedford, MA) at 35 V overnight or at 80V for 90 min. Membranes were blocked with 5% (w/v) milk in Tris Buffered Saline with Tween-20 (TBS-T), and incubated with primary antibodies at their respective concentrations (see Table 1) on a shaker for 3 hours at room temperature or on a shaker overnight in a 4°C room. Blots were washed for 10 min in TBS-T before incubating with their respective horseradish peroxidase (HRP) secondary antibodies (Jackson ImmunoResearch Laboratories, West Grove, PA) at 1:2,000 concentrations for 1 hour at room temperature. Immunoblots were then exposed using enhanced chemiluminescence (GE Healthcare, Piscataway, NJ). Primary antibodies used include anti-α-tubulin, phospho-Akt (S473), total Akt (all from Cell Signaling Technology, Beverly, MA), anti-SM myosin (Biomedical Technologies Inc, Stoughton, MA), anti smooth muscle α–actin, anti-calponin (both Sigma-Aldrich, St. Louis, MO), anti-SM22α (Abcam, Cambridge, MA), anti-GAPDH (Fitzgerald Industries, Acton, MA), phospho-FAK (Y397) (Millipore, Bedford, MA), total FAK (Santa

Cruz Biotechnology, Santa Cruz, CA), phospho-PDGFRβ (T1021, Santa Cruz Biotechnology, Santa Cruz, CA), total PDGFRβ (Cell Signaling Technology, Danvers, MA), anti-GAPDH (Fitzgerald International Industries, Acton, MA), MRTF-A (C19; Santa Cruz Biotechnology, Santa Cruz, CA), phospho-p44/42 MAPK (phospho-ERK1/2; Cell Signaling Technology, Danvers, MA) and p44/42 MAPK (ERK1/2; Cell Signaling Technology, Danvers, MA). The concentrations at which each antibody was used for Western blot and immunofluorescent staining are summarized in Table 1. Western blot results were quantified using NIH ImageJ (National Institutes of Health, Bethesda, MD).

Immunofluorescent Staining, Confocal Imaging and Analysis

Cells were seeded on collagen IV-coated, 22 mm (diameter) round coverslips at 5,000 cells/coverslip and allowed to attach overnight. They were then starved in 1% serum media for 24 hours. Cells stained for smooth muscle α-actin (Sigma-Aldrich, St. Louis, MO, 1:100), MRTF-A (H-140; Santa Cruz Biotechnology, Santa Cruz, CA, 1:50) and vinculin-FITC (Sigma-Aldrich, St. Louis, MO, 1:200) were fixed with 4% paraformaldehyde in 0.1 M phosphate buffer for 10 min at room temperature after washing twice with PBS. Cells that were used for Y397 pFAK (Millipore, Bedford, MA, 1:50) staining were fixed with an ice-cold 1:1 acetone-methanol (both from Fisher Scientific, Pittsburg, PA) solution at -20°C for 5 min after washing twice with PBS. Cells that were treated with 10ng/mL TGF-β1 were incubated for another 72 hours in fresh 1% serum medium after the initial 24 hours of serum starvation and fixed with 4% paraformaldehyde as described above. At the end of fixation, coverslips were washed three more times with PBS and stored at 4°C until use.

For staining, cells were first permeabilized for 10 min in 0.1% Triton X-100 (Fisher Scientific, Pittsburgh, PA) in PBS. Then, coverslips were inverted for 1 hour over a drop of blocking solution containing 5% donkey serum (Jackson ImmunoResearch Laboratories, West Grove, PA) in PBS. Incubation with primary antibodies at their respective concentrations was performed also by inverting the coverslips onto 50 µl drops of antibody diluted in blocking solution and leaving them at 4°C overnight. Coverslips were washed three times for 2 min each in PBS and fluorescein isothiocyanade (FITC)-conjugated secondary antibody (Jackson ImmunoResearch Laboratories, West Grove, PA) diluted in blocking solution was used for one hour at room temperature in the dark. Another three two-minute washes were performed, and, if necessary, a final 30-minute incubation in 1:40 Texas Red phalloidin (Life Technologies, Grand Island, NY) in blocking solution was performed at room temperature in the dark. After final three two-minute washes, coverslips were air-dried for 5 min and mounted using Vectashield mounting media with DAPI (Vector Laboratories, Burlingame, CA) and sealed with nail polish.

Images were taken from random fields of the coverslips using a confocal microscope (Nikon A1, Nikon Instruments, Melville, NY) at constant settings for all coverslips in an experiment. Images were analyzed using Nikon NIS Elements software. Pearson correlation coefficients for colocalization of blue (DAPI) or green (MRTF-A) were calculated for at least 20 cells per slide on at least 3 slides for each bar presented on the graph. Additionally, MRTF-A nucleus/cytoplasm ratios were calculated by measuring the mean intensity of the nuclear versus the cytoplasmic staining of cells (7 slides per genotype, 10-30 cells per slide). Calculating the relative colocalization of phalloidin and SM α-actin was done as with MRTF-A and DAPI by estimating the Pearson correlation coefficient. Focal adhesion size

was estimated by measuring at least 30 randomly selected focal adhesions for at least 3 images per slide for at least 3 slides for each bar on the graph. Measurements were performed by a blinded volunteer in order to avoid involuntary biasing of results.

SMC Proliferation Assays

Cell proliferation was measured by quantifying BrdU incorporation into the DNA of cells. SMCs were plated on 96-well plates, coated with collagen IV, seeded at 5,000 cells/well and allowed to attach overnight in complete media. The cells were then starved in 1% serum media with or without inhibitors for 24 hours. BrdU reagent was added to the wells 30 min after serum starvation/inhibitor treatment. The plates were then fixed and quantified with an ELISA assay according to the manufacturer's protocol (Millipore, Bedford, MA). The inhibitors used include PF573228 (FAK inhibitor – Tocris Bioscience, Ellisville, MO) at a 1μM concentration, 10μM Imatinib mesylate (Selleck Chemicals, Houston TX), 20 μM LY294002 (PI3K inhibitor - Cell Signaling Technology, Danvers MA), and 10 μM U0126 (MEK inhibitor – Sigma Aldrich, St. Louis, MO). Dimethyl sulfoxide (DMSO; 0.6 uL per 2.5 mL media) was used as vehicle control.

F/G Actin Assays

The ratio of polymerized to unpolymerized actin was measured using an F/G actin assay (Kit BK-037, Cytoskeleton, Denver, CO). Cells were seeded on 60 mm collagen IV – coated dishes at 200,000 cells/dish and left in complete media to attach overnight. The next

day cells were washed once in PBS and serum starved in 1% SmBM for 24 hours. At the end of the 24 hours, cells were either treated with 10ng/ml TGF-β1 for 72 hours or directly lysed for the assay according to manufacturer's protocol. Briefly, cells were lysed, collected into centrifuge tubes and sheared with a bent 26½ – gauge needle. Wildtype controls were treated either with 10μM phalloidin (positive control) or with 10μM cytochalasin D (negative control). Cells were spun down for 5 min at 376 x *g*, transferred into ultracentrifuge tubes and spun in an ultracentrifuge (Optima TLX Ultracentrifuge, Rotor TLA-110, Beckman Coulter, Brea, CA) for 1 hour at 126,000 x *g* and 37°C in a rotor that was pre-warmed to 37°C for a minimum of 1 hour. Supernatant and pellet were then separated and the pellet was resuspended in ice-cold lysis buffer with 10μM cytochalasin D or F-actin destabilization buffer and sheared with 26½ - gauge needle every 15 min for one hour on ice.

Sixteen microliters of each sample were then loaded on an SDS-PAGE gel and processed for immunoblot analysis with α-SMA (Sigma- Aldrich, St. Louis, MO).

Actin Filament Breakdown Assay

Five thousands cells were seeded on collagen IV-coated coverslips and left to attach for one hour before complete medium was added and the cells were incubated overnight. Next, cells were serum-starved for 24 hours, at the end of which they were resuspended in fresh 1% serum medium and treated with 10ng/ml TGF-β1 for 48 hours. At the end of the 48 hours, SMCs were treated with 0.5 μM Latrunculin A (Cayman Chemicals, Ann Arbor, MI) for 0hr, 5 min, 10 min, 15 min or 1 hour. Coverslips were fixed with 4% paraformaldehyde

as previously described, immunostained for smooth muscle α-actin and total actin (phalloidin) and viewed under a Confocal microscope.

RhoA/Rac1 Activation Assays

Activation of RhoA and Rac1 were measured by G-LISA assays according to manufacturer's protocol (Kits BK-124/128, Cytoskeleton, Denver, CO). Briefly, cells were seeded onto collagen-IV coated 60 mm dishes at 200,000 cells/ dish and were grown overnight in complete SmBM at 37°C. SMCs were then serum starved in 1% SmBM for 24 hours, at the end of which they were treated with or without lypophosphatidic acid (LPA; Sigma-Aldrich, St. Louis, MO) for 15 min for Rac1 activation. Cells were then washed with ice-cold PBS, lysed in 120µl of lysis buffer with protease inhibitors in a 4°C room and snap frozen after a 12 µL aliquot was taken out for protein quantification. Protein levels were quantified for each sample using 10µL of the aliquot and 300 µL of the provided Precision Red Protein Quantification Reagent at OD 600 nm. For both RhoA and Rac1 activation assays, 0.3-0.5 µg of protein were used per well in a provided reaction plate for subsequent G-LISA analysis. Reactions were performed in duplicate or triplicate.

Statistical Analysis

Student t-tests were used to compare samples from each genotype to wildtype for all experiments. P-values were considered significant (*) when $p<0.05$, highly significant (**)

at $p<0.01$ and (***) $p<0.001$. Error bars on each graph represent either the standard deviation (s.d.) or 95% confidence intervals (C.I.), as indicated in the respective legends.

Table1: Antibody Product and Dilution Information

Antibody	Company	IB	IF
Primary antibodies:			
α-tubulin	Cell Signaling Technology, Danvers, MA	1:500	---
α-smooth muscle actin	Sigma-Aldrich, St. Louis, MO	1:1,000	1:100
SM22α	Abcam, Cambridge MA	1:1,000	---
Calponin 1	Sigma-Aldrich, St. Louis, MO	1:1,000	---
SM-MHC	Biomedical Technologies Inc, Stoughton, MA	1:1,000	---
GAPDH	Fitzgerald Industries International, Acton, MA	1:20,000	---
pAKT (Ser473)	Cell Signaling Technology, Danvers, MA	1:500	---
Total AKT	Cell Signaling Technology, Danvers, MA	1:1,000	---
pFAK	Millipore, Bedford, MA	1:500	1:25
Total FAK	Santa Cruz Biotechnology, Santa Cruz, CA	1:1,000	---
pPDGFRβ	Santa Cruz Biotechnology, Santa Cruz, CA	1:500	---
Total PDGFRβ	Cell Signaling Technology, Danvers, MA	1:1,000	---
Vinculin	Sigma-Aldrich, St. Louis, MO	---	1:200
MRTF-A (H140)	Santa Cruz Biotechnology, Santa Cruz, CA	---	1:50
p42/44 MAPK	Cell Signaling Technology, Danvers, MA	1:1,000	---
Phospho-p44/42 MAPK	Cell Signaling Technology, Danvers, MA	1:500	---
MRTF-A (C19)	Santa Cruz Biotechnology, Santa Cruz, CA	1:500	---
Secondary Antibodies:			
Mouse-FITC	Jackson ImmunoResearch Laboratories, West Grove, PA	---	1:200
Rabbit-FITC	Jackson ImmunoResearch Laboratories, West Grove, PA	---	1:200
Mouse HRP	Jackson ImmunoResearch Laboratories, West Grove, PA	1:2,000	---
Rabbit HRP	Jackson ImmunoResearch Laboratories, West Grove, PA	1:2,000	---

CHAPTER THREE: Actin Filament Formation and Stability in *Acta2*$^{+/+\ R258C\ TG}$ and *Acta2*$^{+/-\ R258C\ TG}$ Mouse Aortic Smooth Muscle Cells

Introduction

In order to confirm the importance of α-actin for the normal functioning of vascular SMCs, we first characterized an *Acta2* null mouse model. This model was first described by Schildmeyer *et al* (2000), who found that the loss of α-actin did not affect the development of the vasculature in these mice but led to decreased aortic contractility, as well as decreased blood pressure. Further, these mice were described to have impaired milk ejection ability (85-86), similar to MRTF-A deficient mice (24-25). Interestingly, compensatory expression of skeletal actin was noted in the aortas of $Acta2^{-/-}$ mice (84).

Detailed study of the aortas of the $Acta2^{-/-}$ mice using echocardiography and histology established that the *Acta2* null mice develop significant aortic dilatations by 8 weeks of age (**Fig. 3.1A)**, coupled with an increase in medial thickness, which reaches significance at 1 year (**Fig. 3.1B)**. These mice have increased density of SMCs in the aortic wall at 4 weeks, which decreases as their aortic diameter progressively increases with age (**Fig. 3.1B**). Further, $Acta2^{-/-}$ mice have increased numbers of elastic lamellae in their aortas (**Fig. 3.1B)** and mild proteoglycan accumulation with age, in agreement with the mild aortic disease phenotype (87). These findings are, unsurprisingly, more pronounced but similar to our findings in the $Acta2^{+/+\ R258C\ TG}$ and $Acta2^{+/-\ R258C\ TG}$ mice.

Assessment of the levels of expression of contractile genes and proteins in explanted aortic $Acta2^{-/-}$ SMCs showed that these SMCs are highly differentiated by the classical definition of increased expression of contractile markers (**Fig.3.1C**). While there were no differences in total actin levels in the cells, there was a compensatory increase in γ-SM actin levels in these cells. Immunofluorescent staining for MRTF-A and quantification of the ratio

between the nuclear and cytoplasmic fraction indicated that MRTF-A is significantly more nuclear in *Acta2*$^{-/-}$ SMCs (**Fig. 3.1D, E**). Thus, the loss of α-actin in these SMCs leads to increase in γ-actin filaments, differential MRTF-A localization in the nucleus, expression of high levels of contractile markers and, therefore, a differentiated phenotype despite the decrease in whole aorta contractility (87). We wanted to test whether introducing the R258C mutation in α-actin conferred a similar phenotype or, on the contrary, a less differentiated phenotype as a result of filament disruption and MRTF sequestration in the cytoplasm.

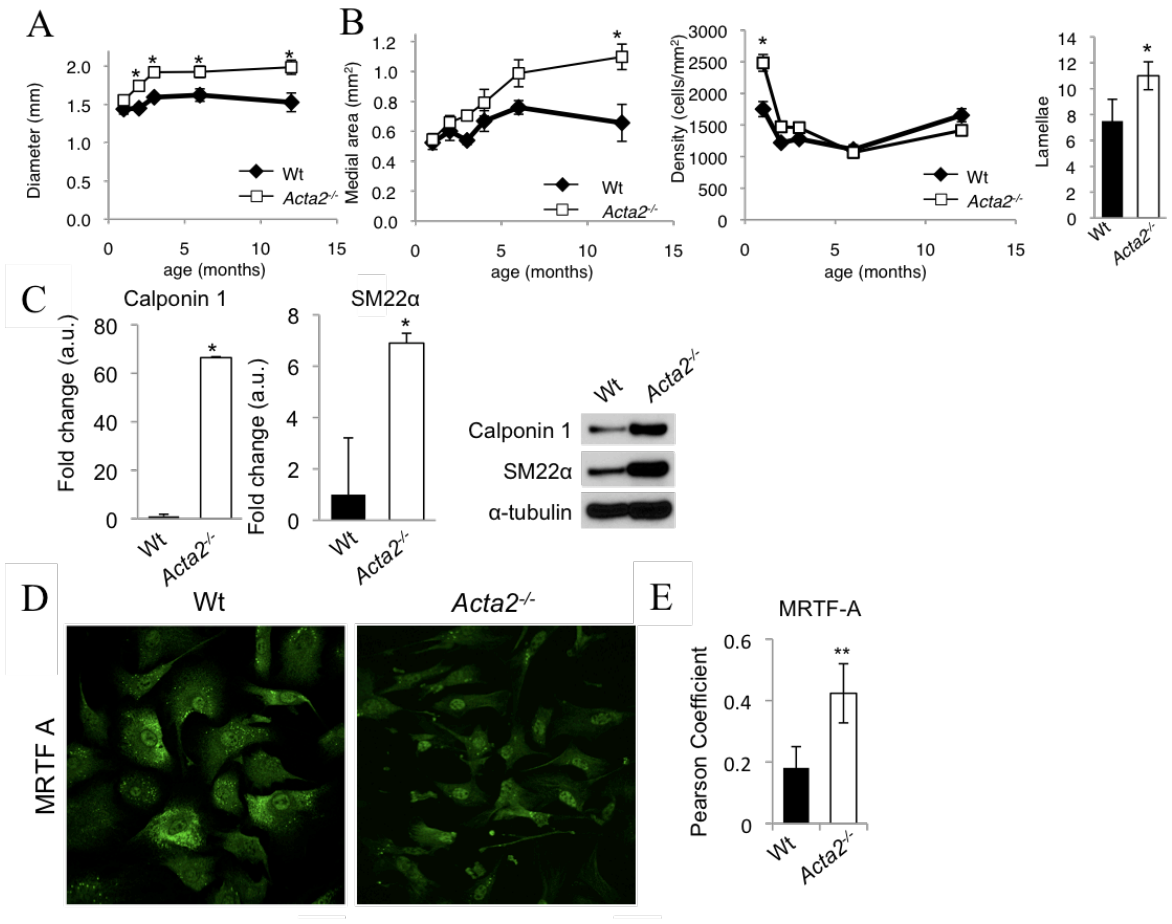

Figure 3.1: Aortic and Vascular Smooth Muscle Cell Phenotype of *Acta2*$^{-/-}$ Mice. **A.** *Acta2*$^{-/-}$ mice have significantly larger aortic diameters starting at 8 weeks. From J. Cao, MD PhD and colleagues (unpublished data) (87), with permission. **B.** Medial area in *Acta2*$^{-/-}$ mice increased with age, while cell density decreases. *Acta2*$^{-/-}$ mice have significantly more

elastic layers in their aortas. From J. Cao, MD PhD and colleagues (unpublished data) (87), with permission. **C.** SMCs from the ascending aorta of *Acta2*$^{-/-}$ mice express contractile markers at significantly greater levels compared to wildtype. **D.** MRTF-A is predominantly localized in the nucleus of *Acta2*$^{-/-}$ SMCs. **E.** Quantification shows that nuclear MRTF-A localization in *Acta2*$^{-/-}$ SMCs is significantly greater than in wildtype SMCs. *p<0.05; error bars represent ±standard error of the mean (s.e.m.) **C,D,E** from C. Papke, PhD and colleagues (unpublished data) (88), with permission.

Results

RNA from explanted aortic SMCs was used to generate cDNA for quantitative real-time PCR (**Fig. 3.2A**). All results are normalized to *Gapdh* and presented as fold change compared to wildtype (which is set to 1). Smooth muscle cells from *Acta2*$^{+/+\ R258C\ TG}$ mice show a significant increase in expression of all smooth muscle contractile genes. *Acta2*$^{+/-\ R258C\ TG}$ SMCs, on the other hand, only show a significant increase in expression of smooth muscle myosin heavy-chain (*Myh11)* and calponin 1 (*Cnn1)* genes, while *Acta2* and *SM22α*, another SMC-specific contractile marker, levels are unchanged. *Acta2*$^{+/-}$ SMCs show no significant difference in gene expression compared to wildtype SMCs for any of the contractile markers. These SMCs also exhibited a lot of variability between different experimental repeats, making them a less reliable control. Thus, while *Acta2*$^{+/+\ R258C\ TG}$ SMCs showed a consistent and significant increase in contractile gene expression, *Acta2*$^{+/-\ R258C\ TG}$ SMCs only express significantly more *Cnn1* and *Myh11* mRNA and have expression similar to wildtype cells for other contractile genes. The observed increase in *Myh11* in both transgenic lines confirms that the explanted cells are in fact SMCs and not fibroblasts, as differentiated fibroblasts express most smooth muscle contractile genes at comparable levels except for *Myh11* (14).

Contractile protein levels as shown by a quantified Western blot in **Fig. 3.2B** (quantification in **Appendix 3A**) indicate that the increased contractile gene expression in *Acta2*$^{+/+\ R258C\ TG}$ SMCs is matched by a similar increase in contractile protein expression. All proteins but myosin heavy chain (SM-MHC) were expressed at higher levels compared to the wildtype, and myosin levels were unchanged. However, both *Acta2*$^{+/-}$ and *Acta2*$^{+/-\ R258C\ TG}$ SMCs express lower levels of α-actin and SM22α compared to wildtype cells. Calponin 1 was more strongly expressed in *Acta2*$^{+/-\ R258C\ TG}$ compared to wildtype cells, and SM-MHC protein levels were unchanged. *Acta2*$^{+/-}$ SMCs had comparable expression levels to the *Acta2*$^{+/-\ R258C\ TG}$ (**Appendix 3A**)

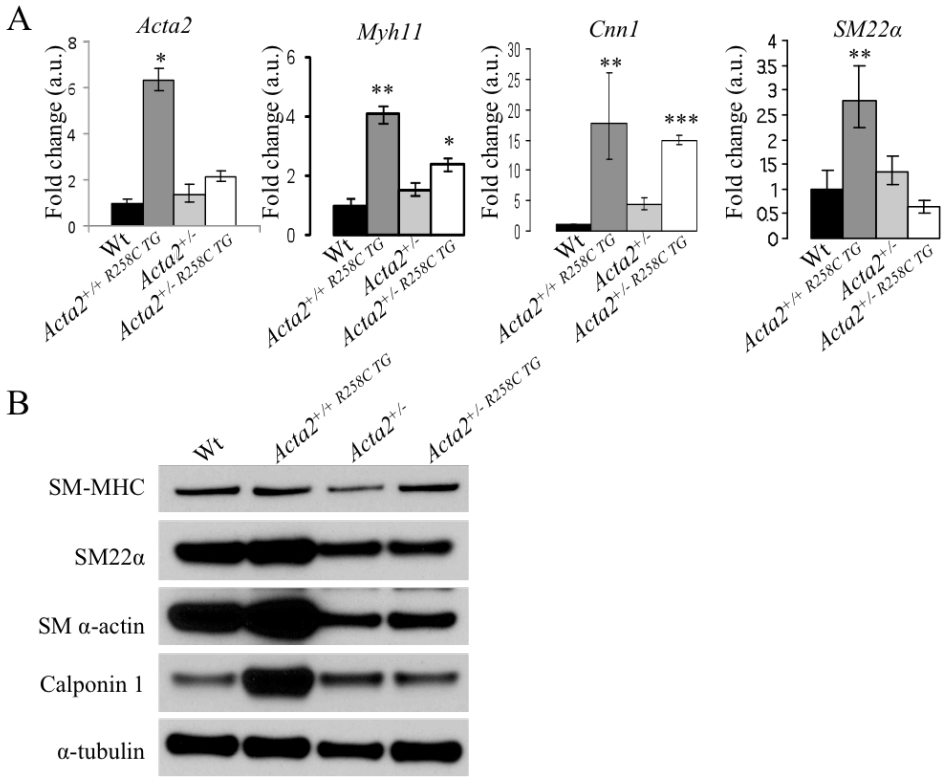

Figure 3.2: Contractile Gene and Protein Expression in Wildtype (WT), *Acta2*$^{+/+\ R258C\ TG}$, *Acta2*$^{+/-}$ and *Acta2*$^{+/-\ R258C\ TG}$ SMCs. A. Quantitative real-time PCR data for the expression of the contractile genes *Acta2, Myh11, Cnn1* and *SM22α* in all four genotypes. Wildtype is set to 1 for each assay and gene expression in the other genotypes is

presented as a fold difference from the wildtype. All results are normalized to *Gapdh.* * $p<0.05$, ** $p<0.01$. Error bars are ±standard deviation (s.d.) **B.** Contractile protein expression, as shown by Western blot. SM-MHC = smooth muscle myosin heavy chain. SM α-actin = smooth muscle-specific α-actin.

Next, we assessed whether α-actin could incorporate into actin filaments by staining smooth muscle cells with α-smooth muscle actin antibody and all filamentous actin with Texas Red phalloidin (**Fig. 3.3A**). Similar to wildtype cells, *Acta2*$^{+/+\ R258C\ TG}$ cells appeared to form proper filaments without any visible pools of unpolymerized α-actin **(Fig. 3.3A)**; there was also no significant difference in the colocalization of red and green in these cells compared to wildtype **(Fig. 3.3B)**. *Acta2*$^{+/-\ R258C\ TG}$ and *Acta2*$^{+/-}$ SMCs, however, had larger pools of unpolymerized α-actin **(Fig. 3.3A)**; hence, α-actin colocalized significantly less with phalloidin in these cells **(Fig. 3.3B)**. In order to quantitatively assess the relative amount of polymerized to unpolymerized α-actin in each cell type, we performed an F/G actin assay on SMCs that were serum-starved for 24 hours (**Fig. 3.3C)**. As expected based on the immunofluorescence results in **Fig. 3.3A**, all of the α-actin in *Acta2*$^{+/-\ R258C\ TG}$ and *Acta2*$^{+/-}$ SMCs was unpolymerized (**Fig. 3.3C, Appendix 3B**). Interestingly, the unpolymerized fraction in *Acta2*$^{+/+\ R258C}$ SMCs based on the F/G actin assay was also much larger than the polymerized (Fig. 3.3C **Appendix 3B)**, which differs from the observations by immunofluorescence and indicates a potential instability in the filaments.

In order to further assess the discrepancy in the results for *Acta2*$^{+/+\ R258C\ TG}$ SMCs' ability to form actin filaments, we performed an F/G actin assay after lysing and then treating the SMCs with phalloidin in order to stabilize the existing filaments (**Fig. 3.3D**). We predicted that performing an F/G actin assay on the pre-treated lysates would allow to better replicate the results from the immunofluorescent staining in **Fig. 3.3A**. Indeed, treating cells

with phalloidin increased the polymerized fraction in all genotypes, with a small unpolymerized fraction remaining only in *Acta2*$^{+/+\ R258C\ TG}$ SMCs, which is also the genotype with the largest amount of total α-actin, too **(Appendix 3C)**. This indicates that in all genotypes, mutant α-actin is able to incorporate in filaments, but phalloidin treatment or other stimulus is required in order for polymerization to happen. Together, the F/G actin assays indicate that at baseline, the *Acta2*$^{+/+\ R258C\ TG}$ SMCs form filaments, which, however, are more prone to breakdown as the unpolymerized actin fraction remains greater than the polymerized.

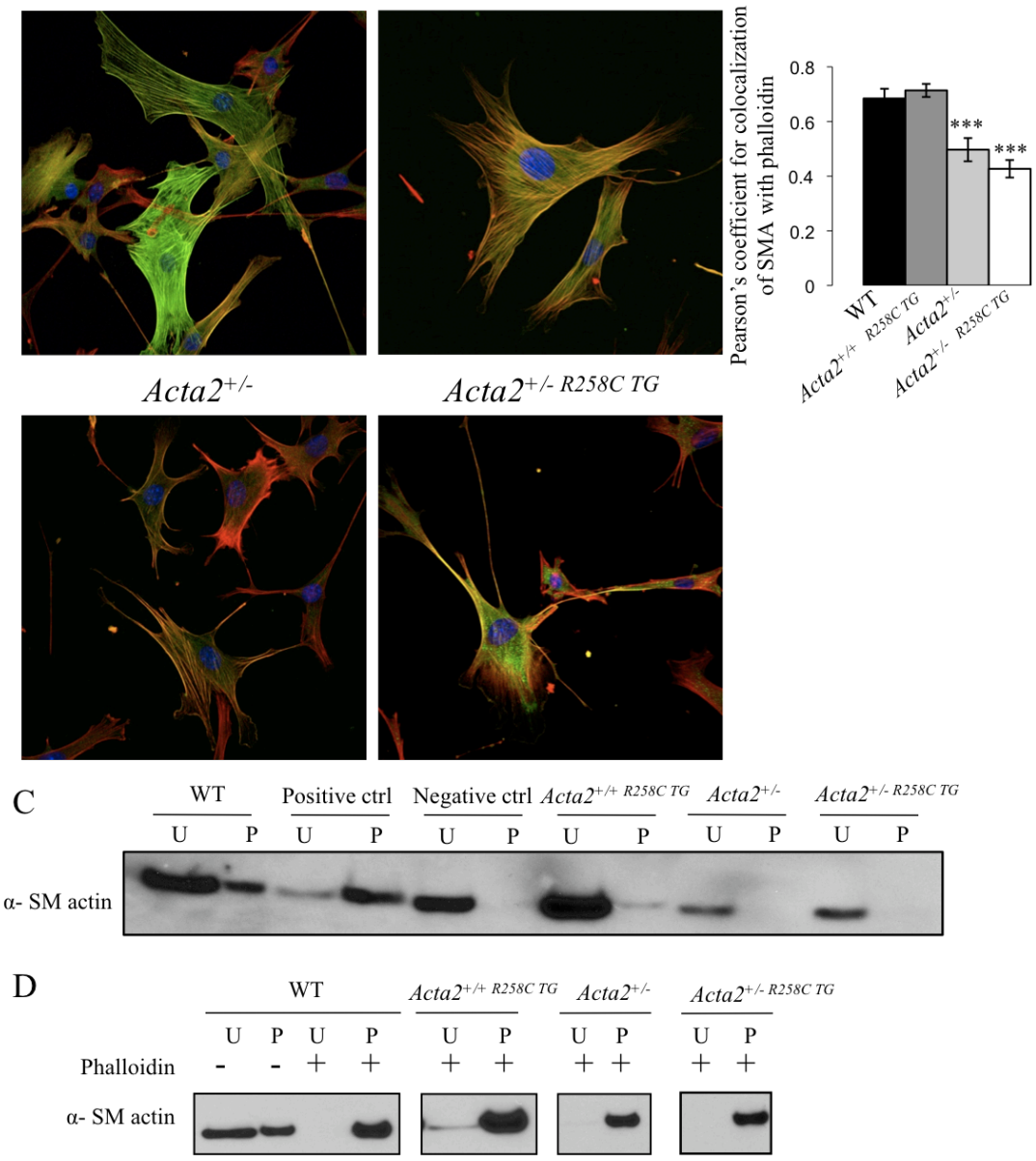

Figure 3.3: Alpha-actin Polymerization in Wildtype (WT), *Acta2*$^{+/+\ R258C\ TG}$, *Acta2*$^{+/-}$ and *Acta2*$^{+/-\ R258C\ TG}$ SMCs at Baseline. A. Immunofluorescent staining for SM α-actin (green), F-actin (phalloidin, red), and nucleus with DAPI after 24 hours of serum starvation. **B.** Quantification of the colocalization of α-SMA and phalloidin, presented by an estimate of the Pearson's correlation coefficient. Results shown are pooled from three independent experiments *** $p<0.001$. Error bars are ± 95% confidence interval (C.I.) **C.** F/G actin assay for all four genotypes. Positive control = wildtype cells after phalloidin treatment. Negative control = wildtype cells after cytochalasin D treatment. U= unpolymerized, P=polymerized. **D.** F/G actin assay for cells with or without phalloidin treatment.

Next, we treated the SMCs with TGF-β1 for 72 hours to reach a more differentiated phenotype (89) and stained for α-SMA and filamentous actin. All SMCs showed at least partial incorporation of α-actin into filaments (**Fig. 3.4A)**. *Acta2*$^{+/+\ R258C\ TG}$ SMCs appeared to incorporate all of their α-actin into filaments, although the filaments often appeared thinner, less organized and more fragile than the wildtype filaments. *Acta2*$^{+/-\ R258C\ TG}$ and *Acta2*$^{+/-}$ SMCs formed few filaments, and they also had pools of unpolymerized actin, indicating that there might be a critical amount of actin required by SMCs in order for polymerization and incorporation into filaments to occur.

When an F/G actin assay was performed on cells treated with TGF-β1 and incubated for 72 hours, we saw that while there was a polymerized fraction of α-actin for all genotypes, the unpolymerized fraction was much greater for all three non-wildtype genotypes compared to the wildtype (**Fig 3.4B, Appendix 3D)**, supporting the prediction that stability of the filaments is impaired as a result of the mutation in α-actin. Taken together, these data show that the non-wildtype SMCs are able to form filaments but require a stimulus, such as TGF-β1 or phalloidin, in order to achieve that.

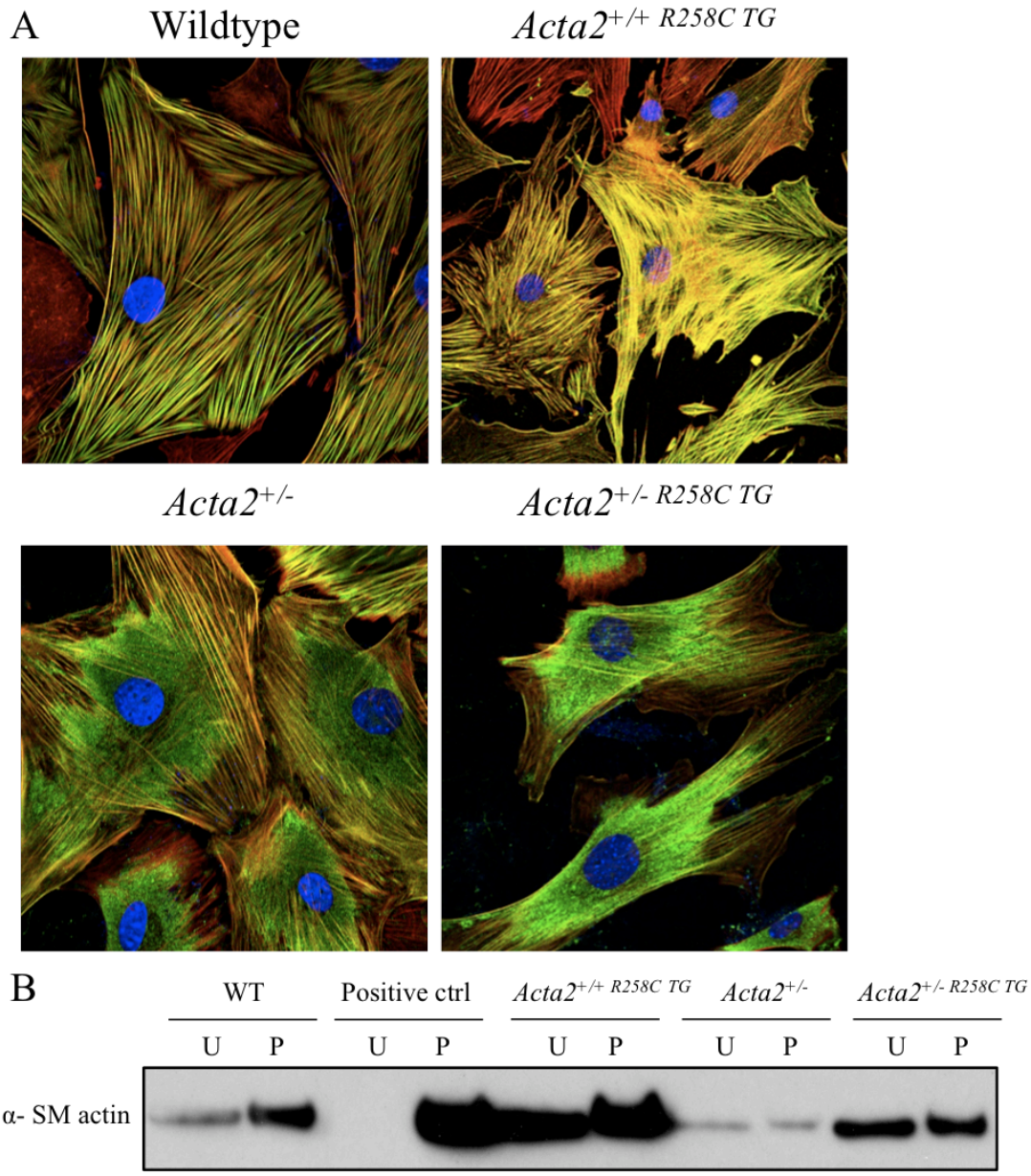

Figure 3.4: Actin Polymerization After 72 Hours of TGF-β1 Treatment. A. Immunofluorescent staining after 72 hours of TGF-β1 treatment for α-SMA (green) and total filamentous actin (phalloidin, red). Nuclei were stained with DAPI (blue). **B.** F/G actin assay after 72 hours of TGF-β1 treatment. Positive ctrl= wildtype cells treated with phalloidin. U=unpolymerized. P=polymerized

In order to test if the *Acta2*$^{+/+\ R258C\ TG}$ filaments break down more quickly than the wildtype filaments as a result of the R258C mutation, we treated coverslips with TGF-β1 for 48 hours, followed by treatment with 0.5 μM Latrunculin A for 0, 5, 10, 15 min and 1 hour.

Immunofluorescence for SM α-actin and phalloidin showed that wildtype SMC filaments have begun to fall apart by 5 min and are almost completely broken down by 15 min of treatment, and missing by 1 hour. In contrast, the *Acta2*$^{+/+\ R258C\ TG}$ SMCs appear to have still some polymerized filaments after one hour of Latrunculin A treatment, and a delayed response at all earlier timepoints (**Fig. 3.5**). As the rate of polymerization during actin treadmilling is the same as the rate of depolymerization, our findings suggest that *Acta2*$^{+/+\ R258C\ TG}$ SMCs surprisingly have less dynamic filaments compared to wildtype SMCs. This finding may be important under conditions of stress, where the ability to quickly respond and assemble new contractile filaments to withstand force across the cell is highly important.

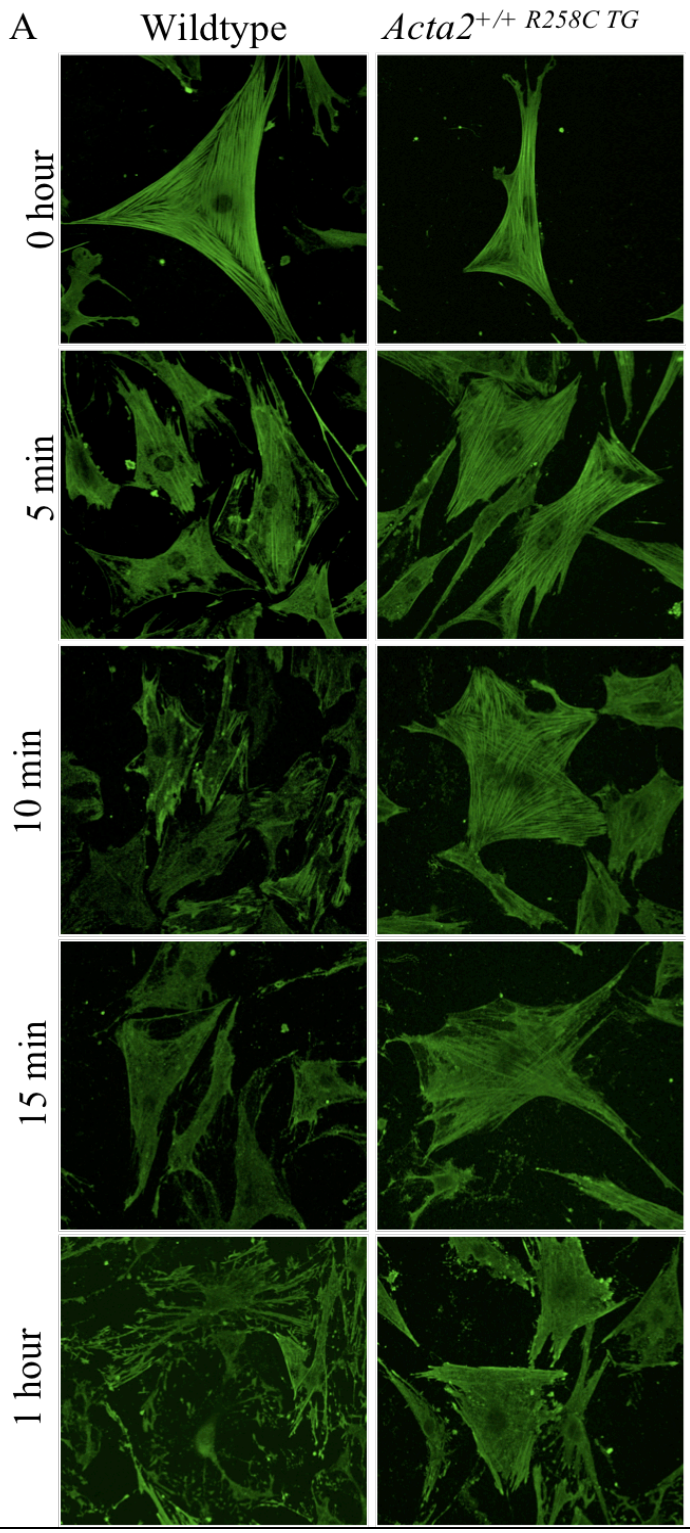

Figure 3.5: Actin Filament Breakdown After Latrunculin A Treatment. Wildtype cells show disrupted filaments as early as 5 min after treatment with 0.5 μM Latrunculin A and complete filament loss by 1 hour, while *Acta2*$^{+/+ R258C TG}$ SMCs have partial filaments even 1 hour post- treatment. Green = α-SM actin.

We next assessed the cellular localization of MRTF-A under the hypothesis that MRTF-A localization would reflect the level of contractile gene expression and the proportion of unpolymerized actin fraction observed for each genotype. Immunofluorescent staining for MRTF-A and the nucleus (with DAPI, **Fig.3.6A**) and quantification of the ratio of nuclear versus cytoplasmic MRTF-A signal using two independent methods indicated differences in the cellular localization of MRTF-A among the four genotypes **(Fig. 3.6B)**, which matched the gene expression data for these cells **(Fig. 3.2A)**. *Acta2*$^{+/+\ R258C\ TG}$ SMCs showed increased colocalization of MRTF-A with the nucleus, which matched the observed increased contractile gene expression and indicated that sufficient filament formation occured in these SMCs to allow MRTF-A translocation. *Acta2*$^{+/-\ R258C\ TG}$ SMCs showed significantly less nuclear localization of MRTF-A, in accordance with the observed large unpolymerized cytoplasmic actin fractions and the lower expression of contractile genes compared to *Acta2*$^{+/+\ R258C\ TG}$ SMCs. Finally, colocalization data for *Acta2*$^{+/-}$ SMCs indicated that, in these cells, a similar proportion of MRTF-A is found in the nucleus when compared to wildtype cells. This also matches contractile gene expression data for the heterozygous cells, which showed no significant difference in the contractile gene expression when compared to wildtype cells. Interestingly, we also found increased expression of total MRTF-A in all three non-wildtype cell lines (**Fig. 3.6C, Appendix 3E**). Finally, expression of *c-fos* was significantly increased in the *Acta2*$^{+/-\ R258C\ TG}$ SMCs, in line with increased cytoplasmic MRTF-A localization in these cells (**Fig. 3.6D**).

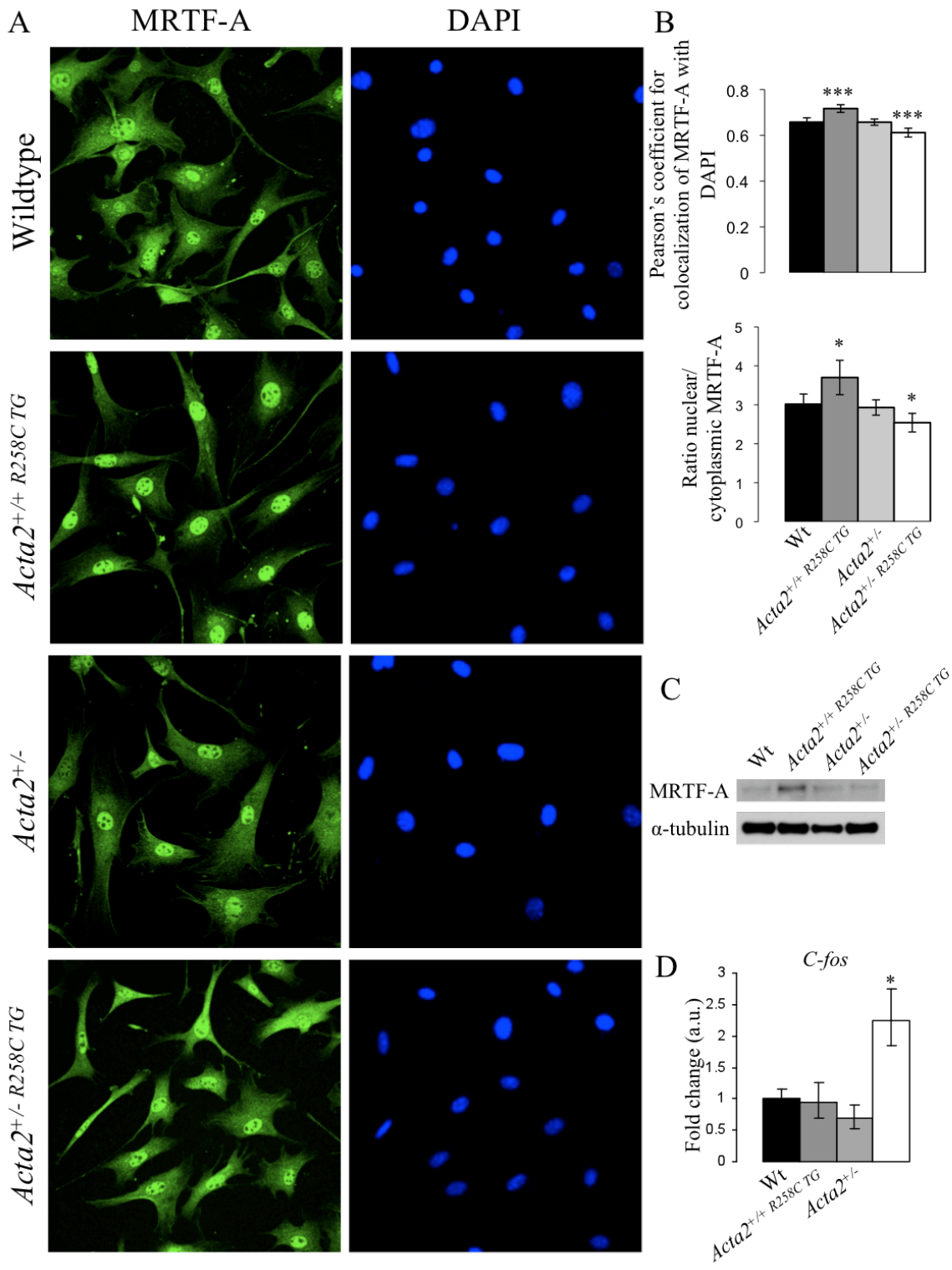

Figure 3.6: MRTF-A Localization and Expression in Wildtype (WT), *Acta2*$^{+/+\ R258C\ TG}$, *Acta2*$^{+/-}$ and *Acta2*$^{+/-\ R258C\ TG}$ SMCs A. Staining with MRTF-A (green) and DAPI (blue) reveals differential localization of MRTF-A in the four genotypes **B.** Nuclear localization of

MRTF-A, presented by the Pearson correlation coefficient for blue and green (top) and as a ratio of nuclear/cytoplasmic intensity of staining ratio (bottom) indicates significantly greater colocalization of MRTF-A with the nucleus in *Acta2*$^{+/+\ R258C\ TG}$ SMCs, and significantly less colocalization of MRTF-A with DAPI in *Acta2*$^{+/-\ R258C\ TG}$ SMCs. There is no significant difference between wildtype cells and *Acta2*$^{+/-\ R258C\ TG}$ SMCs. The results shown are pooled from three (top) or two (bottom) independent experiments. *p<0.05 ***p<0.001. Error bars± 95% C.I. **C.** MRTF-A expression in the *Acta2*$^{+/+\ R258C\ TG}$ SMCs and the *Acta2*$^{+/-}$ SMCs is increased compared to WT SMCs. **D.** *C-fos* expression is increased only in *Acta2*$^{+/-\ R258C\ TG}$ SMCs. *p<0.05. Error bars ± s.d.

So far we have been able to show that mouse smooth muscle cells expressing an *Acta2 R258C* mutant transgene in an *Acta2*$^{+/+}$ or *Acta2*$^{+/-}$ background exhibit a change in contractile gene and protein expression, actin filament stability, and MRTF-A localization. The *Acta2*$^{+/+\ R258C\ TG}$ SMCs are able to form filaments, which allows for MRTF-A to translocate to the nucleus and potentially drives the expression of contractile markers. Thus, *Acta2*$^{+/+\ R258C\ TG}$ SMCs are differentiated by the classical definition of showing increased expression of contractile markers. *Acta2*$^{+/-}$ SMCs, on the other hand, have pools of unpolymerized α-actin and limited filament formation, and even 3 days after TGF-β1 treatment, they still have only about 50% of α-actin incorporated in filaments. MRTF-A localization in the *Acta2*$^{+/-\ R258C\ TG}$ SMCs is more cytoplasmic than in wildtype cells, and together with the modest increases in contractile gene expression and the lower contractile protein expression, it points to a less differentiated phenotype due to impaired filament formation. Finally, all three non-wildtype genotypes require an external stimulus to efficiently incorporate monomeric actin into filaments, and *Acta2*$^{+/+\ R258C\ TG}$ SMCs appear to have more brittle but less dynamic filaments compared to wildtype SMCs.

CHAPTER FOUR: Focal Adhesion Alterations in *Acta2*$^{+/+\ R258C\ TG}$ and *Acta2*$^{+/-\ R258C\ TG}$ Mouse Aortic Smooth Muscle Cells

Introduction

As explained in chapter one, focal adhesions (FAs) are clusters of proteins around integrin receptors at the plasma membrane, which connect the cytoskeleton and actomyosin contractile unit to the extracellular matrix. FAs are signal- and mechanotransducers, and their maturation in fibroblasts has been shown to depend on both actin polymerization and on myosin motor function (43-44). We studied the importance of α-actin and myosin function for the maturation of focal adhesions using SMCs from a mouse model that has decreased myosin function (48), as well as in SMCs from mice lacking α-actin (88). Interestingly, we found differences in the focal adhesion alterations due to the defect in myosin motor function and the ones due to loss of α-actin.

In SMCs from the $Myh11^{R247C/R247C}$ mice, which have significantly impaired myosin function, we found that compared to wildtype SMCs, the $Myh11^{R247C/R247C}$ SMCs had smaller focal adhesions as determined by staining for vinculin and activated focal adhesion kinase (FAK), coupled with increased Rac1 activation and decreased RhoA activation. These cells were also de-differentiated; activating RhoA using the bacterial endotoxin CN03 was able to restore the differentiated phenotype. Further, increased proliferation in these SMCs was attenuated by blocking FAK (48). This study indicated the key role that focal adhesion maturity and composition plays in regulating the SMC phenotype in response to the cell's contractile unit activity.

Focal adhesion maturation was also determined in SMCs from the *α*-actin deficient mice. Analysis of focal adhesion size, number and localization using total internal reflection fluorescent (TIRF) microscopy after immunostaining revealed dramatic differences in the

size, number and localization of focal adhesions in *Acta2*$^{-/-}$ SMCs. Compared to wildtype SMCs, *Acta2*$^{-/-}$ SMCs have fewer focal adhesions, localized exclusively at the cell periphery rather than throughout the cell (**Fig. 4.1A,B**). Further, the *Acta2*$^{-/-}$ SMC focal adhesions are significantly larger in size as compared by both vinculin and pFAK staining (**Fig. 4.1B**). Finally, while RhoA activation was not changed, Rac1 was significantly more activated (**Fig. 4.1C**), consistent with less mature focal adhesions (88). Together, these data indicate that loss of α-actin leads to a major reorganization and alteration of focal adhesions in these SMCs, but that the exact changes are profoundly different compared to those in mice with a defect in myosin motor function.

Given these findings, we hypothesized that FAs will also be altered in *Acta2*$^{+/+\ R258C\ TG}$ and *Acta2*$^{+/-\ R258C\ TG}$ SMCs as a result of the impaired actin filament formation and stability.

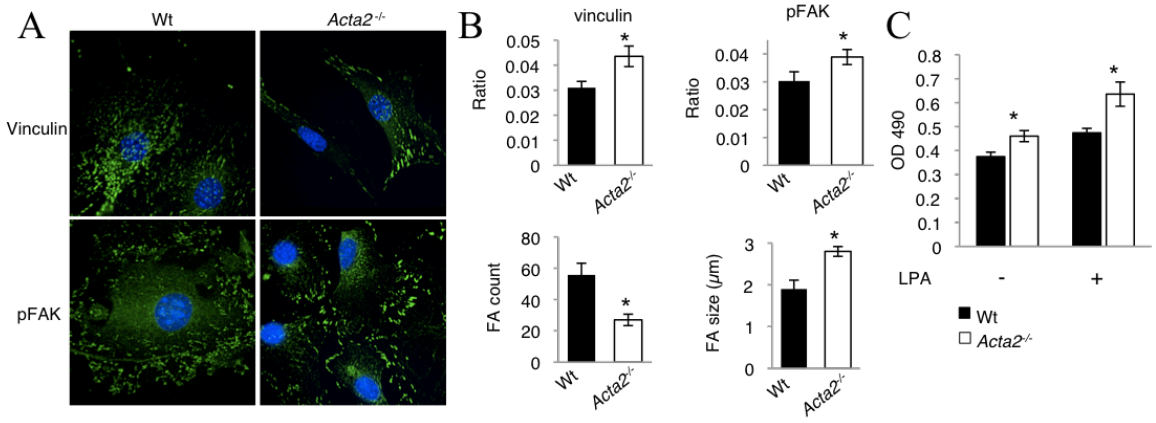

Figure 4.1: Focal Adhesion (FA) Alterations in *Acta2*$^{-/-}$ SMCs. A. Total Internal Reflection Fluorescent (TIRF) microscopy images of pFAK- and vinculin-stained wildtype and *Acta2*$^{-/-}$ SMCs. **B.** Quantification of the intensity and number of FAs in wildtype and *Acta2*$^{-/-}$ SMCs. Ratio = ratio of protein area to total cell area. **C.** Rac1 is more activated in *Acta2*$^{-/-}$ compared to wildtype SMCs; Quantified by G-LISA. *p< 0.05. Error bars ± s.d. From C. Papke, PhD and colleagues (unpublished data) (88), with permission.

Results

Smooth muscle cells from all four genotypes were first immunostained with a vinculin antibody and examined under a laser confocal microscope (**Fig. 4.2A)**. Quantification of the focal adhesion size as assessed by the vinculin staining indicated that *Acta2*$^{+/+\ R258C\ TG}$, *Acta2*$^{+/-}$ and *Acta2*$^{+/-\ R258C\ TG}$ SMCs all had significantly larger focal adhesions compared to wildtype cells. Importantly, the focal adhesions of *Acta2*$^{+/-\ R258C\ TG}$ SMCs were also significantly larger than both the *Acta2*$^{+/-}$ and the *Acta2*$^{+/+\ R258C\ TG}$ focal adhesions (**Fig. 4.2B)**. Further, compared to the wildtype SMCs, *Acta2*$^{+/+\ R258C\ TG}$ and *Acta2*$^{+/-\ R258C\ TG}$ SMCs had fewer and more peripherally localized focal adhesions, similar to the ones in the *Acta2*$^{-/-}$ SMCs.

The observed increase in focal adhesion size in non-transgenic SMCs was replicated when the focal adhesions were quantified by immunofluorescent staining for activated FAK (pFAK; **Fig. 4.2A,B).** Additionally, the differences between the *Acta2*$^{+/+\ R258C\ TG}$, *Acta2*$^{+/-}$ *and Acta2*$^{+/-\ R258C\ TG}$ SMCs were all highly significant, suggesting a very distinct pattern of FAK activation based on the genetic alteration (**Fig. 4.2A,B)**. These observations were confirmed by Western blot as well – while the *Acta2*$^{+/+\ R258C\ TG}$ had similar levels of activated FAK compared to the wildtype cells, both the *Acta2*$^{+/-}$ and the *Acta2*$^{+/-\ R258C\ TG}$ SMCs had more activated FAK (**Fig. 4.2C**). The ratio of pFAK/FAK was elevated for all non-wildtype SMCs, and consistently highest in the *Acta2*$^{+/-\ R258C\ TG}$ SMCs (**Appendix 3F**). Akt, a common downstream target of activated FAK, was significantly less activated in the *Acta2*$^{+/+\ R258C\ TG}$ and the *Acta2*$^{+/-}$ SMCs, but comparable to wildtype in *Acta2*$^{+/-\ R258C\ TG}$. A comparison of the ratios of pAkt/Akt for all four genotypes confirmed decreased Akt

activation in the non-wildtype SMCs (**Fig. 4.2D, Appendix 3F)**. These data suggest that there are differences in FAK activation, and that Akt is not the major downstream pathway activated by FAK in these SMCs.

Given that the size and arrangement of the focal adhesions in the *Acta2*$^{+/+\ R258C\ TG}$ and the *Acta2*$^{+/-\ R258C\ TG}$ SMCs resemble the ones from SMCs lacking α-actin, we tested whether the transgenic SMCs also had more Rac1 activation. Consistent with previous findings and the expectation that focal adhesions are immature, we found that in the *Acta2*$^{+/+\ R258C\ TG}$ SMCs Rac1 was significantly more activated, but RhoA remained unchanged (**Fig. 4.2D)**. Interestingly, we saw a significant decrease in the activation of Rac1 in the *Acta2*$^{+/-}$ SMCs and a similar but even more dramatic decrease in the *Acta2*$^{+/-\ R258C\ TG}$ SMCs. RhoA activation was unchanged in the *Acta2*$^{+/-}$ SMCs but significantly lower in the *Acta2*$^{+/-\ R258C\ TG}$ cells (**Fig. 4.2D)**.

Taken together, data indicate that both transgenic cells lines have alterations in their focal adhesion composition and size. *Acta2*$^{+/+\ R258C\ TG}$ SMCs have larger focal adhesions, which contain more activated FAK and greater Rac1 activation. *Acta2*$^{+/-\ R258C\ TG}$ SMCs also have significantly larger focal adhesions as quantified by vinculin and pFAK staining, as well as even higher levels of activated FAK as quantified by Western blot. However, Rac1 is *decreased* in these SMCs compared to wildtype cells, similar to *Acta2*$^{+/-}$ SMCs.

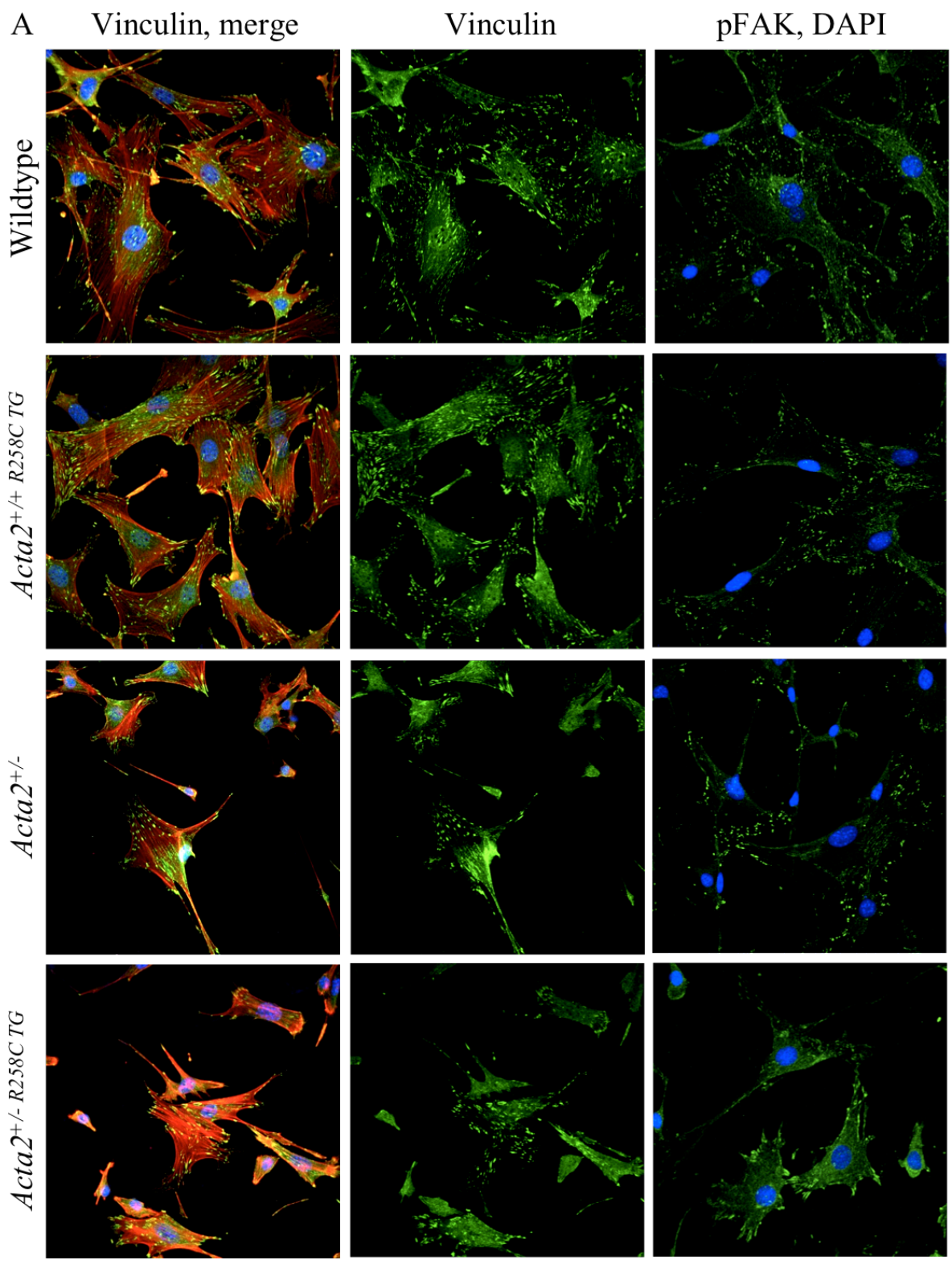
A
Vinculin, merge
Vinculin
pFAK, DAPI
Wildtype
Acta2+/+ R258C TG
Acta2+/-
Acta2+/- R258C TG

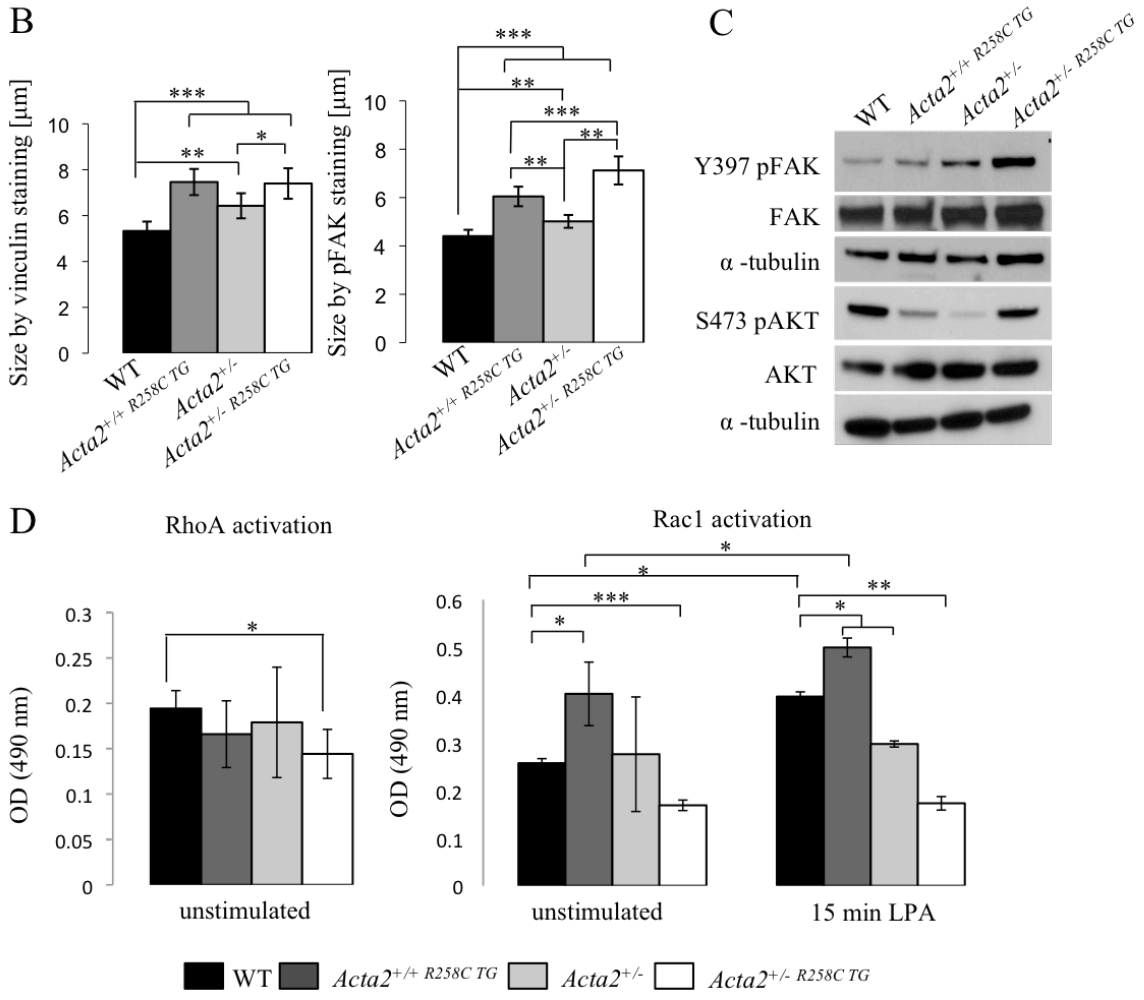

Figure 4.2: Focal Adhesions Are Altered in *Acta2*$^{+/+\ R258C\ TG}$ and *Acta2*$^{+/-\ R258C\ TG}$ SMCs. **A.** Immunofluorescent staining for vinculin (green), total filamentous actin (phalloidin, red) and nucleus (DAPI, blue), or pFAK (green) and nucleus (DAPI, blue). **B.** Quantification of focal adhesion size in *Acta2*$^{+/+\ R258C\ TG}$ and *Acta2*$^{+/-R258C\ TG}$ SMCs indicates that focal adhesions are significantly larger in these SMCs compared to the wildtype. *Acta2*$^{+/-}$ SMCs are only significantly larger than wildtype SMCs when size is determined by pFAK staining. Results are pooled from three independent experiments for vinculin and two for pFAK. *p<0.05, **p<0.01, *** p<0.001. Error bars ± 95% CI. **C.** Western blot showing increased activation of FAK in all three non-wildtype genotypes. Akt activation, however, is lower compared to the wildtype for all of them. **D.** G-LISA assays for RhoA and Rac1 activation show that there is a significant decrease in RhoA activation in *Acta2*$^{+/-\ R258C\ TG}$ SMCs but no change in the others compared to wildtype. Rac1 is significantly more activated in *Acta2*$^{+/+\ R258C\ TG}$ SMCs compared to the wildtype in unstimulated and LPA-stimulated cells, and significantly less activated in *Acta2*$^{+/-\ R258C\ TG}$ SMCs under both conditions and in *Acta2*$^{+/-}$ SMCs after LPA stimulation. RhoA activation is pooled from 3 experiments, Rac1 is a representative experiment (one of three repeats) *p<0.05, **p<0.01. ***p<0.001. Error bars ± s.d.

CHAPTER FIVE: Proliferation in *Acta2*$^{+/+\ R258C\ TG}$ and *Acta2*$^{+/-\ R258C\ TG}$ Mouse Aortic Smooth Muscle Cells

Introduction

Increased proliferation is the hallmark of dedifferentiated smooth muscle cells. Explanted SMCs and dermal fibroblast cells from patients with mutations in *ACTA2* and *MYH11* show increased proliferation (**Fig. 1.5B**) (17; 68; 70). These patients also have a high occurrence of vascular occlusive diseases in a number of smaller arteries, possibly due to increased SMC proliferation.

The proliferative, occlusive vascular pathology observed in humans is retained the *Acta2*$^{-/-}$ mice *in vivo* and in culture. Aortic SMCs explanted from the ascending aortas of the knockout mice proliferate more in culture compared to wildtype SMCs (**Fig.5.1A**). When we performed carotid artery ligations to assess the response to vascular injury in the *Acta2*$^{-/-}$ mice, we unsurprisingly found that the carotid arteries of these mice were almost completely occluded 21 days post-injury (**Fig. 5.1B,C**). The abnormal and significant increase in neointima formation confirmed a pathologic proliferative response of these SMCs *in vitro* and *in vivo* (88).

In trying to identify the mechanism by which a defect in contractile properties leads to increased proliferation, we assessed the contribution of the impaired focal adhesion maturation resulting from the loss of α-actin to increased proliferation in the *Acta2*$^{-/-}$ SMCs. Work in different types of cancer has focused on the role of FAK in proliferation (90-92), and more recently a role for FAK was established in cell proliferation in human lung epithelial cells under conditions of continuous stretch and stress (93), which bear resemblance to the conditions in the vasculature, too. Thus, we chose to determine whether the increased activation of FAK was at least in part responsible for increased proliferation,

and found that using a FAK-specific inhibitor, we were in fact fully able to block proliferation (**Fig. 5.1C, D**) (88).

In cancer, FAK has been shown to interact with growth factor receptors, and this cross-talk contributes to increased tumor proliferation (94-96). Therefore, we assessed if there is any abnormal growth factor involvement in the *Acta2*$^{-/-}$ SMCs as well. There are several growth factor receptors in SMCs that play key roles in modifying the smooth muscle cell phenotype, but the most likely candidate for driving proliferation in the *Acta2*$^{-/-}$ SMCs, the platelet-derived growth factor receptor beta (PDGFRβ), was studied. PDGFRβ is a potent activator of SMC proliferation and migration and is highly important in the development of the vasculature, as well as in response to injury when SMCs switch back to a dedifferentiated phenotype (97-99). Indeed, PDGFRβ had increased expression at the mRNA level in the *Acta2*$^{-/-}$ SMCs (**Fig. 5.1F**). There was more total PDGFRβ protein as well as more activated PDGFRβ, as assessed by phosphorylation of tyrosine 1021 in the α-actin-deficient SMCs, but the ratio of total to activated PDGFRβ was unchanged (**Fig. 5.1F**) (88). Importantly, treating the SMCs with the tyrosine kinase inhibitor imatinib mesylate, an FDA-approved cancer drug (100), was able to decrease proliferation in the *Acta2*$^{-/-}$ SMCs to wildtype levels by decreasing PDGFRβ activation (**Fig. 5.1G,H**;) (88). Imatinib treatment has been shown to be effective in treating pulmonary arterial hypertension (101-102). It has also been shown to reduce excessive neointima formation after carotid artery ligation in a neurofibromatosis mouse model, which developed occlusive vascular disease (103), and it also prevented excessive neotintima formation in *Acta2*$^{-/-}$ mice (**Fig. 5.1I**) (88), highlighting the potential relevance of this drug in treating patients with occlusive vascular diseases due to mutations in *ACTA2*.

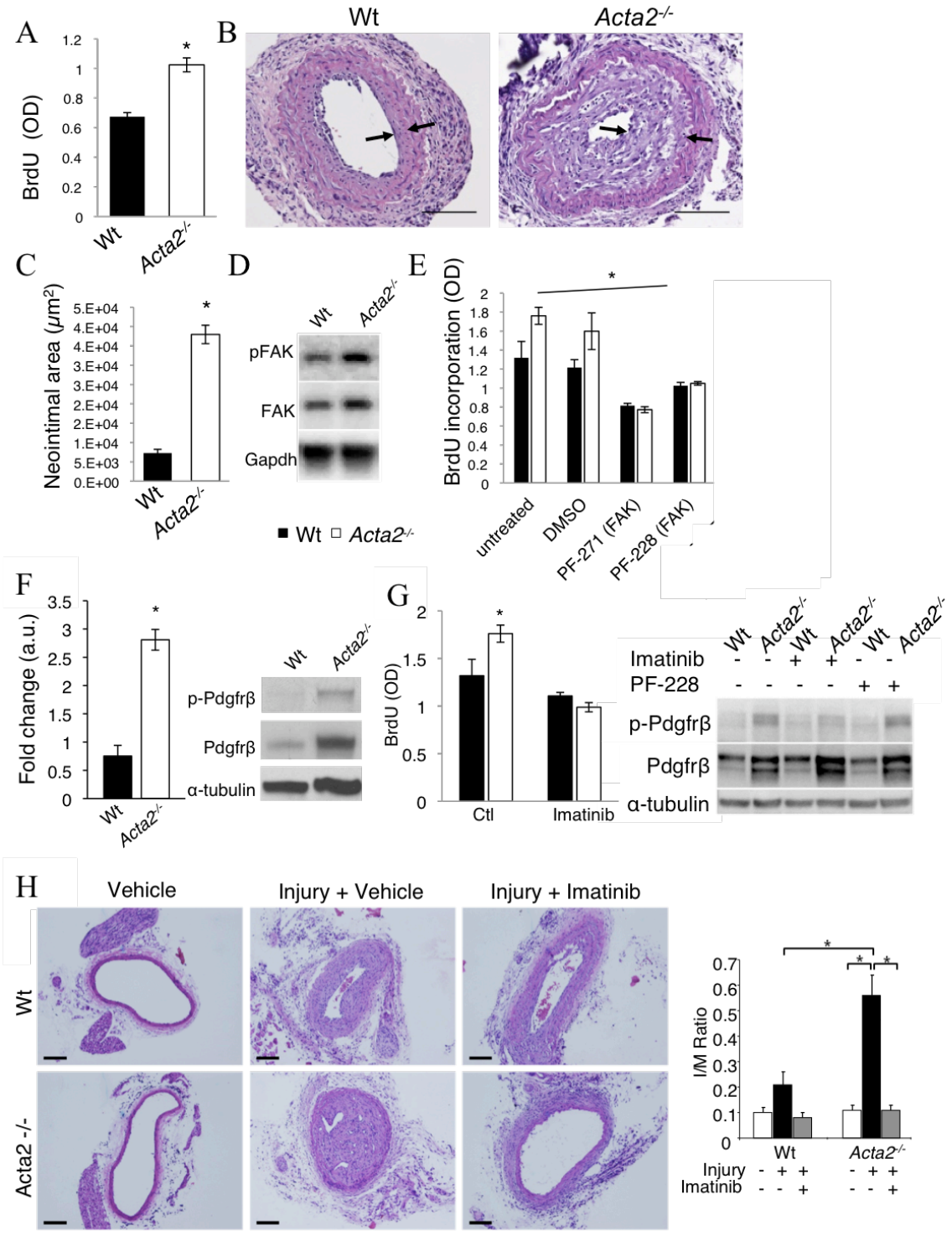

Figure 5.1: Increased SMC Proliferation in *Acta2*$^{-/-}$ Mice *in Vivo* and in Culture Is Driven by FAK and PDGFRβ Activation and Can Be Attenuated by Inhibition of FAK in Culture and by Imatinib Both in Culture and *in Vivo*. **A.** Proliferation in *Acta2*$^{-/-}$ SMCs is significantly increased compared to wildtype SMCs. *p<0.05. Error bars ± s.d. **B.** *Acta2*$^{-/-}$ mice have increased neointima formation 21 days after carotid artery ligation. **C.**

Quantification of carotid ligation response confirms significant increase in neointima formation in *Acta2*$^{-/-}$ mice. *p<0.05. Error bars ± s.e.m. **D.** Western blot showing increased Y397 pFAK expression in *Acta2*$^{-/-}$ SMCs. **E.** Two different FAK inhibitors are able to attenuate proliferation in *Acta2*$^{-/-}$ SMCs. *p<0.05. Error bars ± s.d. **F.** Increased *Pdgfrb* gene expression and total and activated PDGFRβ expression in *Acta2*$^{-/-}$ SMCs. Error bars ± s.d. **G.** Imatinib treatment attenuates proliferation in *Acta2*$^{-/-}$ SMCs. *p<0.05. Error bars ± s.d. **H.** Imatinib, but not PF573228 (PF-228; FAK inhibitor), can partially reduce PDGFRβ activation. **I.** Treating carotid artery ligation site with imatinib post-ligation prevents pathologic neointima formation in *Acta2*$^{-/-}$ mice. *p<0.05 Figures from C. Papke, PhD and colleagues (unpublished work), with permission.

We performed carotid artery ligation on the *Acta2*$^{+/+\ R258C\ TG}$ and *Acta2*$^{+/-\ R258C\ TG}$ mice in order to assess their response to injury, and found that 21 days post-surgery, the *Acta2*$^{+/+\ R258C\ TG}$ mice did not have significantly greater neointima formation compared to wildtype mice, but the *Acta2*$^{+/-\ R258C\ TG}$ mice did, as well as significantly thicker media and a significantly larger media/intima ratio **(Fig. 1.9A, B**) (81). Therefore, we wanted to assess whether proliferation was increased in the smooth muscle cells of the *Acta2*$^{+/+\ R258C\ TG}$ and *Acta2*$^{+/-\ R258C\ TG}$ mice, and whether the pathways found to drive the proliferation in *Acta2*$^{-/-}$ SMCs are also implicated here. Given the many parallels between the *Acta2* $^{R258C\ TG}$ and *Acta2*$^{-/-}$ models *in vivo* and in culture, we hypothesized that SMCs with the *R258C* mutation will proliferate more, and that the pathways driving this response will involve FAK activation and the PDGFRβ.

Results

In order to assess proliferation, we performed a BrdU ELISA assay on our SMCs. Data indicate that both *Acta2*$^{+/+\ R258C\ TG}$ and *Acta2*$^{+/-\ R258C\ TG}$ SMCs proliferate more than wildtype SMCs in culture, with the *Acta2*$^{+/-\ R258C\ TG}$ SMCs proliferating even more than

Acta2$^{+/+\ R258C\ TG}$ SMCs (**Fig. 5.2A)**. *Acta2*$^{+/-}$ SMCs showed such dramatic variation in proliferation between different runs of the assay under identical conditions that we chose not to include them in our comparison of proliferative ability.

We first wanted to test the role of FAK in driving the increased proliferation. We already showed that FAK is not activating the PI3K-Akt pathway, a survival pathway, which suggests that FAK may instead be differentially activating proliferative pathways. In order to test whether FAK activation was driving the increased proliferation in the *Acta2*$^{+/+\ R258C\ TG}$ and *Acta2*$^{+/-\ R258C\ TG}$ SMCs, we treated the SMCs with 1μM PF573228, a highly specific FAK inhibitor. Data presented in **Fig. 5.2B** indicates that treating SMCs with the PF573228 was able to partially decrease the proliferation in *Acta2*$^{+/-\ R258C\ TG}$ SMCs, but not in *Acta2*$^{+/+\ R258C\ TG}$ SMCs, consistent with differences in pFAK levels in these SMCs. Further, when we used the PI3K inhibitor LY294002 we found a paradoxical increase in proliferation (**Fig. 5.2C**), consistent with compensatory activation of MAPK pathways in the LY294002-treated SMCs.

Next, we wanted to assess the potential role of the PDGFRβ in proliferation. We determined mRNA expression and protein levels using quantitative real-time PCR and Western blot and found an increase in the expression of the *Pdgfrb* gene only in the *Acta2*$^{+/+\ R258C\ TG}$ SMCs (**Fig. 5.2D**) and of phosphorylated PDGFRβ in the *Acta2*$^{+/+\ R258C\ TG}$ and *Acta2*$^{+/-}$ SMCs, but not in the *Acta2*$^{+/-\ R258C\ TG}$ SMCs (**Fig. 5.2D, Appendix 3H**). Interestingly, ERK1/2, which is downstream of the PDGFRβ, as well as many other proliferative pathways, was also only activated in the *Acta2*$^{+/+\ R258C\ TG}$ SMCs (**Fig. 5.2E**, **Appendix 3G**). We tested whether a MEK inhibitor, U0126, could block proliferation in the *Acta2*$^{+/+\ R258C\ TG}$ SMCs, and found, unsurprisingly, that to be the case (**Fig. 5.2F**). However,

when we tested whether imatinib could block proliferation in all cell lines, we found only a partial effect on the *Acta2*$^{+/+\ R258C\ TG}$ SMCs but a much stronger effect in the *Acta2*$^{+/-\ R258C\ TG}$ SMCs, in which imatinib brought proliferation down to wildtype levels (**Fig. 5.2G)**.

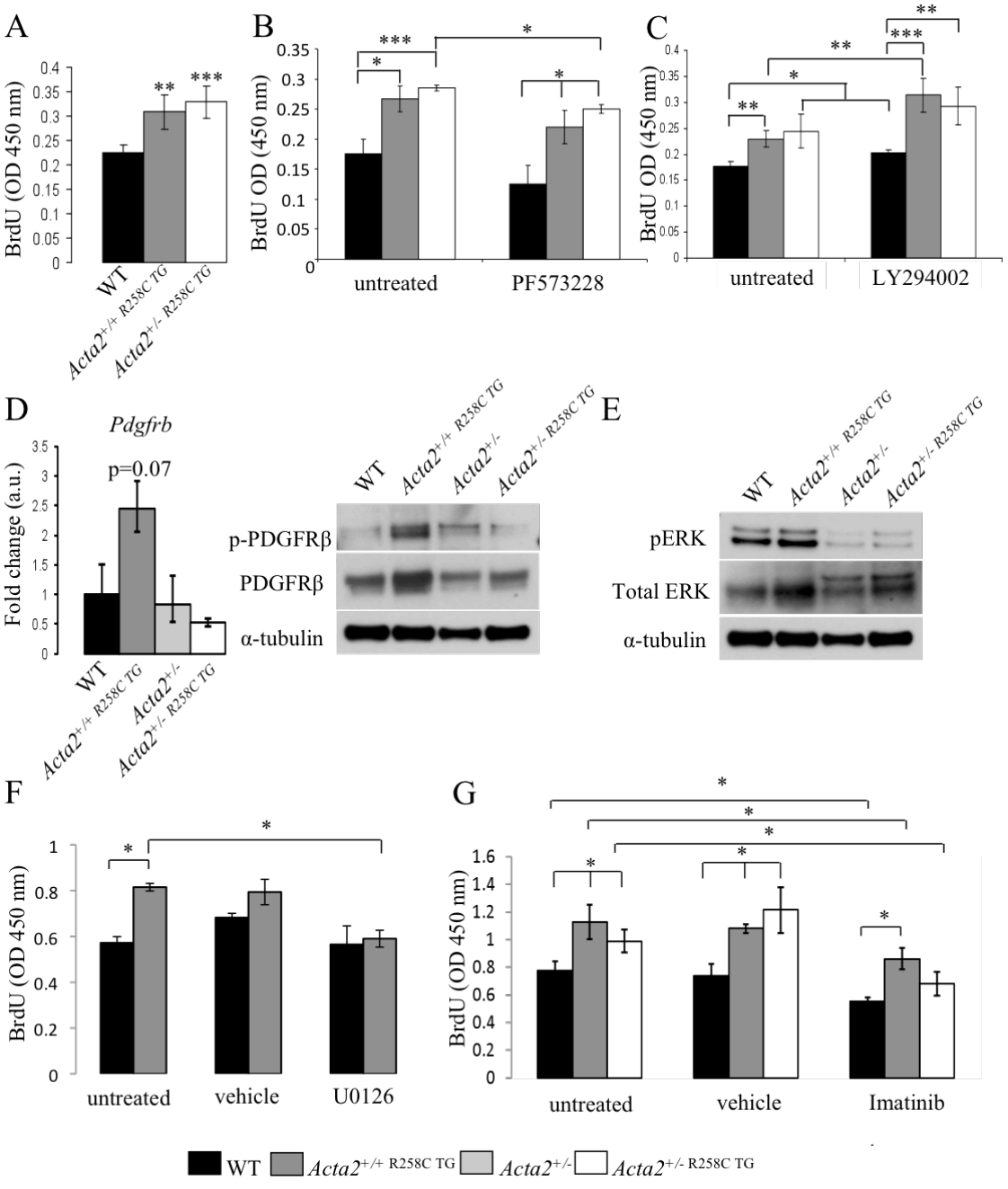

Figure 5.2: Proliferation Is Increased in *Acta2*$^{+/+\ R258C\ TG}$ and *Acta2*$^{+/-\ R258C\ TG}$ SMCs and

Can Be Partially Attenuated by Imatinib and PF573228. A. Both *Acta2*$^{+/+\ R258C\ TG}$ and *Acta2*$^{+/-\ R258C\ TG}$ SMCs proliferate more than wildtype SMCs. **B.** Treating SMCs with 1μM PF573228 (FAK inhibitor) significantly attenuates proliferation only in the *Acta2*$^{+/-\ R258C\ TG}$ SMCs. *p<0.05 ***p<0.001. **C.** Treating cells with 20μM LY294002 causes an increase in proliferation in all cell lines, including wildtype. **D.** *Pdgfrb* expression is only borderline significantly increased in *Acta2*$^{+/+\ R258C\ TG}$ SMCs, but not in any other cell line. The *Acta2*$^{+/+\ R258C\ TG}$ SMCs also have more activated PDGFRβ, as well as total receptor. **E.** Phosphorylated ERK is only elevated slightly in *Acta2*$^{+/+\ R258C\ TG}$ SMCs, and it is lower than the wildtype in *Acta2*$^{+/-}$ and *Acta2*$^{+/-\ R258C\ TG}$ SMCs. **F.** Treatment with 10μM U0126, a MEK inhibitor, can completely block proliferation in *Acta2*$^{+/+\ R258C\ TG}$ SMCs. **G.** 10μM Imatinib treatment partially blocks proliferation in *Acta2*$^{+/+\ R258C\ TG}$ SMCs and completely in *Acta2*$^{+/-\ R258C\ TG}$ SMCs. *p<0.05, **p<0.01, ***p<0.001.All error bars ±s.d.

CHAPTER SIX: Discussion

An overarching goal of our lab is to understand how mutations in contractile and other proteins can cause such profound and devastating vascular diseases in patients so that we can improve clinical management and treatment for these patients. We sought to characterize the aortic smooth muscle cell phenotype of transgenic mice carrying the *Acta2 R258C* mutation in order to determine whether the mutation had a dominant negative effect and whether decreasing the ratio of wildtype to mutant actin would increase the severity of the phenotype. Our *in vivo* data indicating decreased aortic contractility in the $Acta2^{+/+\ R258C\ TG}$ mice and increased neotintima formation in response to carotid injury in the $Acta2^{+/-\ R258C\ TG}$ mice point towards a dual effect of the mutation – impaired contractile properties and increased proliferation. Further, we observed an increase in both neotintima formation post-injury and in aortic disease when we introduced mutant α-actin in mice with an $Acta2^{+/-}$ background compared to the $Acta2^{+/+\ R258C\ TG}$ mice, which suggested that the $Acta2^{+/-\ R258C\ TG}$ mice develop vascular pathology similar to that in patients who are heterozygous for the *ACTA2* R258C mutation. These findings led us to hypothesize that the phenotype of SMCs explanted from these two mutant mouse models will similarly become more severe when the ratio of wildtype to mutant α-actin is decreased. Data presented here confirms this hypothesis but also highlights the dramatic differences in the pathways activated in the $Acta2^{+/+\ R258C\ TG}$ versus $Acta2^{+/-\ R258C\ TG}$ SMCs caused by the decrease in wildtype to mutant α-actin content. Finally, these findings suggest a key role of α-actin in modulating SMC phenotype and function.

In assessing the ability of the $Acta2^{+/+\ R258C\ TG}$ SMCs and $Acta2^{+/-\ R258C\ TG}$ SMCs to form α-actin filaments, we found some interesting differences. Immunofluorescent staining revealed that the $Acta2^{+/+\ R258C\ TG}$ SMCs formed actin filaments but the $Acta2^{+/-\ R258C\ TG}$

SMCs had large pools of unpolymerized actin and few filaments. Even 72 hours post-TGF-β1 treatment, most of the actin in the *Acta2*$^{+/- \ R258C \ TG}$ remained in monomeric form. Interestingly, when we performed an F/G actin assay, we found that *both* cell lines lacked pelleted filaments, suggesting that the *Acta2*$^{+/+ \ R258C \ TG}$ filaments visualized in the cells are unstable when stressed. Treating the cells with phalloidin prior to centrifugation effectively stabilized the polymerized actin in *Acta2*$^{+/+ \ R258C \ TG}$ SMCs, allowing it to be pelleted. This result indicates that the cells are in fact able to form filaments, as observed with immunofluorescence, but these filaments cannot withstand the shearing and agitation required in preparation for the F/G actin assay. Interestingly, the *Acta2*$^{+/- \ R258C \ TG}$ SMCs also produced a pellet after treatment with phalloidin. Phalloidin addition has been known to reduce the critical concentration required for actin polymerization to occur *in vitro*, in addition to accelerating new filament formation by promoting actin nucleation (104). Thus, our finding in the *Acta2*$^{+/- \ R258C \ TG}$ SMCs suggested that phalloidin may cause α-actin to polymerize more effectively and/or stabilize the filaments that are formed.

Concomitant with an increase in the percentage of cells staining positively for actin filaments in both the *Acta2*$^{+/+ \ R258C \ TG}$ SMCs and, to a lesser extent, the *Acta2*$^{+/- \ R258C \ TG}$ SMCs, at 72 hours post-TGF-β1 treatment, about 50% of actin appeared in the polymerized fraction of both cell types. Therefore, growth factor stimulation induced a more differentiated phenotype and more stable filaments in these SMCs. This finding may also be relevant *in vivo*, where stimulation by the extracellular matrix, TGF-β1, biomechanical forces, or other factors may promote similar α-actin filament stability in the SMCs, which could potentially preserve the integrity of the arterial wall resulting in less vascular disease than what would be expected based on the cellular defects.

The findings in the *Acta2*$^{+/-\ R258C\ TG}$ SMCs were also seen in part in the *Acta2*$^{+/-}$ SMCs. Both SMCs showed few filaments by immunofluorescence both after 24 hours of serum starvation and after 72 hours of TGF-β1 treatment, suggesting that the wildtype α-actin haploinsufficiency contributes to decreased actin polymerization, which further supports the hypothesis that actin does not reach a critical concentration in these SMCs and hence polymerization is difficult to initiate. The *Acta2*$^{+/-}$ SMCs also responded to phalloidin treatment prior to performing an F/G actin assay, as we observed pelleting of almost the all α-actin, as well as to TGF-β1 treatment which allowed for approximately 50% polymerization to occur, again suggesting that the inherent ability of these, like the *Acta2*$^{+/-\ R258C\ TG}$, SMCs to polymerize is not impaired.

While haploinsufficiency of wildtype actin is alone sufficient to inhibit actin polymerization based on the findings by F/G actin assay and immunofluorescent staining, there is evidence for additional effects of the R258C mutation on actin polymerization in the *Acta2*$^{+/-\ R258C\ TG}$ SMCs. Even though it is difficult to separate the effects of the loss of the wildtype allele and the mutant transgene insertion on actin filament formation, it is notable that the *Acta2*$^{+/-\ R258C\ TG}$ SMCs express similar levels of total α-actin compared to the *Acta2*$^{+/-}$ SMCs, and yet α-actin integrates into filaments less well than in the heterozygous SMCs (**Fig. 3.3A, B**). This observation is supported by preliminary *in vitro* studies using human α-actin expressed in a bacculovirus system, which suggest that the critical concentration of α-actin R258C mutant monomers required for polymerization to occur is higher than in the wildtype, and thus more protein is required for filaments to begin to form (Kathleen Trybus, PhD, and colleagues, personal communication). This subtle difference between the two heterozygous genotypes is masked when the cells are treated with TGF-β1

because of increased expression of *Acta2* and other contractile proteins in both cell lines. Further, downstream changes resulting from the defect in actin filament formation in the *Acta2*$^{+/-\ R258C\ TG}$ and *Acta2*$^{-/-}$ SMCs, such as MRTF-A localization, focal adhesion size or proliferation ability, were different in these two cell lines. Therefore, we conclude that the *Acta2*$^{+/-\ R258C\ TG}$ SMC phenotype is unique and more severe than either the *Acta2*$^{+/+\ R258C\ TG}$ or *Acta2*$^{+/-}$ SMCs due to the presence of increased mutant to wildtype α-actin in these cells. This conclusion is also supported by the more severe phenotypes observed *in vivo* in these mice (**Fig. 1.8C**).

The hypothesis that the R258C mutant actin forms brittle filaments is also supported by preliminary *in vitro* data from the Trybus lab (Kathleen Trybus, PhD, and colleagues, personal communication). An assessment of flexural rigidity of the wildtype and mutant α-actin showed that the mutant was less flexible when compared to the wildtype, with a tendency to break. Measuring the *in vitro* motility of the wildtype and mutant α-actin revealed that myosin moved the R258C and R258H mutant actins significantly more slowly compared to the wildtype (Kathleen Trybus, PhD, and colleagues, personal communication). While experiments have not yet been conducted with mixed wild-type: mutant actin, as they are found in vascular SMCs in individuals with heterozygous *ACTA2* mutations and in our mouse mutant SMCs, these preliminary data provide further support to our observations in culture.

Our finding that the *Acta2*$^{+/+\ R258C\ TG}$ filaments break down more slowly than the wildtype following treatment with Latrunculin A are also in agreement with the *in vitro* findings by Dr. Trybus and colleagues (personal communication). First, the *Acta2*$^{+/+\ R258C\ TG}$ SMCs express significantly more α-actin compared to the wildtype SMCs and form more,

but thinner, filaments as assessed by immunofluorescent staining. Therefore, the effects of the Latrunculin A treatment might appear less striking in the *Acta2*$^{+/+\ R258C\ TG}$ SMCs compared to the wildtype cells because there are more filaments depolymerizing simultaneously. This is a plausible but probably only partial explanation since even after one hour of treatment, the *Acta2*$^{+/+\ R258C\ TG}$ SMCs still have intact filaments whereas the wildtype SMCs have no filaments by 15 minutes. It is, therefore, likely that the *Acta2*$^{+/+\ R258C\ TG}$ filaments are also less dynamic compared to wildtype filaments. This conclusion is supported by structural predictions that this mutation disrupts the opening and closing of the ATP binding cleft (17). Actin depolymerization requires ATP breakdown into ADP+Pi, followed by subsequent Pi release (35). Therefore, a defect in the ATP binding region, which affects Pi release, could lead to slower depolymerization. Alternatively, it is possible that Latrunculin A is not able to bind mutant actin and hence has only partial effect in the *Acta2*$^{+/+\ R258C\ TG}$ SMCs. Further studies *in vitro* will be required to thoroughly assess the filament dynamics of this mutant. Ultimately, our experiments suggest that the *Acta2*$^{+/+\ R258C\ TG}$ SMC filaments do not dissociate more quickly than wildtype filaments in cultured SMCs, but when force is applied to these cells as in the shearing step prior to F/G actin assays, the filaments fall apart easily. It is tempting to speculate that the constant stretch and force on the aortic wall *in vivo* has a similar effect on the filament integrity as does shearing in culture. This hypothesis could potentially be tested by introducing hypertension, a common risk factor for TAAD in humans, in the *Acta2*$^{+/+\ R258C\ TG}$ mice, and thus increasing the force exerted on the aortic wall. Assessment of the F/G actin ratios in the aortic SMCs may demonstrate increased monomeric actin in the SMCs exposed to increased pressures.

The differential localization of MRTF-A in the SMCs, along with the corresponding changes in contractile gene expression and protein levels, provide a link between impaired actin filament formation/stability and SMC phenotype. *Acta2*$^{+/+\ R258C\ TG}$ SMCs had significantly more nuclear MRTF-A staining compared to the wildtype SMCs, and corresponding increases in all contractile protein levels that were assessed. This confirms our observation that the filaments in these SMCs are intact, and perhaps even more numerous than in wildype cells, allowing MRTF-A localization in the nucleus. The *Acta2*$^{+/-\ R258C\ TG}$ SMCs, on the other hand, had significantly less MRTF-A in the nucleus than the wildtype cells, which is in agreement with the observation that these SMCs have large pools of monomeric actin, which sequesters MRTF-A in the cytoplasm. Surprisingly, these SMCs had no difference in the gene expression levels of *Acta2* and *SM22α* compared to the wildtype cells, and increased expression of *Cnn1* and *Myh11*, suggesting that constitutively nuclear transcription co-factors like myocardin, may partially compensate for the cytoplasmic sequestration of MRTF-A. Interestingly, the *Acta2*$^{+/-}$ SMCs did not show a significant difference in the ratio of nuclear to cytoplasmic MRTF-A compared to the wild-type, but were significantly different from the *Acta2*$^{+/-\ R258C\ TG}$ SMCs. Further, the heterozygous SMCs also did not show a difference in the expression of any contractile genes compared to wildtype. Both *Acta2*$^{+/-\ R258C\ TG}$ and *Acta2*$^{+/-}$ SMCs, however, showed lower protein expression levels than expected based on the gene expression data, suggesting that they both may have increased protein turnover as well. This prediction could be tested by performing a time-course assay with the translation inhibitor cycloheximide in order to assess how quickly proteins are degraded after inhibition. Taken together, we have observed three unique phenotypes in our three genotypes. The *Acta2*$^{+/+\ R258C\ TG}$ mice form filaments

and are highly differentiated based on MRTF-A nuclear localization and increased contractile marker expression; the *Acta2*$^{+/-}$ SMCs form very few filaments and do not show any changes in contractile gene expression and MRTF-A localization but have a decrease in contractile markers at the protein level; finally, the *Acta2*$^{+/- \ R258C \ TG}$ SMCs have almost no filament formation, decreased nuclear MRTF-A localization but partial increase in contractile gene expression, coupled with a *decrease* in contractile protein levels.

Given the differential localization of MRTF-A in each cell line, we would have predicted that the *Acta2*$^{+/+ \ R258C \ TG}$ and *Acta2*$^{+/- \ R258C \ TG}$ SMCs would have opposite rates of proliferation. Interestingly, we found that both cell lines proliferated significantly more than the wildtype SMCs. This finding is consistent with the established SRF: MRTF phenotype switching axis for the *Acta2*$^{+/- \ R258C \ TG}$ SMCs – sequestering MRTF-A in the cytoplasm allows SRF to bind other transcription factors that promote *c-fos* expression and cell growth. While it is surprising that the *Acta2*$^{+/+ \ R258C \ TG}$ SMCs did not show a decrease in proliferation, these data are consistent with findings from the *Acta2*$^{-/-}$ SMCs, which also showed a significant increase in contractile marker levels in conjunction with increased proliferation (88). It has been shown previously that SMC precursor cells display this dual phenotype during the early stages of vascular development (106). Further, reports have suggested that deficits in contractile protein expression may not be required for growth and proliferation to be initiated (107), and, conversely, that differentiation of SMCs in culture also does not require a loss of proliferative activity (106; 108). Therefore, there is evidence for an uncoupling of the two ends of the smooth muscle cell phenotypic spectrum, which could help explain the unique phenotype we observed in the *Acta2*$^{+/+ \ R258C \ TG}$ and *Acta2*$^{-/-}$ SMCs.

With regard to the SRF: MRTF axis, the increased proliferation, in addition to contractile gene expression, suggests that growth signals may be promoting proliferation independently of SRF. Alternatively, SRF expression levels may be higher in these SMCs, and so enough SRF is present to bind both types of transcriptional co-factors. Support for the uncoupling between growth and differentiation via the SRF: MRTF axis was also found in the dedifferentiated *Myh11*$^{R247C/R247C}$ SMCs (48). While RhoA activation restores differentiation by inducing actin polymerization and driving MRTF-A back in the nucleus, proliferation was not correspondingly attenuated by this process (48). Therefore, MRTF-A translocation out of the nucleus can "sensitize" SMCs to proliferative stimuli, but localization of MRTF-A in the nucleus does not prevent the SMCs from being sensitive to other proliferation signals.

Mutations in contractile proteins identified in our lab have been shown to uniformly decrease contractility and force generation in the aorta. As the demonstrated or hypothesized decreased contractility is the underlying defect linking the mutations causing thoracic aortic disease, we wanted to explore the link between the phenotypic changes and force generation. We focused on focal adhesions, which are crucial signal transduction centers and integration points for signaling and mechanical cues (39; 42). The composition of focal adhesions depending on their maturity can drive additional cell processes and pathways that will affect the cellular phenotype, and the progression of maturation of these focal adhesions is dependent on increasing force generation across the cell driven by actin and myosin filaments. For example, activators of RhoA are only found in mature focal adhesions (44); RhoA regulates myosin light chain phosphorylation and actin stress fiber formation, hallmarks of a differentiated cell. Activators of Rac1, on the other hand, are enriched in less

mature FAs (44), and Rac1 is involved in proliferative and migratory signaling downstream of growth factor receptors like the PDGFRβ (109), the angiotensin type 1 receptor (110), and it may also be activated in response to reactive oxygen species (111).

We found in both the *Acta2*$^{+/+\ R258C\ TG}$ and *Acta2*$^{+/-\ R258C\ TG}$ SMCs that the focal adhesions are fewer, more peripherally localized and larger compared with wildtype cells. Further, these SMCs were enriched in activated FAK, suggested to play a role in focal adhesion strengthening (112-113), in addition to focal adhesion turnover (114-115). These findings are in line with the *Acta2*$^{-/-}$ SMC findings (88), providing further support to the hypothesis that the disruptive effect of the R258C mutation induces a smooth muscle cell phenotype similar to the one resulting from the complete loss of α-actin. Interestingly, the *Acta2*$^{+/+\ R258C\ TG}$ SMCs had a significant increase in the activation of Rac1 but no change in RhoA activation, also in line with the *Acta2*$^{-/-}$ SMCs. However, the *Acta2*$^{+/-\ R258C\ TG}$ SMCs and *Acta2*$^{+/-}$ SMCs showed a paradoxical decrease in Rac1, and the *Acta2*$^{+/-\ R258C\ TG}$ SMCs had a slight but significant decrease in RhoA activation, which was unique to this cell line and hence further supports an additive effect of the genetic alterations. This indicates that there may be a decrease in total Rac1 and RhoA production or expression. The exact mechanism, by which the loss of an α-actin allele could lead to a decrease in Rac1 and RhoA activation, remains unclear, but probably stems directly from the altered focal adhesion content. A summary of these findings if presented in **Fig. 6.1.**

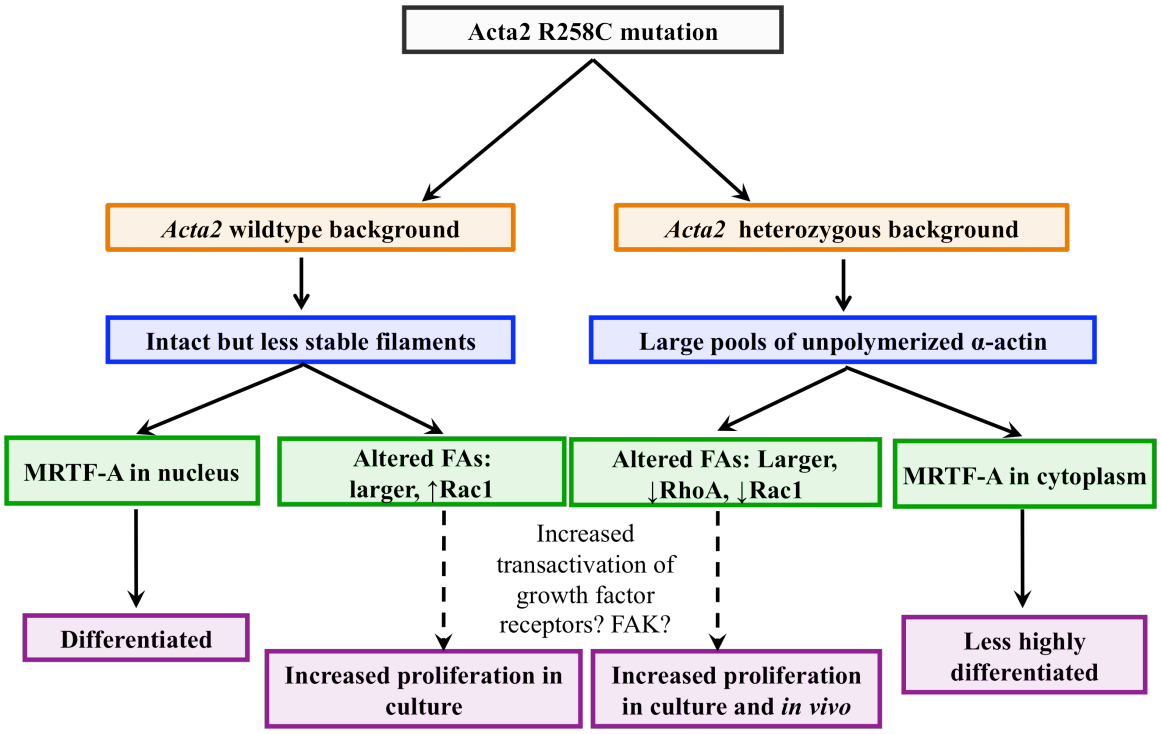

Figure 6.1: Model of the Effects of the *Acta2 R258C* Mutation in *Acta2*$^{+/+\ R258C\ TG}$ and *Acta2*$^{+/-\ R258C\ TG}$ SMCs

Our lab's work is the first to address how mutations in contractile proteins affect the focal adhesion phenotype. Thus, we are observing not only novel SMC phenotypes, but also previously undescribed focal adhesion phenotypes. While work has been done to disrupt actin polymerization or myosin II motor activity using specific inhibitors (43-44; 113), the indirect effects of impaired contractile ability (coming from altered interactions with partner molecules, for example) on focal adhesion maturation have not been addressed. Loss of actin filament stability induces the formation of large focal adhesions, which are traditionally considered to be more mature. However, the peripheral localization of these adhesions (which suggests they are nascent), the activation of FAK, together with the increase in Rac1 for the *Acta2*$^{+/+\ R258C\ TG}$ SMCs and the decrease in RhoA in the *Acta2*$^{+/-}$

$^{R258C\ TG}$ SMCs, indicate that the focal adhesions are not maturing properly. Thus, the dual nature of the observed SMC phenotype is reflected in the focal adhesion phenotype, too.

We also wanted to test whether the proliferative pathways identified in the *Acta2*$^{-/-}$ SMCs were similarly activated in the mutant cells. Our studies clearly indicate a role for FAK in driving proliferation. While FAK inhibitor treatment had a modest effect on attenuating proliferation in the *Acta2*$^{+/+\ R258C\ TG}$ SMCs, it had a partial but significant effect in the *Acta2*$^{+/-\ R258C\ TG}$ SMCs, which also had the greatest increase in activated FAK as seen by Western blot. Together with the observation that Akt is not more activated in the SMCs expressing more activated FAK, this data suggests that a key role for FAK in these SMCs is in stimulating proliferative pathways.

In addition to assessing the contribution of FAK to proliferation in our SMCs, we tested for growth factor receptor activation, focusing on the platelet-derived growth factor receptor β (PDGFRβ). Expression of the receptor at the mRNA level was only marginally significantly increased in the *Acta2*$^{+/+\ R258C\ TG}$ SMCs. At the protein level, both the activated receptor and total receptor protein levels were increased in these cells, which is in agreement with findings in the *Acta2*$^{-/-}$ SMCs (88). Therefore, we tested whether imatinib could block proliferation in our SMCs like it did for the null cells. The fact that imatinib reduced proliferation to wildtype levels in the *Acta2*$^{+/-\ R258C\ TG}$ SMCs and only partially in the *Acta2*$^{+/+\ R258C\ TG}$ SMCs was surprising given the lack of increased activation in the PDGFRβ, but it may possibly indicate a greater sensitivity of these SMCs to inhibitors of proliferation like imatinib. Alternatively, imatinib, as a multi-target tyrosine kinase inhibitor, may be affecting proliferation through any of its other main targets, such as Bcr/Abl and C-kit (116). However, Bcr in SMCs is downstream of PDGF (117). C-kit, on the other hand, is more

highly expressed in endothelial cells than SMCs (118), but its expression can increase in VSMCs in response to injury (119). These data suggest that it is less likely that these tyrosine kinases play a role in driving proliferation in culture. However, their increased expression in response to injury (117; 119), together with the significant enrichment of c-kit positive stem cells in the media of TAAD patients reported by Shen and colleagues (120), suggests a role for multi-target tyrosine kinase inhibitors like imatinib in treating vascular disease in patients with *ACTA2* mutations.

One surprising finding from this study is the similarity in the cellular phenotypes of the $Acta2^{-/-}$ SMCs and the $Acta2^{+/+\ R258C\ TG}$ SMCs. These SMCs have similar contractile gene and protein expression, proliferation, MRTF-A localization, focal adhesion alterations and response to imatinib treatment (88). The mouse models also display similar aortic pathology, but the $Acta2^{+/+\ R258C\ TG}$ mouse pathology is predictably less severe than the pathology of actin-deficient mice. Furthermore, wildtype SMCs treated with an α-actin disrupting peptide also exhibit alterations in agreement with data presented here (88). These findings suggest that the dominant negative effect of the R258C mutation, even with wildtype α-actin present, can almost recapitulate the complete loss of the gene and gene product in vitro. Furthermore, while the cellular phenotype that we characterized in the $Acta2^{+/-\ R258C\ TG}$ SMCs was different from the ones in the $Acta2^{+/+\ R258C\ TG}$ and $Acta2^{-/-}$ SMCs, the $Acta2^{+/-\ R258C\ TG}$ mice develop more significant vascular pathology compared to the other two genotypes. Taking the recurring findings in SMCs from the three models, it appears that alterations or loss of α-actin drive the cellular and vascular phenotype in these mouse models through impaired actin filament stability, focal adhesion rearrangements, FAK activation, and increased proliferation. More work will be needed to detail the exact cause-

and-effect sequence as a result of the mutant α-actin expression and to devise potential treatments for the aortic disease in patients with *ACTA2 R258C* mutations.

In conclusion, the *Acta2*$^{+/+\ R258C\ TG}$ and *Acta2*$^{+/-\ R258C\ TG}$ mice are the first mouse models of a recurring mutation that leads to FTAAD. The aortic phenotype in these mice matches the observations in our patients, verifying that this is a good model of disease. We sought to characterize the phenotype of vascular SMCs explanted from the ascending aorta in order to gain better understanding of the cellular pathology associated with aneurysm development, since little is known about the fate of SMCs in the early stages of disease progression. The findings presented here, coupled with the ones from the *Acta2*$^{-/-}$ mouse model, point towards a unique SMC phenotype resulting from a disruption or complete loss of α-actin filaments, which is simultaneously proliferative and expressing contractile markers (88). The similarity of results amongst our various models suggests that the pathology noted in this study is most likely going to be replicated in SMCs from models of other *ACTA2* mutations. Further, and also importantly, the shared findings between the *Acta2*$^{-/-}$ and *Acta2*$^{+/+\ R258C\ TG}$ SMCs and mice imply that any treatments evaluated for aortic or vascular occlusive disease may potentially be applicable to patients with other mutations in *ACTA2*.

APPENDIX

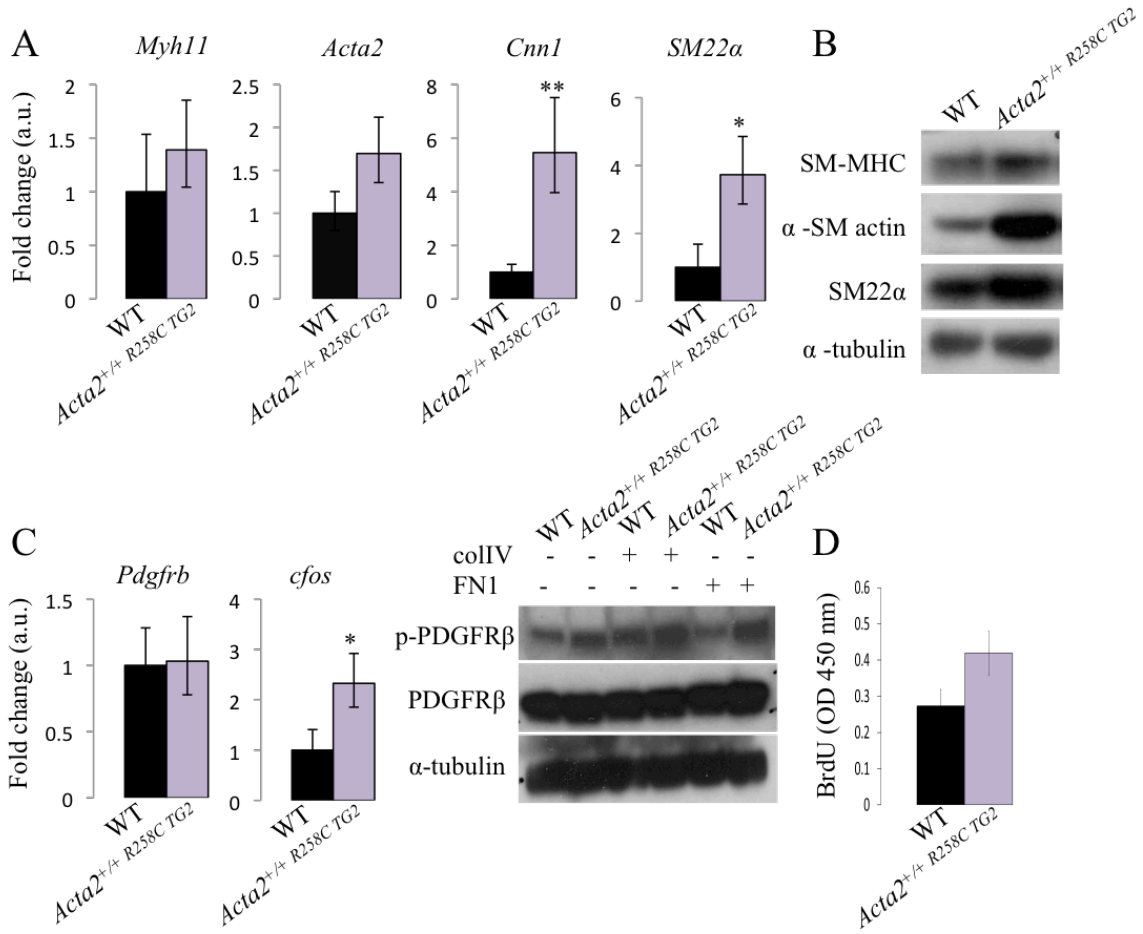

Appendix 1: Characterization of the *Acta2*$^{+/+\ R258C\ TG2}$ SMCs. A. *Acta2*$^{+/+\ R258C\ TG2}$ SMCs express *Cnn1* and *SM22α* at significantly greater levels compared to wildtype cells, and *Acta2* and *Myh11* and comparable levels. *p<0.05, **p<0.01. Error bars ± s.d. **B.** Increased contractile protein expression in *Acta2*$^{+/+\ R258C\ TG2}$ SMCs. **C.** While *Pdgfrb* expression is not increased, *cfos* is significantly more highly expressed in *Acta2*$^{+/+\ R258C\ TG2}$ SMCs, and the PDGFRβ is more activated at the protein level when SMCs are grown on plastic, collagen IV and fibronectin 1 alike. **D.** Proliferation is borderline significantly increased in *Acta2*$^{+/+\ R258C\ TG2}$ SMCs.

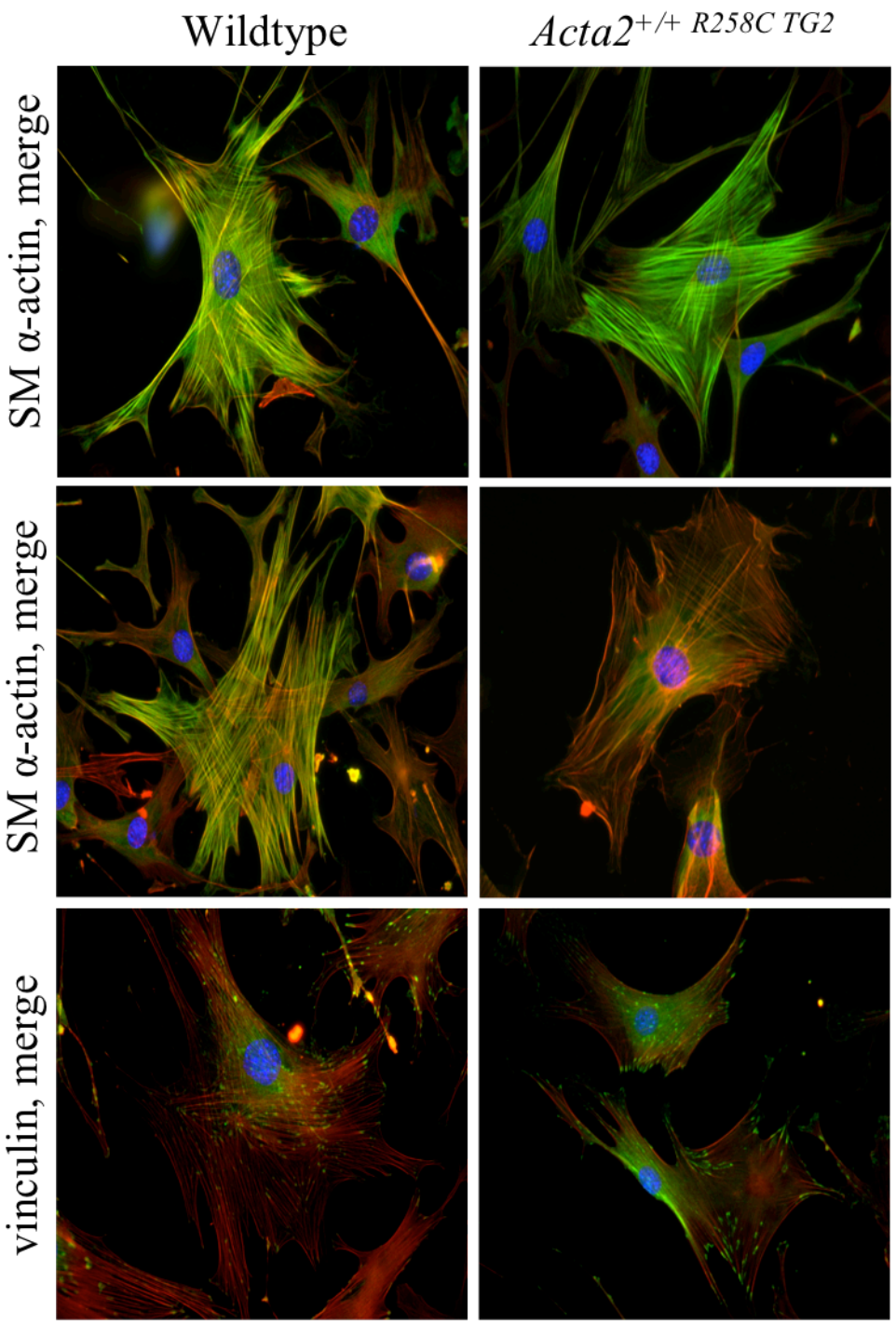

Appendix 2: **Immunofluorescent Staining of Wildtype and *Acta2*$^{+/+\ R258C\ TG2}$ SMCs.** SM α-actin = green, vinculin = green, phalloidin (total filamentous actin) = red, nucleus (DAPI) = blue.

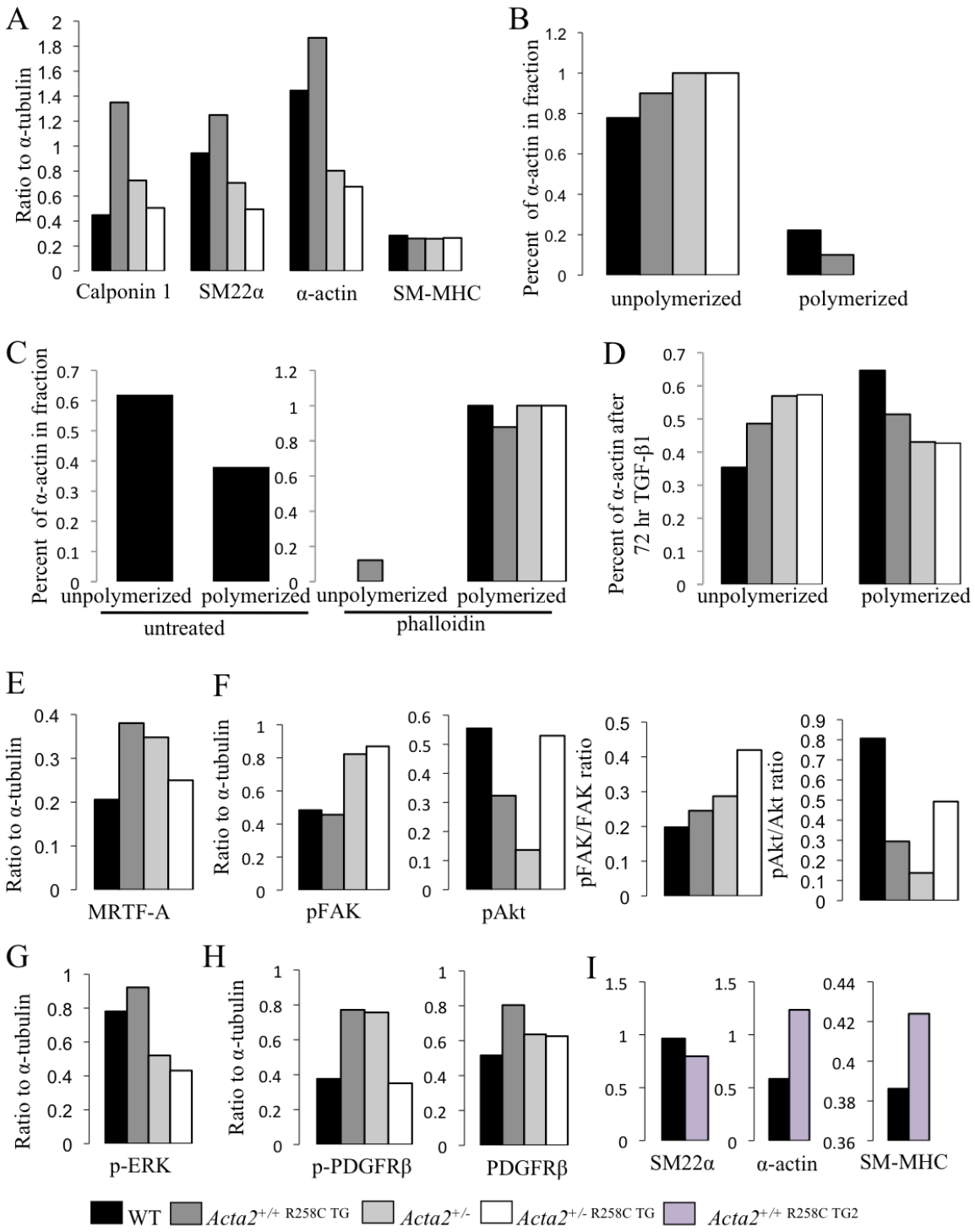

Appendix 3: Quantification of Western Blots.

Bibliography

1. Castellano, J. M., Kovacic, J. C., Sanz, J., and Fuster, V. (2012). Are we ignoring the dilated thoracic aorta? *Ann NY Acad Sci* **1254**, 164-174.
2. IRAD Online.International Registry of Acute Aortic Dissection. <http://www.iradonline.org/index.html>
3. LeMaire, S. A., and Russell, L. (2011). Epidemiology of thoracic aortic dissection. *Nat Rev Cardiol* **8**, 103-113.
4. Milewicz, D. M. (2011). Stopping a Killer: Improving the diagnosis, treatment, and prevention of acute ascending aortic dissections *Circulation* **124**, 1902-1904.
5. Milewicz, D. M., and Regalado, E.(February 13, 2003,updated January 12, 2012).In *GeneReviews* (Pagon, R. A., Bird, T. D., and Dolan, C. R., eds), University of Washington, Seattle, WA, 1993-
6. Milewicz, D. M., Guo, D. C., Tran-Fadulu, V., Lafont, A. L., Papke, C. L., Inamoto, S., Kwartler, C. S., and Pannu, H. (2008). Genetic basis of thoracic aortic aneurysms and dissections: focus on smooth muscle cell contractile dysfunction. *Annu Rev Genomics Hum Genet* **9**, 283-302.
7. Elefteriades, J. A. (2008). Thoracic Aortic Aneurysm: Reading the enemy's playbook. *Yale Journal of Biology and Medicine* **81**, 175-186.
8. El-Hamamsy, I., and Yacoub, M. H. (2009). Cellular and molecular mechanisms of thoracic aortic aneurysms. *Nat Rev Cardiol* **6**, 771-786.
9. Milewicz, D. M., Kwartler, C. S., Papke, C. L., Regalado, E. S., Cao, J., and Reid, A. J. (2010). Genetic variants promoting smooth muscle cell proliferation can result in

diffuse and diverse vascular diseases: evidence for a hyperplastic vasculomyopathy. *Genet Med* **12**, 196-203.

10. Wolinsky, H., and Glagov, S. (1967). A lamellar unit of aortic medial structure and function in mammals *Circ Res* **20**, 99-111.
11. Bunton, T. E., Biery, N. J., Myers, L., Gayraud, B., Ramirez, F., and Dietz, H. C. (2001). Phenotypic alteration of vascular smooth muscle cells precedes elastolysis in a mouse model of Marfan Syndrome *Circ Res* **88**, 37-43.
12. Zhang, X., Shen, Y. H., and LeMaire, S. A. (2009). Thoracic aortic dissection: are matrix metalloproteinases involved? *Vascular* **17**, 147-157.
13. Lowy, J., and Small, J. V. (1970). The organization of myosin and actin in vertebrate smooth muscle. *Nature* **227**, 46-51.
14. Owens, G. K., Kumar, M. S., and Wamhoff, B. R. (2004). Molecular regulation of vascular smooth muscle cell differentiation in development and disease. *Physiol Rev* **84**, 767-801.
15. McDonald, O. G., and Owens, G. K. (2007). Programming smooth muscle plasticity with chromatin dynamics. *Circ Res* **100**, 1428-1441.
16. Yoshida, T., Kaestner, K. H., and Owens, G. K. (2008). Conditional deletion of Krüppel-like factor 4 delays downregulation of smooth muscle cell differentiation markers but accelerates neointimal formation following vascular injury. *Circ Res* **102**, 1548-1557.
17. Guo, D. C., Papke, C. L., Tran-Fadulu, V., Regalado, E. S., Avidan, N., Johnson, R. J., Kim, D. H., Pannu, H., Willing, M. C., Sparks, E., Pyeritz, R. E., Singh, M. N., Dalman, R. L., Grotta, J. C., Marian, A. J., Boerwinkle, E. A., Frazier, L. Q.,

LeMaire, S. A., Coselli, J. S., Estrera, A. L., Safi, H. J., Veeraraghavan, S., Muzny, D. M., Wheeler, D. A., Willerson, J. T., Yu, R. K., Shete, S. S., Scherer, S. E., Raman, C. S., Buja, L. M., and Milewicz, D. M. (2009). Mutations in Smooth Muscle Alpha-Actin (*ACTA2*) Cause Coronary Artery Disease, Stroke, and Moyamoya Disease, Along with Thoracic Aortic Disease *The American Journal of Human Genetics* **84**, 617-627.

18. Kumar, M. S., and Owens, G. K. (2003). Combinatorial control of smooth muscle-specific gene expression. *Arterioscler Thromb Vasc Biol* **23**, 737-747.

19. Parmacek, M. S. (2007). Myocardin-Related Transcription Factors: Critical Coactivators Regulating Cardiovascular Development and Adaptation *Circ Res* **100**, 633-644.

20. Miano, J. M., Long, X., and Fujiwara, K. (2007). Serum response factor: master regulator of the actin cytoskeleton and contractile apparatus. *Am J Physiol Cell Physiol* **292**, C70-C81.

21. Cen, B., Selvaraj, A., and Prywes, R. (2004). Myocardin/MKL family of SRF coactivators: key regulators of immediate early and muscle specific gene expression. *J Cell Biochem* **93**, 74-82.

22. Hoofnagle, M. H., Neppl, R. L., Berzin, E. L., Teg Pipes, G. C., Olson, E. N., Wamhoff, B. W., Somlyo, A. V., and Owens, G. K. (2011). Myocardin is differentially required for the development of smooth muscle cells and cardiomyocytes. *Am J Physiol Heart Circ Physiol* **300**, H1707-H1721.

23. Oh, J., Richardson, J. A., and Olson, E. N. (2005). Requirement of myocardin-related transcription factor-B for remodeling of branchial arch arteries and smooth muscle differentiation *PNAS* **102**, 15122-15127.

24. Hinson, J. S., Medlin, M. D., Lockman, K., Taylor, J. M., and Mack, C. P. (2007). Smooth muscle cell-specific transcription is regulated by nuclear localization of the myocardin-related transcription factors. *Am J Physiol Heart Circ Physiol* **292**, H1170-H1180.

25. Li, S., Chang, S., Qi, X., Richardson, J. A., and Olson, E. N. (2006). Requirement of a myocardin-related transcription factor for development of mammary myoepithelial cells. *Mol Cell Biol* **26**, 5797-5808.

26. Nakamura, S., Hayashi, K., Iwasaki, K., Fujioka, T., Egusa, H., Yatani, H., and Sobue, K. (2010). Nuclear import mechanism for myocardin family members and their correlation with vascular smooth muscle cell phenotype. *J Biol Chem* **285**, 37314-37323.

27. Zhou, J., Hu, G., and Herring, B. P. (2005). Smooth muscle-specific genes are differentially sensitive to inhibition by Elk-1. *Mol Cell Biol* **25**, 9874-9885.

28. Mack, C. P., Somlyo, A. V., Hautmann, M., Somlyo, A. P., and Owens, G. K. (2001). Smooth muscle differentiation marker gene expression is regulated by RhoA-mediated actin polymerization *The Journal of Biological Chemistry* **276**, 341-347.

29. Asparuhova, M. B., Gelman, L., and Chiquet, M. (2009). Role of the actin cytoskeleton in tuning cellular responses to external mechanical stress *Scandinavian Journal of Medicine and Science in Sports* **19**, 490-499.

30. Guettler, S., Vartiainen, M. K., Miralles, F., Larijani, B., and Treisman, R. (2008).RPEL motifs link the serum response factor cofactor MAL but not myocardin to Rho signaling via actin binding. *Mol Cell Biol* **28**, 732-742.

31. Yin, H., Jiang, Y., Li, H., Li, J., Gui, Y., and Zheng, X. L. (2011).Proteasomal degradation of myocardin is required for its transcriptional activity in vascular smooth muscle cells. *J Cell Physiol* **226**, 1897-1906.

32. Kim, H. R., Gallant, C., Leavis, P. C., Gunst, S. J., and Morgan, K. G. (2008). Cytoskeletal remodeling in differentiated vascular smooth muscle is actin isoform dependent and stimulus dependent. *Am J Physiol Cell Physiol* **295**, C768-C778.

33. Gabbiani, G., Schmid, E., Winter, S., Chaponnier, C., de Chastonay, C., Vandekerckhove, J., Weber, K., and Franke, W. W. (1981). Vascular smooth muscle cells differ from other smooth muscle cells: predominance of vimentin filaments and a specific alpha-type actin *PNAS* **78**, 298-302.

34. Lim, S. M., Trzeciakowski, J. P., Sreenivasappa, H., Dangott, L. J., and Trache, A. (2012). RhoA-induced cytoskeletal tension controls adaptive cellular remodeling to mechanical signaling. *Integr Biol (Camb)*

*3*5. Korn, E. D., Carlier, M. F., and Pantaloni, D. (1987). Actin polymerization and ATP hydrolysis *Science* **238**, 638-644.

36. Kueh, H. Y., Brieher, W. M., and Mitchison, T. J. (2008). Dynamic stabilization of actin filaments *PNAS* **105**, 16531-16536.

37. Dominguez, R., and Holmes, K. C. (2011). Actin structure and function. *Annu Rev Biophys* **40**, 169-186.

38. Chrzanowska-Wodnicka, M., and Burridge, K. (1996). Rho-stimulated contractility drives the formation of stress fibers and focal adhesions. *J Cell Biol* **133**, 1403-1415.

39. Huveneers, S., and Danen, E. H. (2009). Adhesion signaling - crosstalk between integrins, Src and Rho. *J Cell Sci* **122**, 1059-1069.

40. Lim, S. M., Kreipe, B. A., Trzeciakowski, J., Dangott, L., and Trache, A. (2010). Extracellular matrix effect on RhoA signaling modulation in vascular smooth muscle cells. *Exp Cell Res* **316**, 2833-2848.

41. Godin, C. M., and Ferguson, S. S. (2010). The angiotensin II type 1 receptor induces membrane blebbing by coupling to Rho A, Rho kinase, and myosin light chain kinase. *Mol Pharmacol* **77**, 903-911.

42. Provenzano, P. P., and Keely, P. J. (2011). Mechanical signaling through the cytoskeleton regulates cell proliferation by coordinated focal adhesion and Rho GTPase signaling. *J Cell Sci* **124**, 1195-1205.

43. Choi, C. K., Vicente-Manzanares, M., Zareno, J., Whitmore, L. A., Mogilner, A., and Horwitz, A. R. (2008). Actin and alpha-actinin orchestrate the assembly and maturation of nascent adhesions in a myosin II motor-independent manner. *Nat Cell Biol* **10**, 1039-1050.

44. Kuo, J., Han, X., Hsiao, C., Yates, J. R., and Waterman, C. M. (2011). Analysis of the myosin-II-responsive focal adhesion proteome reveals a role for βPix in negative regulation of focal adhesion maturation *Nature Cell Biology* **13**, 383-383.

45. Hinz, B. (2006). Masters and servants of the force: the role of matrix adhesions in myofibroblast force perception and transmission. *Eur J Cell Biol* **85**, 175-181.

46. Liu, B., Itoh, H., Louie, O., Kubota, K., and Kent, K. C. (2002). The signaling protein Rho is necessary for vascular smooth muscle migration and survival but not for proliferation. *Surgery* **132**, 317-325.

47. Mack, C. P. (2011). Signaling mechanisms that regulate smooth muscle cell differentiation. *Arterioscler Thromb Vasc Biol* **31**, 1495-1505.

48. Kuang, S. Q., Kwartler, C. S., Byanova, K. L., Pham, J., Gong, L., Prakash, S. K., Huang, J., Kamm, K. E., Stull, J. T., Sweeney, H. L., and Milewicz, D. M. (2012). Rare, Nonsynonymous Variant in the Smooth Muscle-Specific Isoform of Myosin Heavy Chain, MYH11, R247C, Alters Force Generation in the Aorta and Phenotype of Smooth Muscle Cells. *Circ Res* **110** (11), 1411-22.

*4*9. Majesky, M. W. (2007). Developmental basis of vascular smooth muscle diversity. *Arterioscler Thromb Vasc Biol* **27**, 1248-1258.

50. Gadson, P. F., Dalton, M. L., Patterson, E., Svoboda, D. D., Hutchinson, L., Schram, D., and Rosenquist, T. H. (1997). Differential Response of Mesoderm- and Neural Crest-Derived Smooth Muscle to TGF-**β**1: Regulation of c-myb and **α**1 (I) Procollagen Genes. *Experimental Cell Research* **230**, 169-180.

51. Topouzis, S., and Majesky, M. W. (1996). Smooth Muscle Lineage Diversity in the Chick Embryo: Two Types of Aortic Smooth Muscle Cell Differ in Growth and Receptor-Mediated Transcriptional Responses to Transforming Growth Factor-**β.** *Developmental Biology* **178**, 430-445.

52. Elefteriades, J. A., and Farkas, E. A. (2010). Thoracic aortic aneurysm: clinically pertinent controversies and uncertainties. *J Am Coll Cardiol* **55**, 841-857.

53. Brooke, B. S., Habashi, J. P., Judge, D. P., Patel, N., Loeys, B., and Dietz, H. C. (2008). Angiotensin II Blockade and Aortic-Root Dilation in Marfan's Syndrome. *The New England Journal of Medicine* **358**, 2787-2795.

54. National Marfan Foundation. Marfan Syndrome. 2012.<www.marfan.org/marfan>

55. Habashi, J. P., Judge, D. P., Holm, T. M., Cohn, R. D., Loeys, B. L., Cooper, T. K., Myers, L., Klein, E. C., Liu, G., Calvi, C., Podowski, M., Neptune, E. R., Halushka,

M. K., Bedja, D., Gabrielson, K., Rifkin, D. B., Carta, L., Ramirez, F., Huso, D. L., and Dietz, H. C. (2006). Losartan, an AT1 antagonist, prevents aortic aneurysm in a mouse model of Marfan syndrome. *Science* **312**, 117-121.

56. McLoughlin, D., McGuinness, J., Byrne, J., Terzo, E., Huuskonen, V., McAllister, H., Black, A., Kearney, S., Kay, E., Hill, A. D., Dietz, H. C., and Redmond, J. M. (2011). Pravastatin reduces Marfan aortic dilation. *Circulation* **124**, S168-S173.

57. Loeys, B. L., Schwarze, U., Holm, T., Callewaert, B. L., Thomas, G. H., Pannu, H., De Backer, J. F., Oswald, G. L., Symoens, S., Manouvrier, S., Roberts, A. E., Faravelli, F., Greco, M. A., Pyeritz, R. E., Milewicz, D. M., Coucke, P. J., Cameron, D. E., Braverman, A. C., Byers, P. H., De Paepe, A. M., and Dietz, H. C. (2006). Aneurysm Syndromes Caused by Mutations in the TGF-beta Receptor *The New England Journal of Medicine* **355**, 788-798.

58. Loeys-Dietz Syndrome Foundation.Loeys-Dietz Syndrome.2008.<http://loeysdietz.org>

59. Kalra, V. B., Gilbert, J. W., and Malhotra, A. (2011). Loeys-Dietz syndrome: cardiovascular, neuroradiological and musculoskeletal imaging findings. *Pediatr Radiol* **41**, 1495-504; quiz 1616.

60. Ong, K. T., Perdu, J., De Backer, J., Bozec, E., Collignon, P., Emmerich, J., Fauret, A. L., Fiessinger, J. N., Germain, D. P., Georgesco, G., Hulot, J. S., De Paepe, A., Plauchu, H., Jeunemaitre, X., Laurent, S., and Boutouyrie, P. (2010). Effect of celiprolol on prevention of cardiovascular events in vascular Ehlers-Danlos syndrome: a prospective randomised, open, blinded-endpoints trial. *Lancet* **376**, 1476-1484.

61. Prakash, S. K., LeMaire, S. A., Guo, D. C., Russell, L., Regalado, E. S., Golabbakhsh, H., Johnson, R. J., Safi, H. J., Estrera, A. L., Coselli, J. S., Bray, M. S., Leal, S. M., Milewicz, D. M., and Belmont, J. W. (2010). Rare copy number variants disrupt genes regulating vascular smooth muscle cell adhesion and contractility in sporadic thoracic aortic aneurysms and dissections. *Am J Hum Genet* **87**, 743-756.

62. Kuang, S. Q., Guo, D. C., Prakash, S. K., McDonald, M. L., Johnson, R. J., Wang, M., Regalado, E. S., Russell, L., Cao, J. M., Kwartler, C., Fraivillig, K., Coselli, J. S., Safi, H. J., Estrera, A. L., Leal, S. M., Lemaire, S. A., Belmont, J. W., Milewicz, D. M., and GenTAC Investigators (2011). Recurrent chromosome 16p13.1 duplications are a risk factor for aortic dissections. *PLoS Genet* **7**, e1002118.

63. LeMaire, S. A., McDonald, M. L., Guo, D. C., Russell, L., Miller, C. C., Johnson, R. J., Bekheirnia, M. R., Franco, L. M., Nguyen, M., Pyeritz, R. E., Bavaria, J. E., Devereux, R., Maslen, C., Holmes, K. W., Eagle, K., Body, S. C., Seidman, C., Seidman, J. G., Isselbacher, E. M., Bray, M., Coselli, J. S., Estrera, A. L., Safi, H. J., Belmont, J. W., Leal, S. M., and Milewicz, D. M. (2011). Genome-wide association study identifies a susceptibility locus for thoracic aortic aneurysms and aortic dissections spanning *FBN1* at 15q21.1. *Nat Genet* **43**, 996-1000.

64. Inamoto, S., Kwartler, C. S., Lafont, A. L., Liang, Y. Y., Fadulu, V. T., Duraisamy, S., Willing, M., Estrera, A., Safi, H., Hannibal, M. C., Carey, J., Wiktorowicz, J., Tan, F. K., Feng, X. H., Pannu, H., and Milewicz, D. M. (2010). *TGFBR2* mutations alter smooth muscle cell phenotype and predispose to thoracic aortic aneurysms and dissections. *Cardiovasc Res* **88**, 520-529.

65. Regalado, E. S., Guo, D. C., Villamizar, C., Avidan, N., Gilchrist, D., McGillivray, B., Clarke, L., Bernier, F., Santos-Cortez, R. L., Leal, S. M., Bertoli-Avella, A. M., Shendure, J., Rieder, M. J., Nickerson, D. A., NHLBI GO Exome Sequencing Project, and Milewicz, D. M. (2011). Exome sequencing identifies *SMAD3* mutations as a cause of familial thoracic aortic aneurysm and dissection with intracranial and other arterial aneurysms. *Circ Res* **109**, 680-686.

66. Wang, L., Guo, D. C., Cao, J., Gong, L., Kamm, K. E., Regalado, E., Li, L., Shete, S., He, W. Q., Zhu, M. S., Offermanns, S., Gilchrist, D., Elefteriades, J., Stull, J. T., and Milewicz, D. M. (2010). Mutations in myosin light chain kinase cause familial aortic dissections. *Am J Hum Genet* **87**, 701-707.

67. Zhu, L., Vranckx, R., Khau Van Kien, P., Lalande, A., Boisset, N., Mathieu, F., Wegman, M., Glancy, L., Gasc, J. M., Brunotte, F., Bruneval, P., Wolf, J. E., Michel, J. B., and Jeunemaitre, X. (2006). Mutations in myosin heavy chain 11 cause a syndrome associating thoracic aortic aneurysm/aortic dissection and patent ductus arteriosus. *Nat Genet* **38**, 343-349.

68. Pannu, H., Tran-Fadulu, V., Papke, C. L., Scherer, S., Liu, Y., Presley, C., Guo, D., Estrera, A. L., Safi, H. J., Brasier, A. R., Vick, G. W., Marian, A. J., Raman, C. S., Buja, L. M., and Milewicz, D. M. (2007). *MYH11* mutations result in a distinct vascular pathology driven by insulin-like growth factor 1 and angiotensin II. *Hum Mol Genet* **16**, 2453-2462.

69. Renard, M., Callewaert, B., Baetens, M., Campens, L., Macdermot, K., Fryns, J. P., Bonduelle, M., Dietz, H. C., Gaspar, I. M., Cavaco, D., Stattin, E. L., Schrander-Stumpel, C., Coucke, P., Loeys, B., De Paepe, A., and De Backer, J. (2011). Novel

MYH11 and *ACTA2* mutations reveal a role for enhanced TGFβ signaling in FTAAD. *Int J Cardiol*

70. Guo, D. C., Pannu, H., Tran-Fadulu, V., Papke, C. L., Yu, R. K., Avidan, N., Bourgeois, S., Estrera, A. L., Safi, H. J., Sparks, E., Amor, D., Ades, L., McConnell, V., Willoughby, C. E., Abuelo, D., Willing, M., Lewis, R. A., Kim, D. H., Scherer, S., Tung, P. P., Ahn, C., Buja, L. M., Raman, C. S., Shete, S. S., and Milewicz, D. M. (2007). Mutations in smooth muscle alpha-actin (ACTA2) lead to thoracic aortic aneurysms and dissections. *Nat Genet* **39**, 1488-1493.

71. Morisaki, H. (2009). Mutation of ACTA2 gene as an important cause of familial and nonfamilial nonsyndromatic thoracic aortic aneurysm and/or dissection (TAAD) *Human Mutation* **30**, 1406-1411.

72. Milewicz, D. M., Østergaard, J. R., Ala-Kokko, L. M., Khan, N., Grange, D. K., Mendoza-Londono, R., Bradley, T. J., Olney, A. H., Adès, L., Maher, J. F., Guo, D., Buja, L. M., Kim, D., Hyland, J. C., and Regalado, E. S. (2010). *De novo ACTA2* mutation causes a novel syndrome of multisystemic smooth muscle dysfunction. *Am J Med Genet A* **152A**, 2437-2443.

73. Yoo, E. H., Choi, S. H., Jang, S. Y., Suh, Y. L., Lee, I., Song, J. K., Choe, Y. H., Kim, J. W., Ki, C. S., and Kim, D. K. (2010). Clinical, pathological and genetic analysis of a Korean familiy with thoracic aortic aneurysms and dissections carrying a novel Asp26Tyr mutation *Annals of Clinical and Laboratory Science* **40**

74. Disabella, E., Grasso, M., Gambarin, F. I., Narula, N., Dore, R., Favalli, V., Serio, A., Antoniazzi, E., Mosconi, M., Pasotti, M., Odero, A., and Arbustini, E. (2011). Risk

of dissection in thoracic aortic aneurysms associated with mutations of smooth muscle alpha-actin 2 (ACTA2) *Heart* **97**, 321-326.

75. Hoffjan, S., Waldmüller, S., Blankenfeldt, W., Kötting, J., Gehle, P., Binner, P., Epplen, J. T., and Scheffold, T. (2011). Three novel mutations in the ACTA2 gene in German patients with thoracic aortic aneurysms and dissections. *Eur J Hum Genet* **19**, 520-524.

76. Imai, T., Horigome, H., Shiono, J., and Hiramatsu, Y. (2011). Isolated giant ascending aortic aneurysm in a child- a novel mutation of the ACTA2 gene *European Journal of Cardio-thoracic Surgery* **40**, e156-e157.

77. Mundia, M. M., Demers, R. W., Chow, M. L., Perieteanu, A. A., and Dawson, J. F. (2012). Subdomain location of mutations in cardiac actin correlate with type of functional change. *PLoS One* **7**, e36821.

78. Bergeron, S. E., Wedemeyer, E. W., Lee, R., Wen, K. K., McKane, M., Pierick, A. R., Berger, A. P., Rubenstein, P. A., and Bartlett, H. L. (2011). Allele-specific effects of thoracic aortic aneurysm and dissection alpha-smooth muscle actin mutations on actin function. *J Biol Chem* **286**, 11356-11369.

79. Cao, J., and Villamizar, C. Lab of Dianna Milewicz, MD, PhD, University of Texas Health Science Center in Houston, TX. Unpublished work.

80. Chang, A., Kamm, K. E., and Stull, J. Lab of James Stull, PhD and Kristine E. Kamm, PhD. University of Texas Southwestern Medical Center, Dallas, TX. Unpublished work.

81. Villamizar, C. Lab of Dianna Milewicz, MD, PhD, University of Texas Health Science Center in Houston, TX. Unpublished work.

82. Huang, J., Kamm, K. E., and Stull, J.Lab of James Stull, PhD and Kristine E. Kamm, PhD. University of Texas Southwestern Medical Center, Dallas, TX. Unpublished work.

83. Kumar, A. and Lindner, V. (1997). Remodeling with neointima formation in the mouse carotid artery after cessation of blood flow. *Arterioscler Thromb Vasc Biol* **17**, 2238-2244.

84. Schildmeyer, L. A., Braun, R., Taffet, G., Debiasi, M., Burns, A. E., Bradley, A., and Schwartz, R. J. (2000). Impaired vascular contractility and blood pressure homeostasis in the smooth muscle alpha-actin null mouse. *FASEB J* **14**, 2213-2220.

85. Haaksma, C. J., Schwartz, R. J., and Tomasek, J. J. (2011). Myoepithelial Cell Contraction and Milk Ejection Are Impaired in Mammary Glands of Mice Lacking Smooth Muscle Alpha-Actin *Biology of Reproduction* **85**, 13-21.

86. Weymouth, N., Shi, Z., and Rockey, D. C. (2012). Smooth muscle α actin is specifically required for the maintenance of lactation. *Dev Biol* **363**, 1-14.

87. Papke, C. L., Cao, J., and Villamizar, C. Lab of Dianna Milewicz, MD, PhD, University of Texas Health Science Center in Houston, TX. Unpublished work.

88. Papke, C. L., Cao, J., Kwartler, C. S., Villamizar, C., Byanova, K. L., Lim, S., Wang, M., Rees, M., Chaponnier, C., Gabbiani, G., Khakoo, A. Y., Chandra, J., Trache, A., Zimmer, W., and Milewicz, D. M. Loss of Smooth Muscle α-actin Increases Smooth Muscle Cell Proliferation Through Altered Focal Adhesions and Ligand-Independent Platelet Derived Growth Factor Receptor-β Activation. Unpublished manuscript.

89. Tang, Y., Urs, S., Boucher, J., Bernaiche, T., Venkatesh, D., Spicer, D. B., Vary, C. P., and Liaw, L. (2010). Notch and transforming growth factor-beta (TGFbeta) signaling

pathways cooperatively regulate vascular smooth muscle cell differentiation. *J Biol Chem* **285**, 17556-17563.

90. Schlaepfer, D. D., Hanks, S. K., Hunter, T., and van der Geer, P. (1994). Integrin-mediated signal transduction linked to Ras pathway by GRB2 binding to focal adhesion kinase *Nature* **372**, 786-791.

91. Schlaepfer, D. D., and Hunter, T. (1996). Signal transduction from the extracellular matrix - a role for the focal adhesion protein-tyrosine kinase FAK. *Cell Structure and Function* **21**, 445-450.

92. Wang, D., Grammer, J. R., Cobbs, C. S., Stewart, J. E., Liu, Z., Rhoden, R., Hecker, T. P., Ding, Q., and Gladson, C. L. (2000). p125 focal adhesion kinase promotes malignant astrocytoma cell proliferation in vivo *Journal of Cell Science* **113**, 4221-4230.

93. Chaturvedi, L. S., Marsh, H. M., and Basson, M. D. (2007). Src and focal adhesion kinase mediate mechanical strain-induced proliferation and ERK1/2 phosphorylation in human H441 pulmonary epithelial cells. *Am J Physiol Cell Physiol* **292**, C1701-C1713.

94. Schneller, M., Vuori, K., and Ruoslahti, E. (1997). αvβ3 integrin associates with activated insulin and PDGFβ receptors and potentiates the biological activity of PDGF. *EMBO J* **16**, 5600-5607.

95. Woodard, A. S., García-Cardeña, G., Leong, M., Madri, J. A., Sessa, W. C., and Languino, L. R. (1998). The synergistic activity of αvβ3 integrin and PDGF receptor increases cell migration. *J Cell Sci* **111 (4)**, 469-478.

96. Eliceiri, B. P. (2001). Integrin and Growth Factor Receptor Crosstalk *Circ Res* **89**, 1104-1110.

97. Schwartz, S. M. (1997). Smooth muscle migration in vascular development and pathogenesis. *Transplant Immunology* **5**, 255-260.

98. Myllärniemi, M., Calderon, L., Lemström, K., Buchdunger, E., and Häyry, P. (1997). Inhibition of platelet-derived growth factor receptor tyrosine kinase inhibits vascular smooth muscle cell migration and proliferation. *FASEB J* **11**, 1119-1126.

99. Pichon, S., Bryckaert, M., and Berrou, E. (2004). Control of actin dynamics by p38 MAP kinase - Hsp27 distribution in the lamellipodium of smooth muscle cells. *J Cell Sci* **117**, 2569-2577.

100. National Cancer Institute. Cancer Drug Information - Imatinib Mesylate.<http://www.cancer.gov/cancertopics/druginfo/imatinibmesylate>

101. Ghofrani, H. A., Seeger, W., and Grimminger, F. (2005). Imatinib for the treatment of pulmonary arterial hypertension. *The New England Journal of Medicine* **353**

102. ten Freyhaus, H., Dumitrescu, D., Berghausen, E., Vantler, M., Caglayan, E., and Rosenkranz, S. (2012). Imatinib mesylate for the treatment of pulmonary arterial hypertension. *Expert Opin Investig Drugs* **21**, 119-134.

103. Lasater, E. A., Bessler, W. K., Mead, L. E., Horn, W. E., Clapp, D. W., Conway, S. J., Ingram, D. A., and Li, F. (2008). *Nf1*$^{+/-}$ mice have increased neointima formation via hyperactivation of a Gleevec-sensitive molecular pathway. *Hum Mol Genet* **17**, 2336-2344.

104. Wendel, H., and Dancker, P. (1987). Influence of phalloidin on both the nucleation and the elongation phase of actin polymerization. *Biochimica et Biophysica Acta* **915**, 199-204.

105. Trybus, K. M., Fagnant, Patty and Sckolnick, Maria. 2012. Personal communication.

106. Lee, S. H., Hungerford, J. E., Little, C. D., and Iruela-Arispe, M. L. (1997). Proliferation and differentiation of smooth muscle cell precursors occurs simultaneously during the development of the vessel wall. *Dev Dyn* **209**, 342-352.

107. Owens, G. K., Loeb, A., Gordon, D., and Thompson, M. M. (1986).Expression of smooth muscle-specific alpha-isoactin in cultured vascular smooth muscle cells: relationship between growth and cytodifferentiation. *J Cell Biol* **102**, 343-352.

108. De Mey, J. G., Uitendaal, M. P., Boonen, H. C., Vrijdag, M. J., Daemen, M. J., and Struyker-Boudier, H. A. (1989). Acute and long-term effects of tissue culture on contractile reactivity in renal arteries of the rat. *Circ Res* **65**, 1125-1135.

109. Hawkins, P. T., Eguinoa, A., Qiu, R. G., Stokoe, D., Cooke, F. T., Walters, R., Wennström, S., Claesson-Welsh, L., Evans, T., and Symons, M. (1995). PDGF stimulates an increase in GTP-Rac via activation of phosphoinositide 3-kinase. *Curr Biol* **5**, 393-403.

110. Higuchi, S., Ohtsu, H., Suzuki, H., Shirai, H., Frank, G. D., and Eguchi, S. (2007). Angiotensin II signal transduction through the AT1 receptor: novel insights into mechanisms and pathophysiology. *Clin Sci (Lond)* **112**, 417-428.

111. Vecchione, C., Carnevale, D., Di Pardo, A., Gentile, M. T., Damato, A., Cocozza, G., Antenucci, G., Mascio, G., Bettarini, U., Landolfi, A., Iorio, L., Maffei, A., and Lembo, G. (2009). Pressure-induced vascular oxidative stress is mediated through

activation of integrin-linked kinase 1/βPIX/Rac-1 pathway. *Hypertension* **54**, 1028-1034.

112. Michael, K. E., Dumbauld, D. W., Burns, K. L., Hanks, S. K., and García, A. J. (2009). Focal adhesion kinase modulates cell adhesion strengthening via integrin activation. *Mol Biol Cell* **20**, 2508-2519.

113. Dumbauld, D. W., Shin, H., Gallant, N. D., Michael, K. E., Radhakrishna, H., and García, A. J. (2010). Contractility modulates cell adhesion strengthening through focal adhesion kinase and assembly of vinculin-containing focal adhesions. *J Cell Physiol* **223**, 746-756.

114. Ilic, D., Furuta, Y., Kanazawa, S., Takeda, N., Sobue, K., Nakatsuji, N., Nomura, S., Fujimoto, J., Okada, M., Yamamoto, T., and Aizawa, S. (1995). Reduced cell motility and enhanced focal adhesion contact formation in cells from FAK-deficient mice *Nature* **377**, 539-544.

115. Webb, D. J., Donais, K., Whitmore, L. A., Thomas, S. M., Turner, C. E., Parsons, J. T., and Horwitz, A. F. (2004). FAK-Src signalling through paxillin, ERK and MLCK regulates adhesion disassembly. *Nat Cell Biol* **6**, 154-161.

116. Pardanani, A., and Tefferi, A. (2004). Imatinib targets other than bcr/abl and their clinical relevance in myeloid disorders. *Blood* **104**, 1931-1939.

117. Alexis, J. D., Wang, N., Che, W., Lerner-Marmarosh, N., Sahni, A., Korshunov, V. A., Zou, Y., Ding, B., Yan, C., Berk, B. C., and Abe, J. (2009). Bcr kinase activation by angiotensin II inhibits peroxisome-proliferator-activated receptor gamma transcriptional activity in vascular smooth muscle cells. *Circ Res* **104**, 69-78.

118. Liu, X., Cheng, Y., Yang, J., Xu, L., and Zhang, C. (2012). Cell-specific effects of miR-221/222 in vessels: molecular mechanism and therapeutic application. *J Mol Cell Cardiol* **52**, 245-255.

119. Wang, C. H., Verma, S., Hsieh, I. C., Hung, A., Cheng, T. T., Wang, S. Y., Liu, Y. C., Stanford, W. L., Weisel, R. D., Li, R. K., and Cherng, W. J. (2007). Stem cell factor attenuates vascular smooth muscle apoptosis and increases intimal hyperplasia after vascular injury. *Arterioscler Thromb Vasc Biol* **27**, 540-547.

120. Shen, Y. H., Hu, X., Zou, S., Wu, D., Coselli, J. S., and Lemaire, S. A. (2012). Stem cells in thoracic aortic aneurysms and dissections: potential contributors to aortic repair. *Ann Thorac Surg* **93**, 1524-1533.

Vita

Katerina Lyubomirova Byanova was born in Sofia, Bulgaria on June 18, 1987 and is the daughter of Donka Stoyanova Stoyanova and Lubomir Borissov Bianov. After successfully completing the International Baccalaureate Program and graduating from Red Cross Nordic United World College in Flekke, Norway in May 2005, she went on to attend Amherst College in Amherst, MA, from which she earned the degree of Bachelor of Arts in Biology *cum laude* in May 2009. Katerina enrolled at the University of Texas Graduate School of Biomedical Sciences in August 2010. She will graduate with a Master of Science in June 2012.

Permanent address:

Dianabad, bl.11, entr. 2, ap. 40
Sofia 1172,
Bulgaria

Email: katerinabyanova@gmail.com